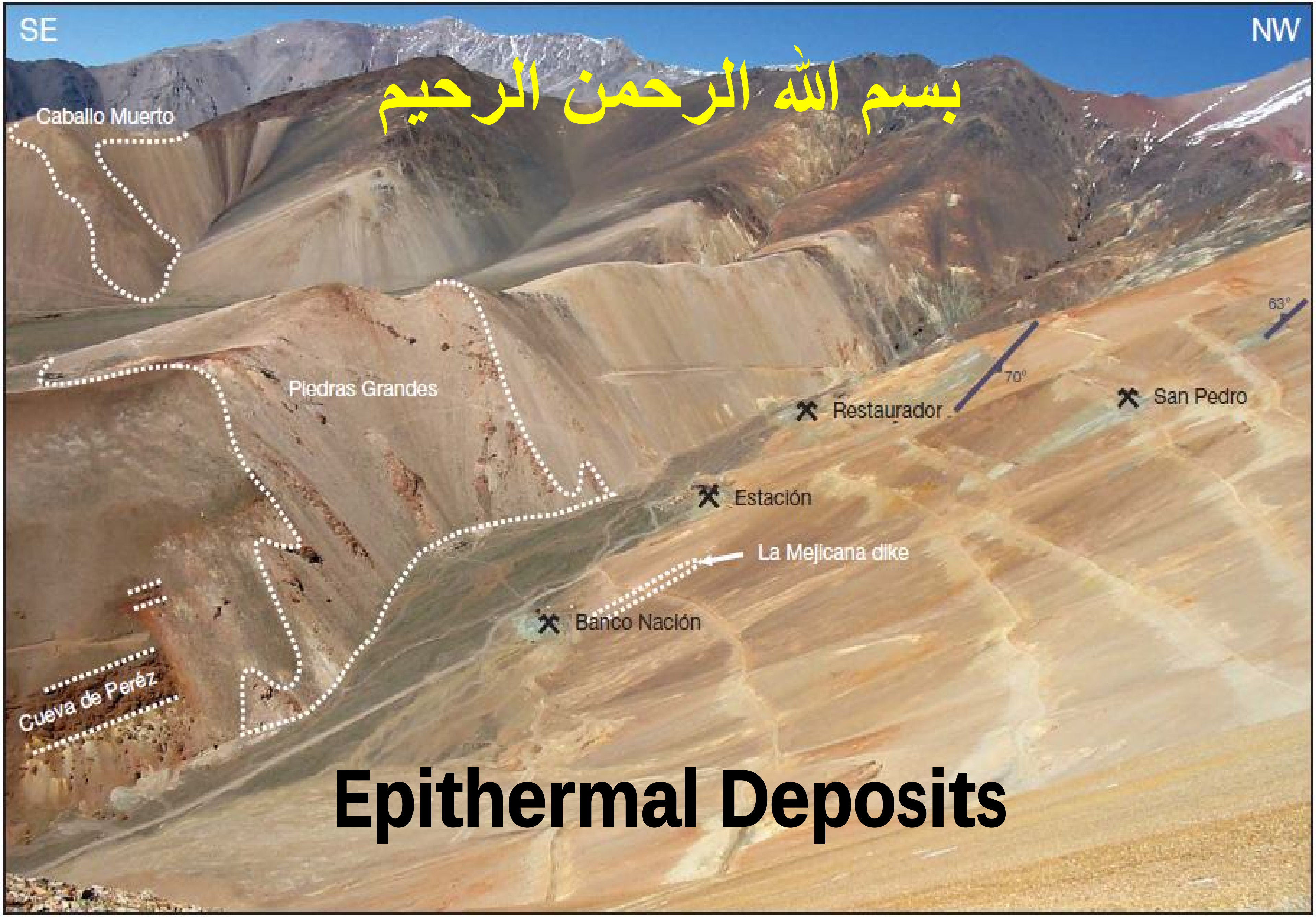

FIG. 3. Photograph of Quebrada La Mejicana looking southwest from La Estrechura. The historic galleries of San Pedro, Restaurador, Estación, and Banco Nación are partly accessible and reflect past Cu-Au-Ag mining activity.

Simplified Definition:

Epithermal deposits of Au (± Ag) comprise veins and disseminations near the Earth's surface (≤1.5 km), in volcanic and sedimentary rocks, sediments, and, in some cases, also in metamorphic rocks. The deposits may be found in association with hot springs and frequently occur at centres of young volcanism.

The ores are dominated primarily by precious metals (Au, Ag), but some deposits may also contain variable amounts base metals such as Cu, Pb, and Zn.

Epithermal Au (—Ag) deposits form in the near-surface environment, from hydrothermal systems typically within 1.5 km of the Earth's surface.

They are commonly found associated with centres of magmatism and volcanism, but form also in shallow marine settings.

Hot-spring deposits and both liquid- and vapour-dominated geothermal systems are commonly associated with epithermal deposits.

The shallow origin of epithermal Au deposits makes them more susceptible to erosion

Epithermal Au deposits have represented a high-grade, readily mineable, exploration target largely in Tertiary and younger volcanic centres, including the Cordillera. However, a number of older epithermal Au deposits have also been discovered, including several Proterozoic examples in Canada.

The ores are dominated primarily by precious metals (Au, Ag), but some deposits may also contain variable amounts base metals such as Cu, Pb, and Zn.

Ore texture; replacement (i.e. by solution and reprecipitation),or open-space filling (e.g. veins, breccias, pore spaces).

The form of deposits originating by open-space filling typically reflects that of the structural control of the hydrothermal fluids (planar vs. irregular fractures, etc).

The deposits are commonly young, generally Tertiary or Quaternary.

They may be of similar age as their host rocks when these are volcanic in origin, or (typically) younger than their host

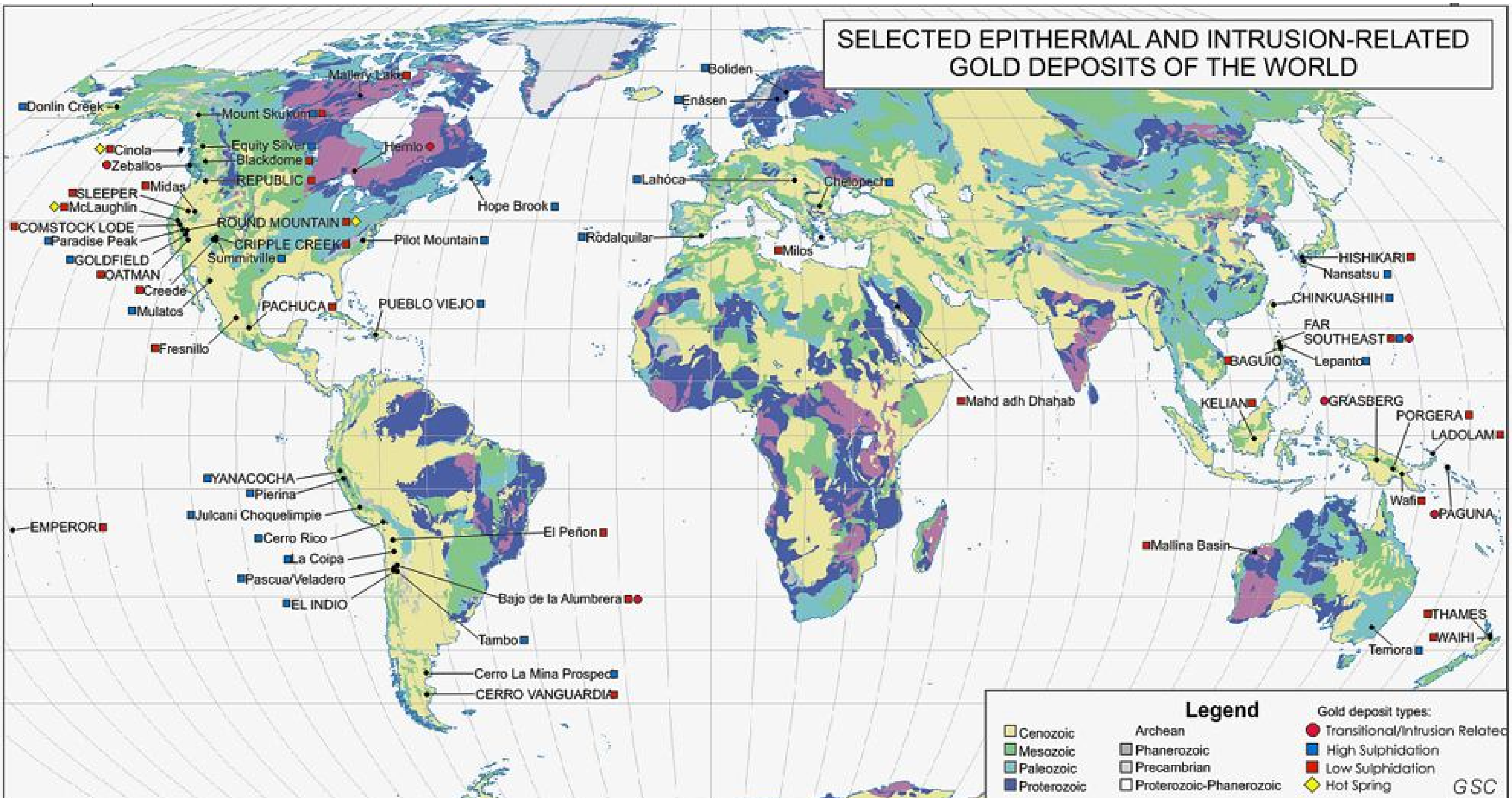

References:
Arancibia et al. 2006; Bethke et al., 2005; Carman, 2003; Deyell et al., 2005; Dubé et al., 1998; Fifarek and Rye, 2005; Goldfarb et al., 2004; Gosselin and Dubé, 2005a,c; Hedenquist et al., 2000; Huston et al., 2002; Klein and Criss, 1988; Naden et al., 2005; Panteleyev, 1996a,b,c, 2005a,b; Poulsen, 1996, 2000; Sillitoe, 1992, 1997; Taylor, 1996, this paper; Turner et al., 2003.

N.B.: Giant and Bonanza Gold deposits indicated by capitalization of deposit name, e.g., EL INDIO.

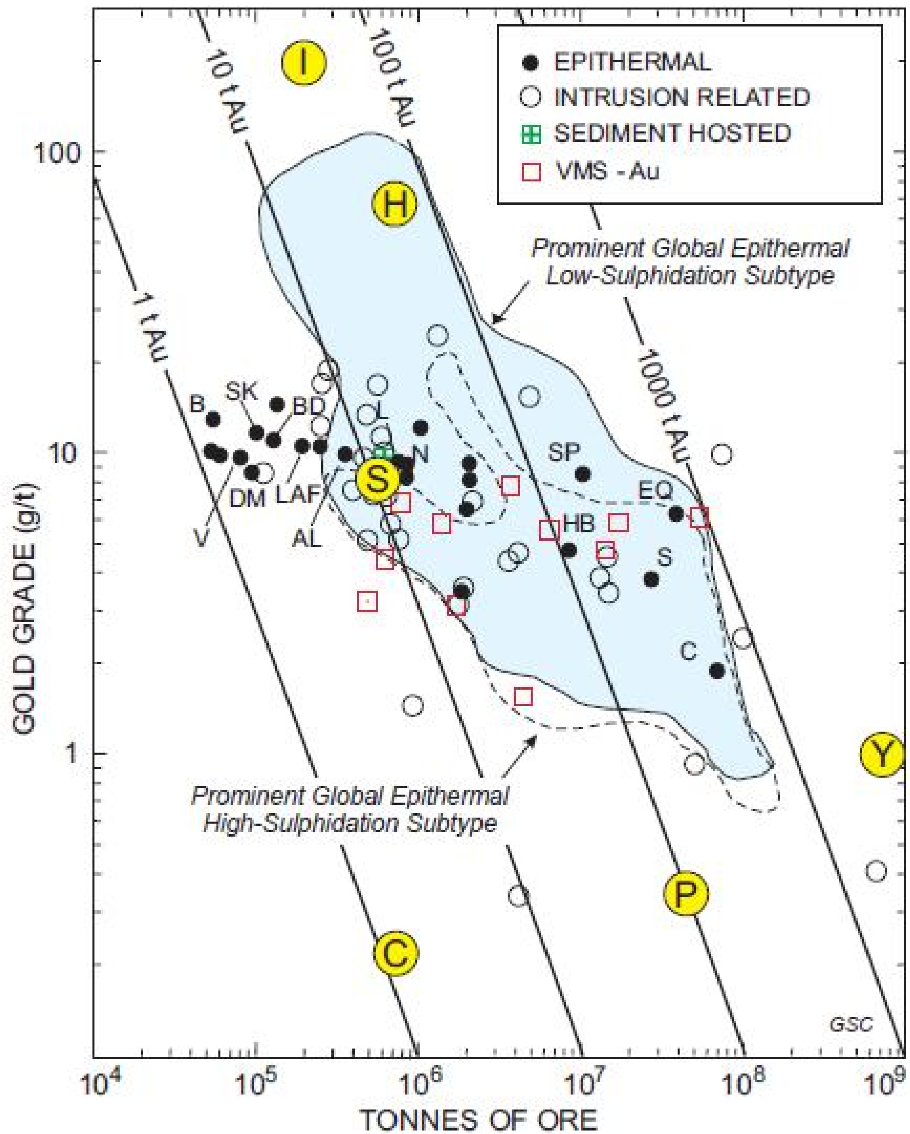

FIGURE 3. Plot of Au grade (g/t) versus tonnage (economic, or reserves+production) for selected Canadian epithermal Au deposits and prominent examples elsewhere in the world, classified by subtype as referred to in the text (Taylor, 2007).

Table 1: History of nomenclature for divisions of epithermal deposit types

Goldfield type			Ransome (1907)
Alunitic kaolinic gold veins	Sericitic zinc-silver veins	Gold-silver-adularia veins Fluoritic tellurium-adularia gold veins	Emmons (1918)
Gold-alunite deposits	Gold-quartz veins in andesite		Lindgren (1933)
	Argentite-gold quartz veins Argentite veins Base metal veins	Gold-quartz veins in rhyolite Gold telluride veins Gold selenide veins	
Secondary quartzite (Altered host rock)			Fedorov (1903); Nakovnik (1933)
Acid	Alkaline		Sillitoe (1977)
Epithermal			Buchanan (1981)
Enargite-gold			Ashley (1982)
		Hot-spring type	Giles and Nelson (1982)
High sulfur	Low sulfur		Bonham (1986, 1988)
Acid sulfate	Adularia-sericite		Hayba et al. (1985), Heald et al. (1987)
High sulfidation	Low sulfidation		Hedenquist (1987)
Alunite-kaolinite	Adularia-sericite		Berger and Henley (1989)
	Type 1 adularia-sericite	Type 2 adularia-sericite	Albino and Margolis (1991)
High sulfidation	High sulfide + base metal, low sulfidation	Low sulfide + base metal, low sulfidation	Sillitoe (1993)
Lithocap (Altered host rock)			Sillitoe (1995)
High sulfidation	Western andesite assemblage, low sulfidation	Bimodal basalt-rhyolite assemblage, low sulfidation	John et al. (1999); John (2001)
HIGH SULFIDATION (HS)	INTERMEDIATE SULFIDATION (IS)	LOW SULFIDATION (LS)	Hedenquist et al. (2000)

Note: CAPITALIZED names used in this presentation

From Sillitoe and Hedenquist, 2003. See this paper, as well as Einaudi et al., 2003, for sources of references listed

Table 2.2 Characteristics of high- and low-sulfidation epithermal deposits

High-sulfidation	**Low-sulfidation**
Oxidized sulfur species (SO_2, SO_4^{2-}, HSO_4^-) in ore fluid/vapor	Reduced sulfur species (HS^-, H_2S) in ore fluid/vapor
Also referred to as	
Gold–alunite, acid–sulfate, alunite–kaolinite	Adularia–sericite, hotspring-related
Fluids	
Acidic pH, probably saline initially, dominantly magmatic	Near-neutral pH, low salinity, gas-rich (CO_2, H_2S), dominantly meteoric
Alteration assemblage	
Advanced argillic (zonation: quartz–alunite–kaolinite–illite–montmorillonite–chlorite)	Adularia–sericite (zonation: quartz/chalcedony–calcite–adularia–sericite–chlorite)
Metal associations	
Au–Cu (lesser Ag, Bi, Te)	Au–Ag (lesser As, Sb, Se, Hg)

Robb, 2005

	High sulfidation (HS)	Low sulfidation (LS)
Genetically related volcanic rocks	Mainly andesite-rhyodacite	Andesite-rhyodacite-rhyolite
Deposit form	Disseminated: dominant, replacement: common, stockwork: minor	Open-space veins: dominant, stockwork: common, disseminated & replacement: minor
Alteration Zone	Areally extensive & visually prominent	Commonly restricted and visually subtle
Quartz gangue	Fine-grained, massive, mainly replacement origin; residual, slaggy (vuggy) quartz commonly hosts ore	Chalcedony &/or quartz displaying crustiform, colloform, bladed, cockade & carbonate-replacement textures; open space filling
Carbonate gangue	Absent	Ubiquitous, commonly managanoan
Other gangue	Barite widespread with ore; native sulfur commonly fills open spaces	Barite & (or) fluorite present locally; barite commonly above ore
Sulfide abundance	10-90 vol% mainly fine-grained, partly laminated pyrite	1-20 vol%, but typically <5 vol%, predominantly pyrite
Metals present	Cu, Au, As (Ag, Pb)	Au and (or) Ag (Zn, Pb, Cu)

TABLE 1. Comparative mineralogical, geological, and production data for selected epithermal Au deposits in Canada and several non-Canadian type examples.*

District and/or deposit	Age[1] Host [Min.]	Size[2] Ore[5]	(R+P) Au[6]	Grade[3]	Ag/Au	Base Metal	%S	Ad	Al	Cpy	En	Ss	Ags	Sp	Gn	Ba	Fl	Rc	Cc	Ank	Host rock	Alt'n.[7] vn → w.r.	Form[8]
								Mineralogy[4]										Carbonates					
HIGH-SULPHIDATION TYPE:[9] *Volcanic host rocks*																							
Toodoggone River, B.C.	189-198;182																						
Al (Bonanza; Thesis)	[196]	0.348	3.21	9.6					X	X		X	X	X	X	X					and./dacite	Si/A	vn
BV	[190-197]	0.053	0.55	10.4		x										X					andesite		vn,bx
Equity Silver, B.C.[14]	57.2 [>48;57.2]	31.42	24.41	4.2	128.2	X				X		X	X	X							dacite/tuff/congl.	A	vn,st,dis
Summitville, Colorado	20.2-22.0 [22.3]	83.51	3.5		1.2	X	5?		XX	XX	X	XX	X	X	X	X					qtz. Latite	Vgy-Si/Qtz-Al/A	repl., vn
Nansatsu, Japan	3.4-7.6 [2.7-5.5]		>18	3-6	0.1-1.0	x	≤10		X		X	x	X	X	X	x			X		andesite	Vgy-Si/Al-A/Ph/P	repl.
El Indio, Chile[19]	13.7 [8.6]	8.7	108	1.7-218	0.5-10	XX	≤30[11]		X	[X]	[XX]	X	x	[x]	[x]	X					rhyodacite	Si/Ph-A (Al-A)	vn,bx
INTERMEDIATE-SULPHIDATION TYPE *(possible example; variant of low-sulphidation subtype)*																							
Stewart-Iskut region, B.C.	210																		X				
Silbak-Premier	[194.8?]	9.622	66.24	7.0	22.6	XX	≤5[12]	X[13]		X		X	X	X	X	X		X	X	X	and./dacite	Si/K/Ph/P	vn,st,bx
LOW-SULPHIDATION TYPE: *Volcanic and plutonic host rocks*																							
Mt. Skukum, Y.T.	53.2 [50.7]	0.200	2.49	25.0	0.9		<1	X	x							x	X	x	XX	x	andesite	Si/±K/Ph/A/P	vn,bx,st
Mt. Nansen, Y.T.	Tertiary	0.288	3.15	11.1	39.0					X				X	X								
Laforma, Y.T.	>140 [78?]	0.191	2.13	11.2		X				X		x		X	x	X			X	X	granodiorite	Ph	vn
Venus, Y.T.	L. Jur.	>0.07	>0.66	9.3	26.5	XX	15-60						x		X	X					and./dacite	Si/A	vn
Toodoggone River, B.C.	189-198;182																						
Lawyers	[180]	0.880	6.73	7.4	46.7	X		X	X	X		X	X	X	X	X					andesite	Si/A/P	st,bx
Baker (Chapelle)		0.055	1.05	19.5	9.1		3-15			X		X	X	X	X				X		and./basalt	Si/Ph/A/P	vn
Blackdome, B.C.	Eocene [>24,<51.5]	0.368	7.35	20.6	3.1	x	≤5	X		X			x	x	x				X		and./dacite	Si/K/A/P	vn,bx
Stewart-Iskut region, B.C.	210																		X				
Sulphurets (Snowfield)	[192.7]	25	0.78	2.4	0.6	X				X		X		X	X	X	X		X		bslt.-and./andesite	K/Ph/A/P	st,vn,dis
Creede, Colorado	Tertiary	1.4	21.0	1.5	400	X		X	x			x	X	X	X	X	X	X					
LOW-SULPHIDATION TYPE: *Sedimentary and/or mixed host rocks*																							
Cinola, B.C.	Tert./Cret. [14]	23.80	58.31	2.45	2	x	≤10		x	x				x	x				X		congl./s.s./shale	Si/A	diss.,bx,
Dusty Mac, B.C.	Eocene	0.093	0.60	7.2	21.5	X	≤15			x			x	x	x		X		X		s.s./sh./and. pyroclastic	Si/A	bx,st
Hishikari, Japan	0.51-1.78/Cret. [0.8-1.0]		121.7	70	1.27	x		XX		X		x	x	X	x				X	x	shale-s.s./and./dacite	Si/A	vn

* Principal deposits plus several others selected to represent part of the spectrum of variation in type and setting; modified from Taylor (1996).

5. tonnes of ore x106; 6. grams of gold (Au) x106; 7. Alteration facies, vein (vn) to wall rock (w.r.): Vgy-Si; vuggy silica; Qtz, quartz; Al, alunite (advanced argillic); Si, silicification; K, potassic; Ph, phyllic (sercitic);
A, argillic/advanced argillic; P, propylitic (sequence from vein to wall rock); 8. Form of deposit (in order of importance) vn, vein; bx, breccia; st, stockwork; diss., disseminated, repl., replacement; 9. Classification is based on available
Abbreviations: %S*, per cent sulphide; Ad, adularia; Al, alunite; Cpy, chalcopyrite; En, enargite; Ss, sulphosalts (e.g., tennantite-tetrahedrite); Ags, silver sulphides; Sp, sphalerite; Gn, galena; Ba, barite; Fl, fluorite; CO3*, carbonate; Rc rhodochrosite; Cc, calcite; Ank, ankerite; XX = abundant; X = present; x = minor to rare; blank = absent or unknown; and. = andesite; bslt. = basalt; congl. = conglomerate; s.s. = sandstone; lms. = limestone; sh. = shale; Tert. = Tertiary;
Cret. = Cretaceous; L. Jur. = Lower Jurassic; *NB: [ ] = not in paragenetic association with Au . (Talor, 2007)*

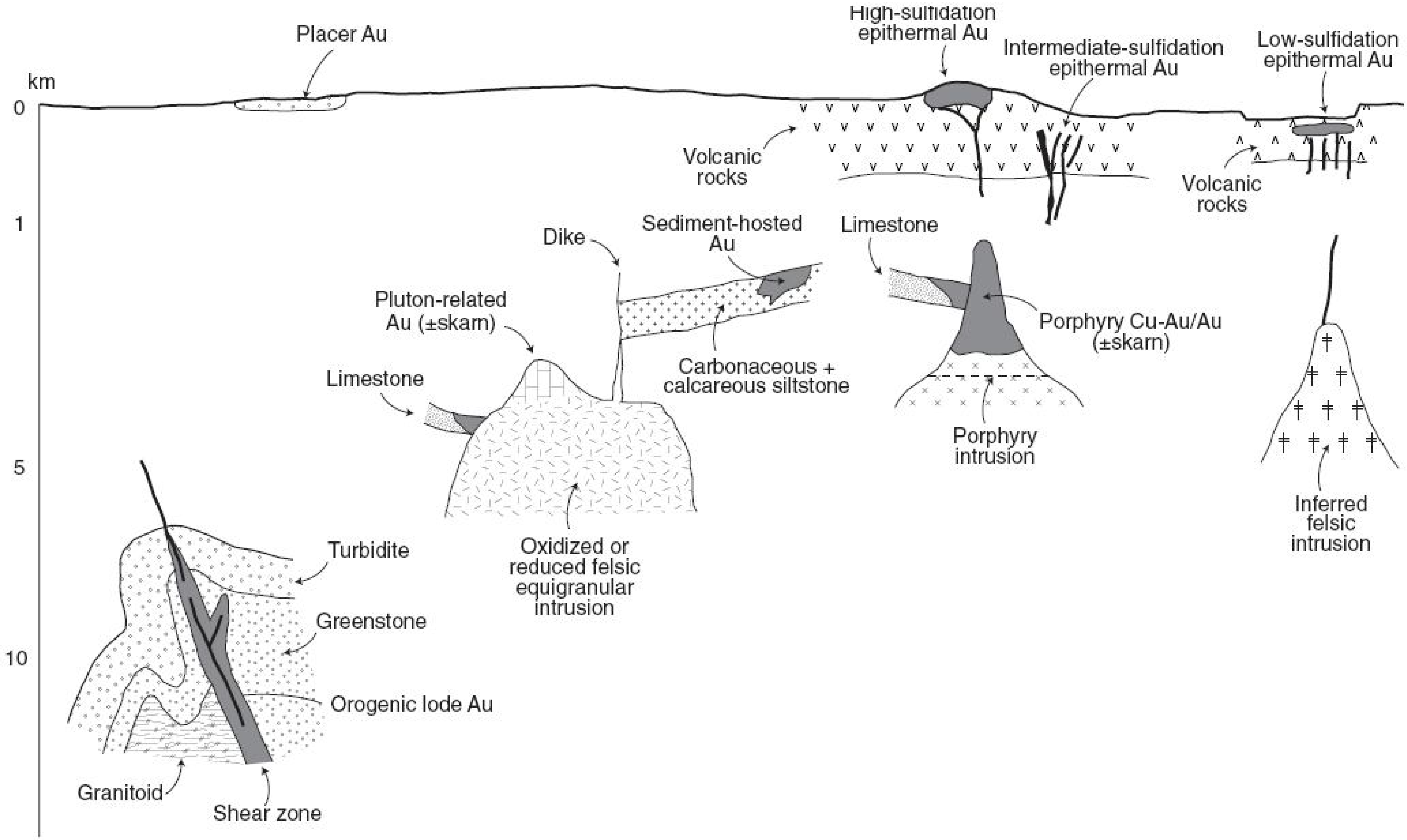

FIG. 1. Schematic geologic settings and interrelationships of the principal gold deposit types in the North and South American Cordillera, inspired by Robert et al. (2007). The approximate depth scale is logarithmic. Selected deposit characteristics are summarized in Table 1. Note that placer gold is most commonly derived by erosion of orogenic and pluton-related deposits.

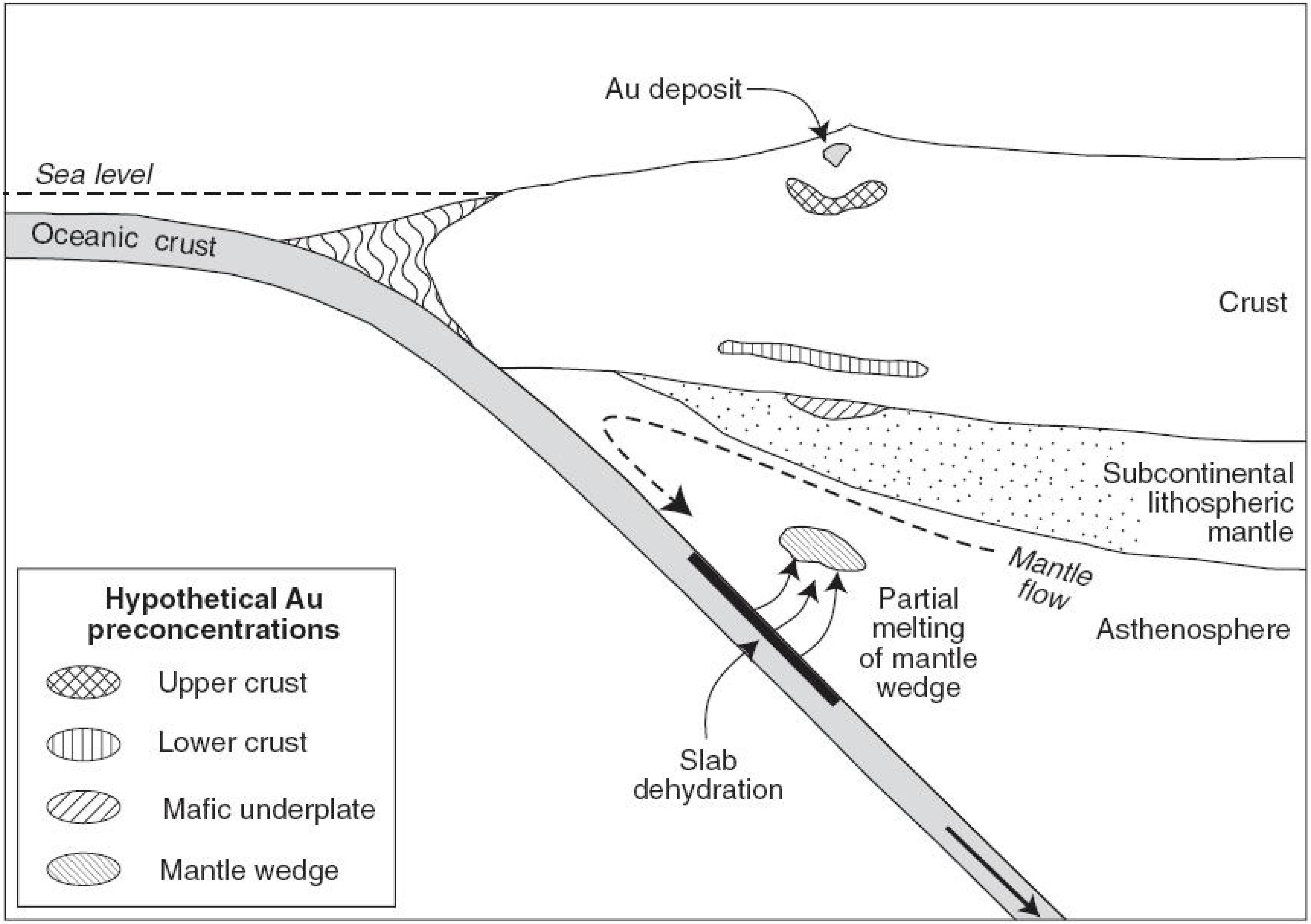

FIG. 11. Cartoon section of a convergent margin to show possible sites of gold (or other metal) concentrations that may be tapped during the magmatism or transcrustal fluid flow responsible for upper-crustal mineralization. Alternatively, another chemical parameter, such as redox state, may influence metal availability. See text for further discussion.

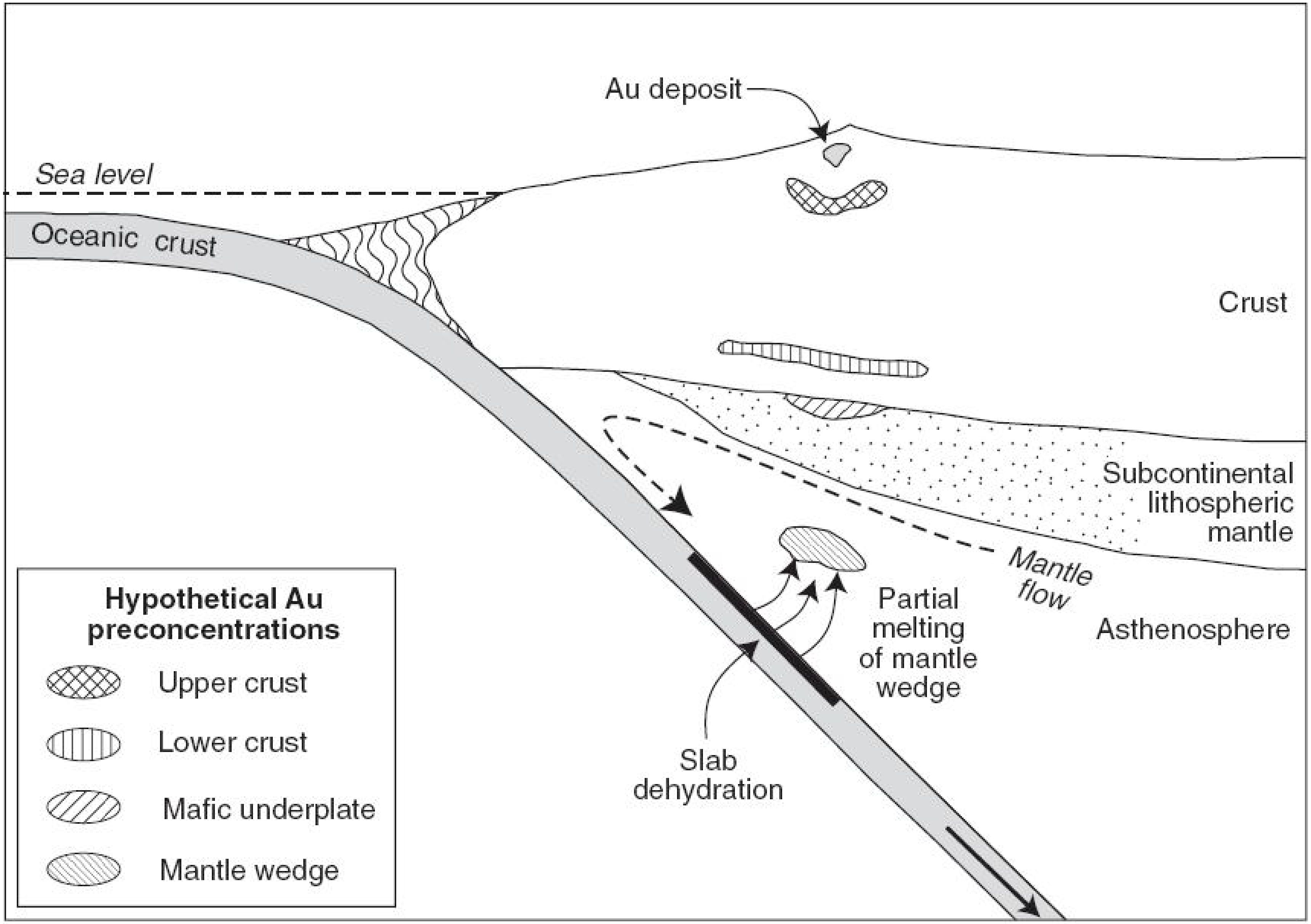

FIG. 11. Cartoon section of a convergent margin to show possible sites of gold (or other metal) concentrations that may be tapped during the magmatism or transcrustal fluid flow responsible for upper-crustal mineralization. Alternatively, another chemical parameter, such as redox state, may influence metal availability. See text for further discussion.

Wallrock alteration in epithermal deposits

Quartz-alunite / high sulfidation deposits

Adularia-sericite / low sulfidation deposits

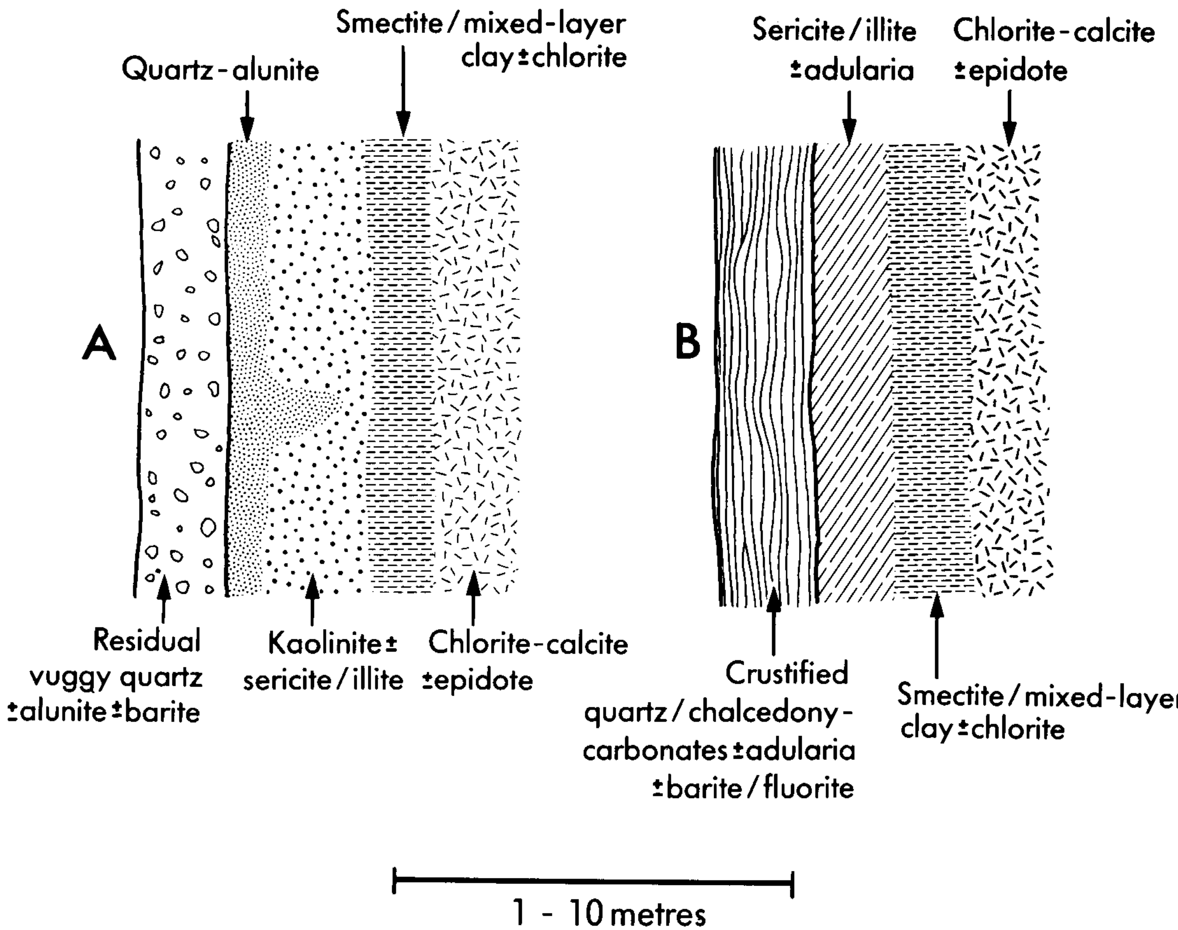

Types of silicic alteration & veining in epithermal deposits

Type	Formation	Where?	Significance	Metals	LS or HS
Sinter	From near-neutral pH hot springs	Only at surface	Paleosurface, topographic (hydrologic) depression, focus of upflow	Var. As, Sb, Hg, Tl (Au, Ag if flared vent)	LS only
Residual silica (opaline)	Moderate leaching, pH ~2–3, 80–90% SiO_2	In vadose zone	Steam-heated origin, above paleowater table	Hg, unless overprint	LS or HS
Chalcedony horizon	Silica remobilized from steam-heated zone; deep fluid may contribute to outflow	At water table, up to 1–2+ km from source	Paleowater table, may be distal from source	Hg if only steam-heated, As, Sb, Au, Ag if deep fluid	LS or HS
Chalcedony veins, colloform bands; crypto-crystalline veins	From low-T fluid, colloids; recrystallized from gel	Shallow depth, <150 m	<200°C, rapidly cooling fluid, boiling at depth; cryptocrystalline at ~200°C	As, Sb, Se, Au, Ag	LS or late HS
Quartz veins, vugs	From cooling solution	>150 m depth	>200°C	Au, Ag, base metals	LS, late HS
Residual silica (vuggy quartz)	Extreme leaching at pH <2, >95% SiO_2	Core of volcanic-hydrothermal system	Permeable core, principal host to high-sulfidation ore	Barren, or Cu, As, Au, Ag	HS only
Silicification	From cooling water	Surface to 500 m, massive <150 m depth	Shallow portion of system, pervasive flow	Trace Au, Ag	LS, mid to late HS

Abbreviations: LS = low sulfidation, HS = high sulfidation

Hedenquist et al. (2000)

Relation between volcanic-hosted epithermal and sub-volcanic types of mineralization

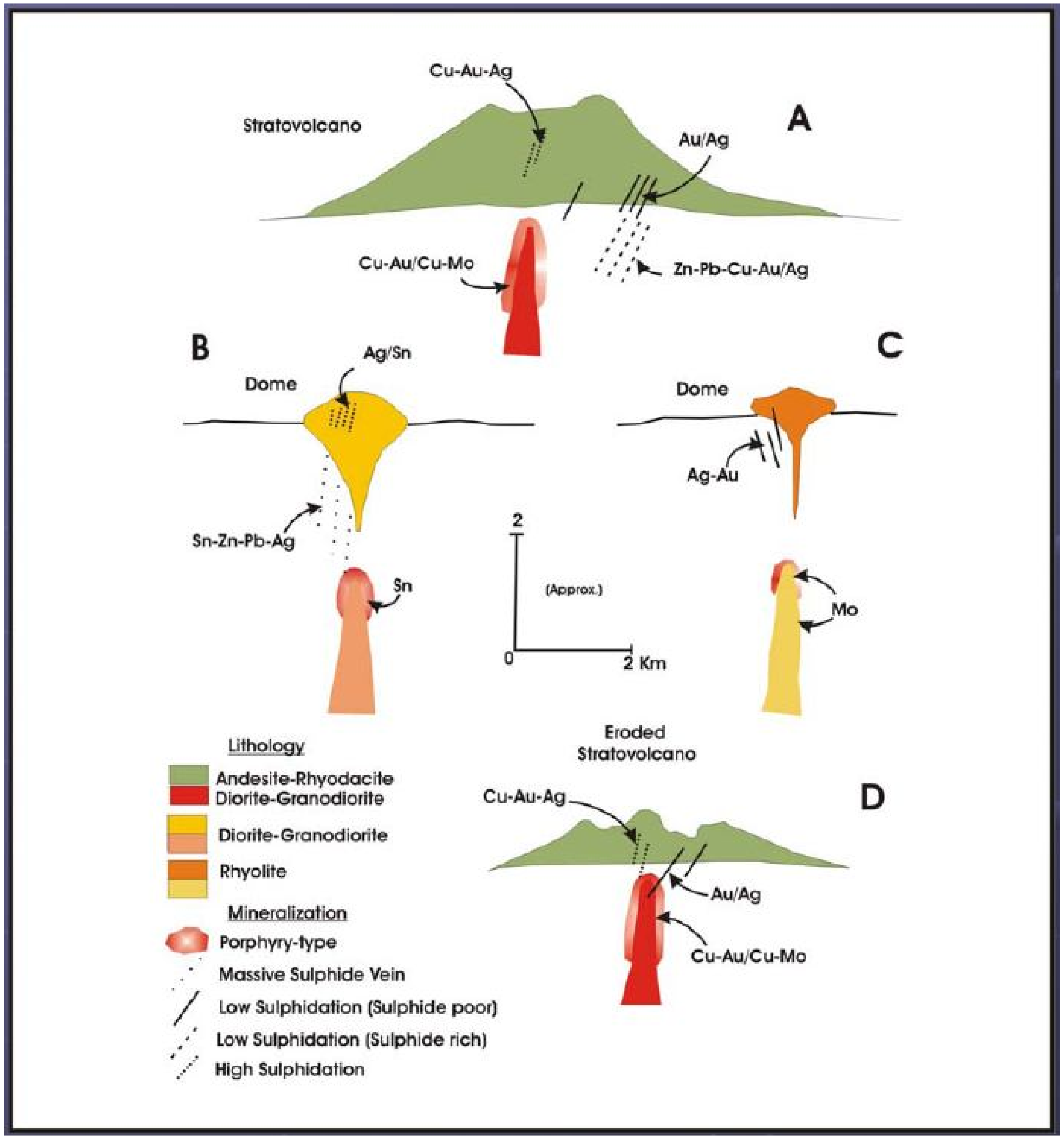

Styles and geometries of epithermal deposits illustrating the influence of structural, hydrothermal and lithologic controls on permeability, i.e., fluid conduits (Sillitoe, 1993)

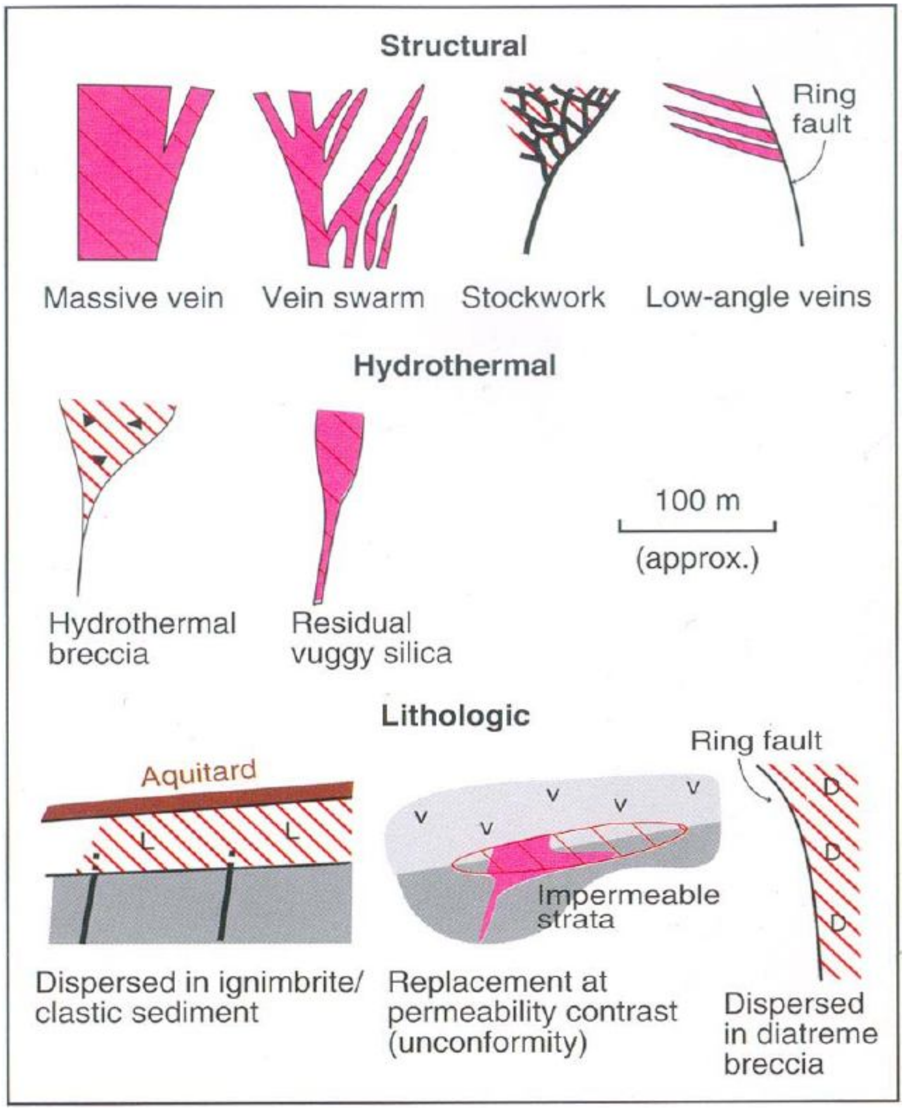

Lithological control in epithermal deposits

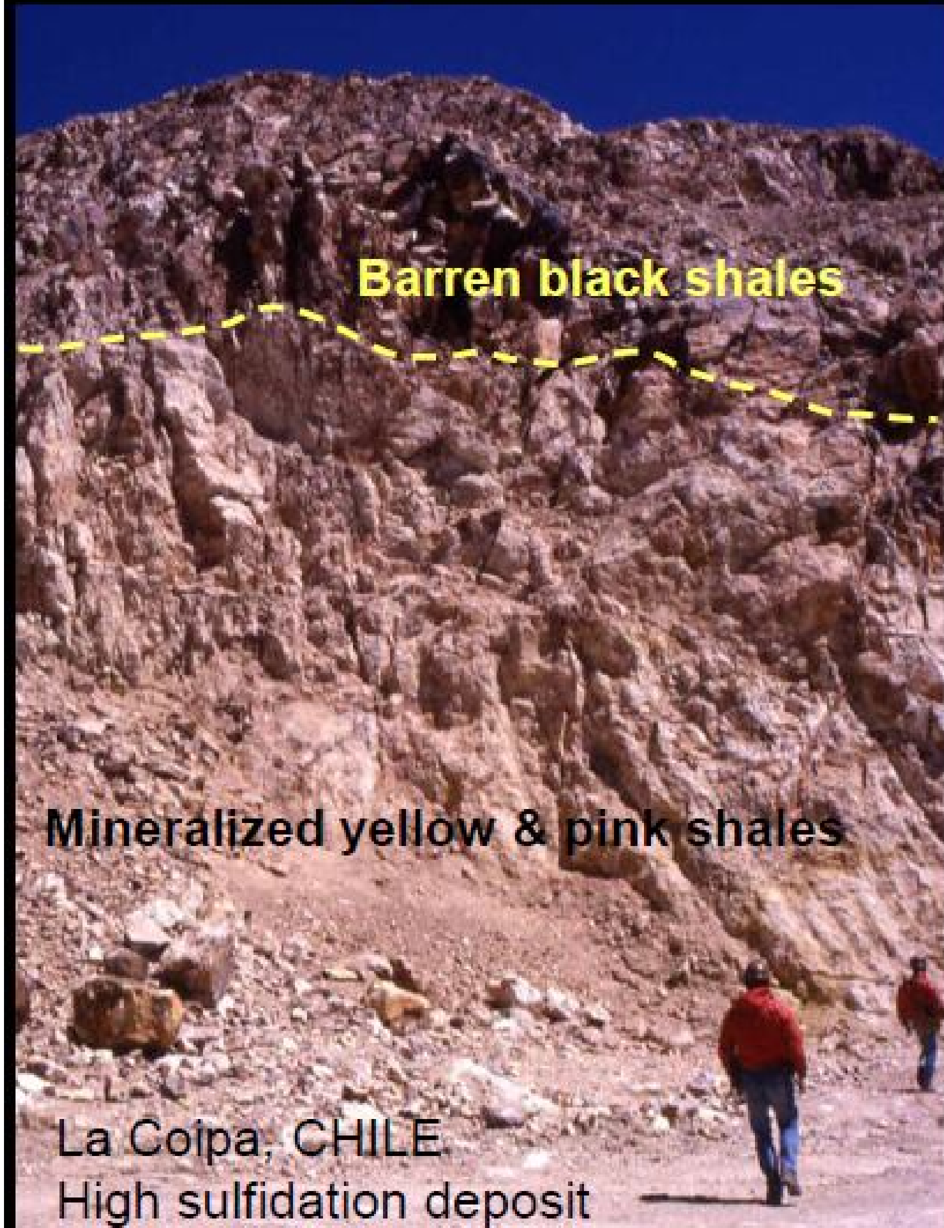

Bedding-controlled alunite replacement in shale

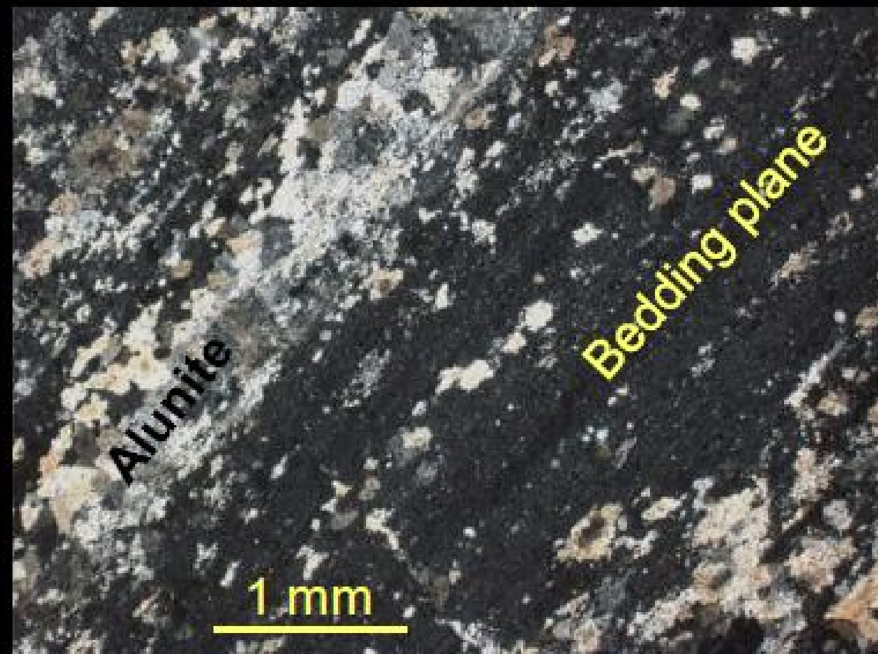

Fluid salinities in epithermal deposits

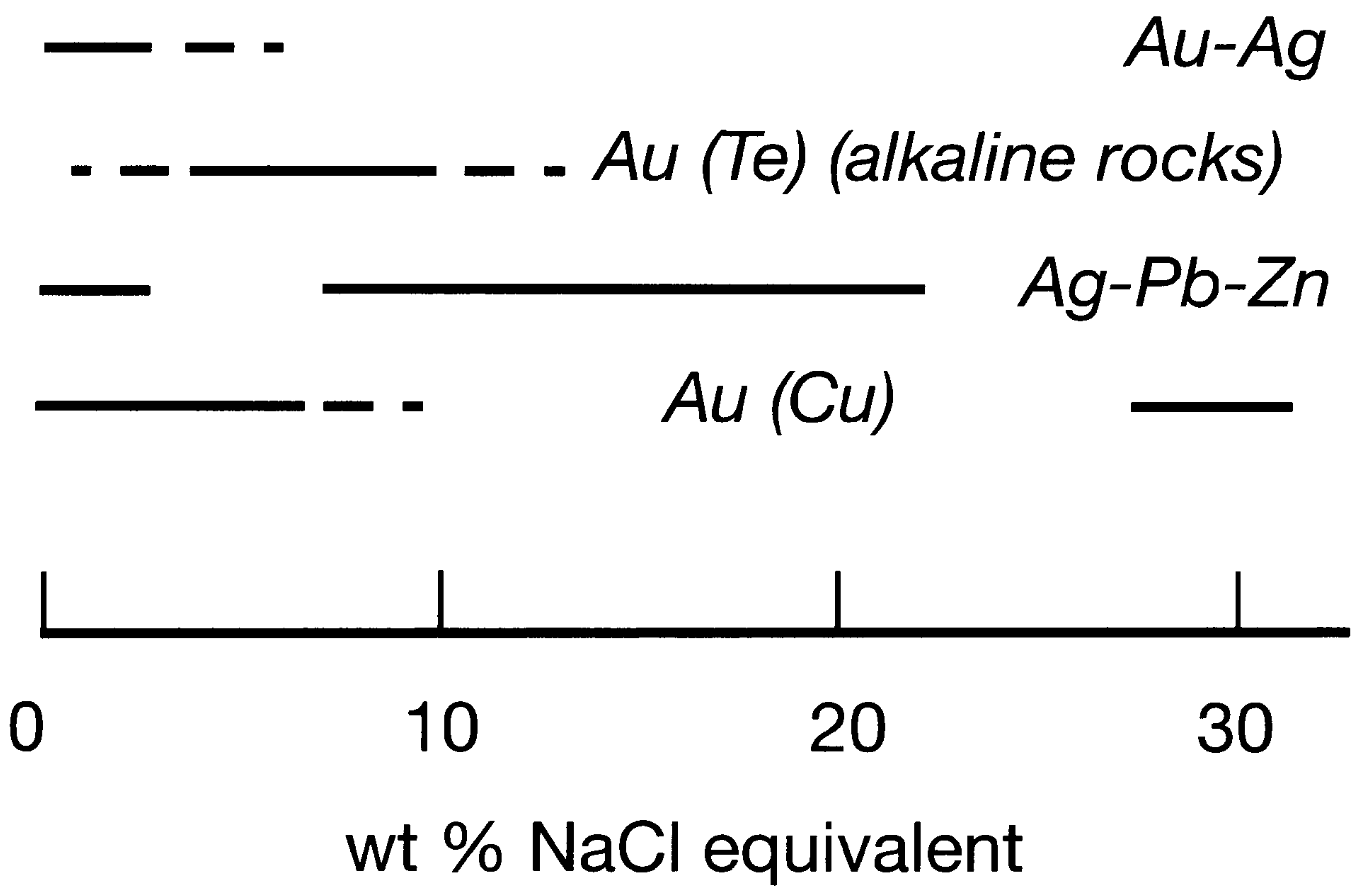

Simmons et al. (2005)

KEY CHARACTERISTICS OF EPITHERMAL DEPOSITS

Deposits classified as epithermal show a wide range of characteristics, including their **tectonic setting**,

character of host rocks, **deposit form**, **mineralogy of ore and gangue**, **hydrothermal alteration** , **assemblage and zoning**, and **ore fluid chemistry**, **temperature** and **pressure** (White and Hedenquist, 1995).

The key characteristics that allow a **simple classification** of epithermal deposits are:

1) the redox state of the ore-forming fluid

2) the metal assemblage of the deposit

- ***Noel C. White and Vincent Poizat*** BHP Minerals International Exploration, Brook House, 229 Shepherds Bush Road, London

C. PUDACK, W. E. HALTER, C. A. HEINRICH, AND T. PETTKE, 2009

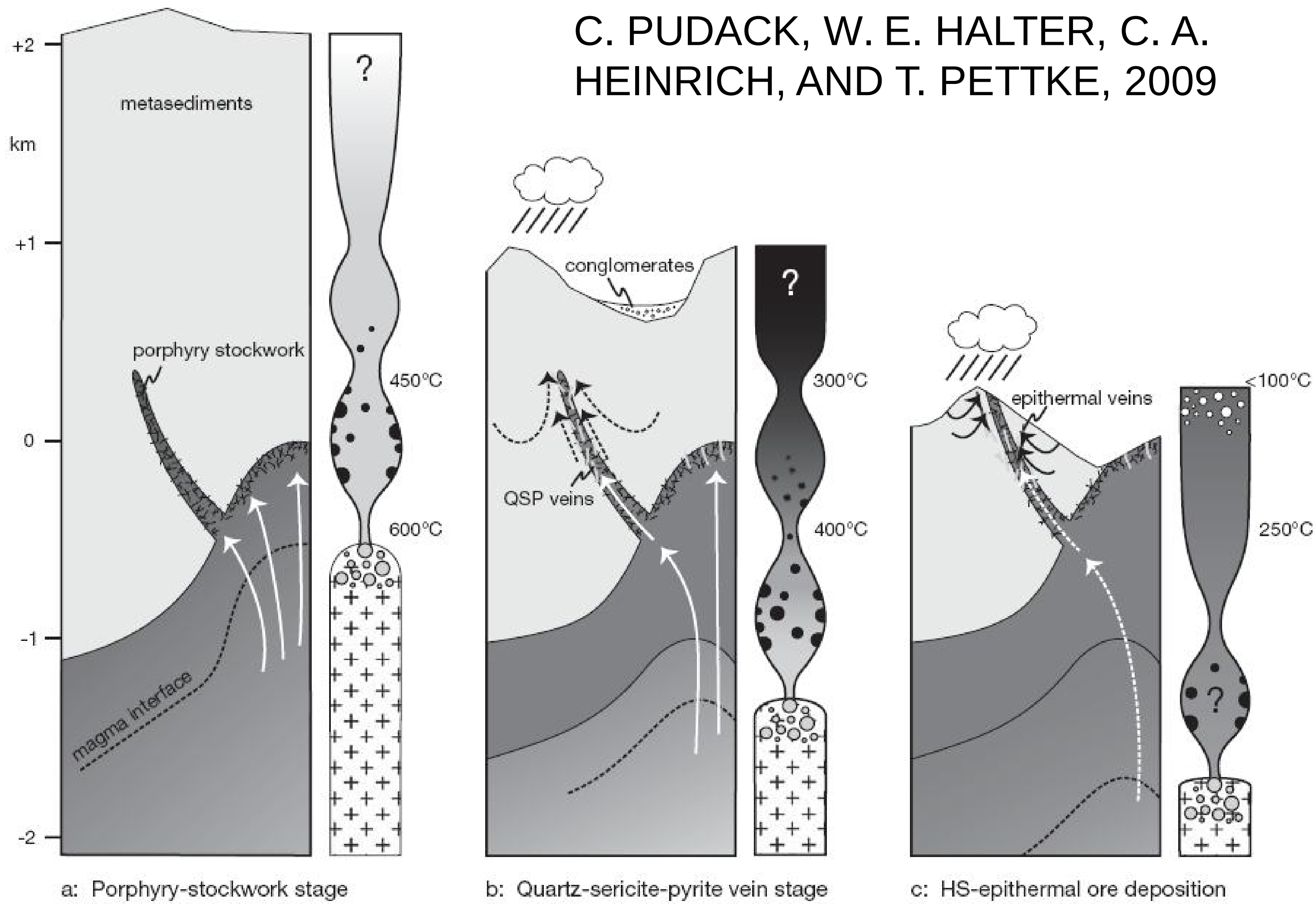

FIG. 11. Schematic cross sections through the Famatina Cu-Mo-Au system, illustrating the inferred fluid evolution paths from the deep porphyry setting (a) through the transitional QSP stage (b) to the shallow high-sulfidation epithermal environment (c), based on continued ascent of magmatic-hydrothermal fluid in a progressively cooling and eroding hydrothermal system. White arrows indicate the source fluid exsolving from a crystallizing magma at progressively greater depth. Black arrows highlight the progressive input of meteoric water. Fluid columns ("chimneys") to the right of each cartoon section schematically illustrate the evolving phase state of the single- and two-phase fluids along their upflow path. Fluids are shaded to denote the fluid density, varying between low-density vapor (white) and dense liquids of various salinities (black). Note that the vaporlike fluid in b and c evolves, through contraction, to become more dense on ascent and cooling, and thus liquid-like at epithermal depths (in contrast to the high-temperature vapor discharge at the surface in a). Constrictions denote confined permeability, which are likely to lead to pressure fluctuations between lithostatic conditions at the magmatic interface, and pressures that are increasingly controlled by the density of the fluid phase where veins are open to the eroding surface, i.e., hydrostatic (or vaporstatic) conditions.

Low-sulfidation styles

1. Low-sulfidation gold-silver deposits

Associated with calc-alkaline volcanic rocks :

-They are typically vein deposits with at most **minor amounts of associated base metals**;

- usually gold and silver are the only economic metals.
- The **veins** are dominated by q**uartz** or **chalcedony and calcite**, usually with a**dularia**, and show a great diversity of textures.
- The veins typically have an extensive envelope of hydrothermal alteration produced by **neutral-pH** mineralising fluids: i.e. pervasive **propylitic** alteration, with the veins surrounded by s**ericitic** alteration, then i**llite-smectite** alteration at shallow levels.
- They are also found in parts of the **central Asian Tethys** belt. A sub-style of these deposits was distinguished by Sillitoe (1993)
- they occur with high-silica **rhyolites** of probable A-type, and are rich in molybdenum and fluorite.

Adularia-sericite / low sulfidation epithermal deposits

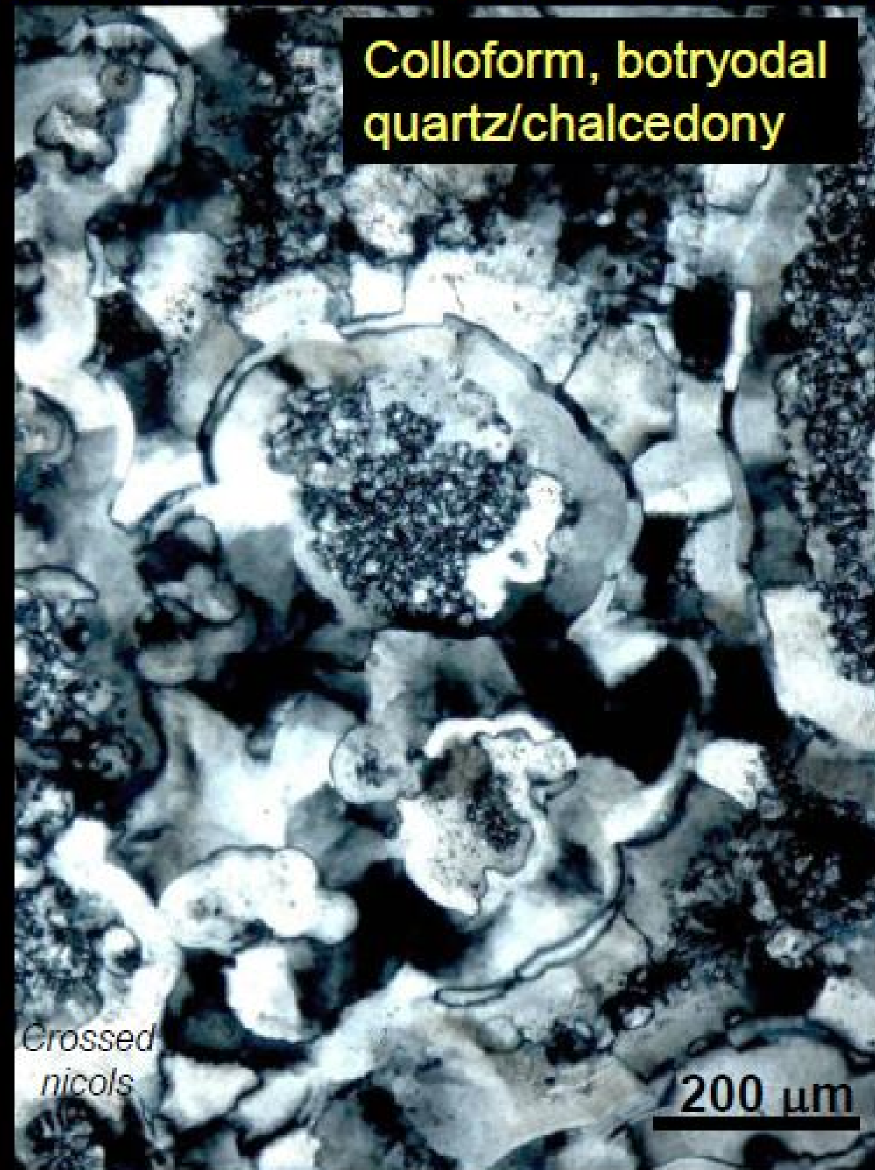

Ovacik, TURKEY

Adularia-sericite / low sulfidation epithermal deposits

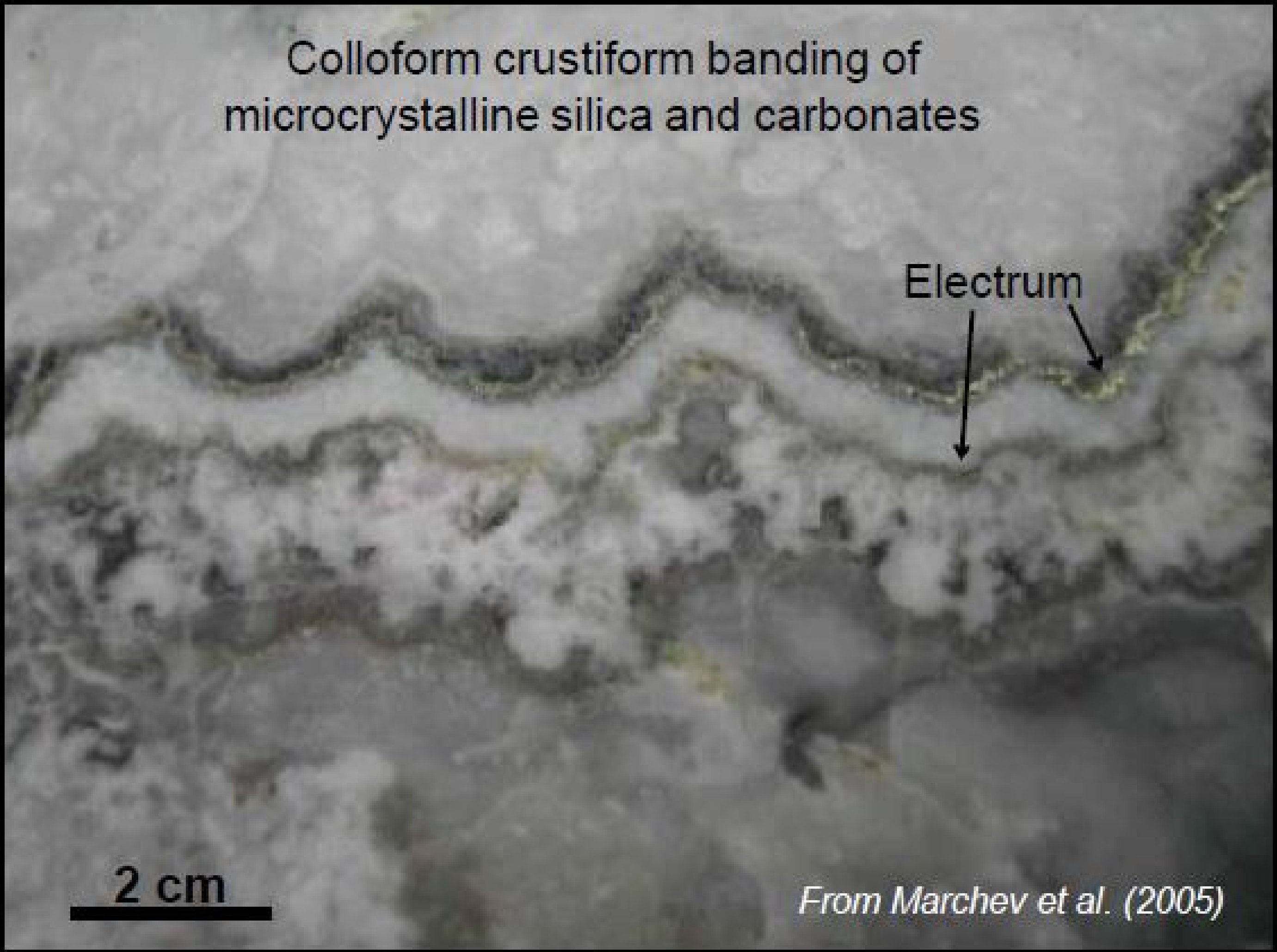

Ada Tepe, BULGARIA

Associated with alkaline igneous rocks :

Deposits of this type (Bonham, 1986) are not very common, but they are economically important.

The best examples are Cripple Creek (USA), Porgera and Ladolam (Papua New Guinea), and Emperor (Fiji).

In most respects they resemble the low sulfidation gold-silver deposits associated with calc-alkaline volcanic rocks **except**:

i) they tend to be unusually large and rich

ii) they are associated with potassium-rich alkaline volcanic and/or intrusive rocks

iii) they are commonly related to alkaline (or shoshonitic) porphyry copper Systems

iv) they may show relatively **narrow** and restricted hydrothermal alteration zones

v) they show evidence of the involvement of a late-stage magmatic fluid in ore-forming processes

vi) they are **tellurium-rich** (other epithermal gold-silver deposits typically have selenium » tellurium).

2. Low-sulfidation silver-gold-base metal deposits

- They show many of the textural and alteration characteristics of gold-silver deposits, but are **usually dominated by** Ag, Pb and Zn mineralisation.
- Au may be present, but is typically (though not always) much less significant than silver.
- Cu may be significant at deeper levels.
- Mn carbonates are common as gangue, and adularia and fluorite may be present
- *These deposits commonly* extend **much deeper** than low sulfidation gold-silver deposits, and to higher paleotemperatures.
- In some cases there may be an increase in tin minerals at greater depths.

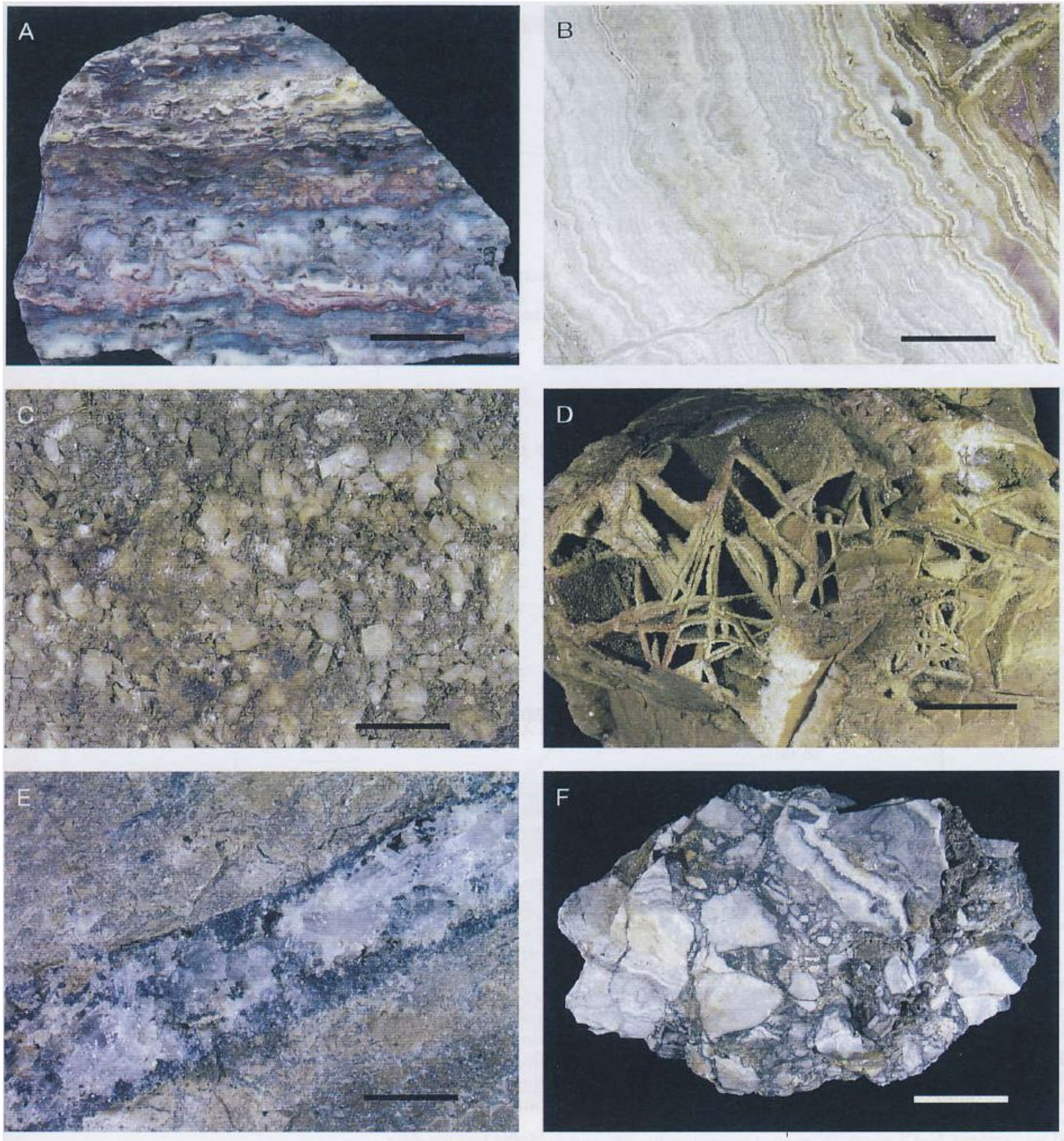

FIG. 6. Photographs of minerals and textures that commonly occur in epithermal deposits associated with quartz ± calcite ± adularia ± illite: A. Cinnabar-bearing silica sinter (Puhipuhi, New Zealand; scale bar = 2 cm). B. Colloform crustiform banding in gold-silver–bearing ore (Martha Hill, New Zealand; scale bar = 2 cm). C. Adularia encrusted on open fracture (Martha Hill, New Zealand; scale bar = 1 cm). D. Lattice textures in which platy calcite is replaced by quartz in gold-silver–bearing ore (Martha Hill, New Zealand; scale bar = 3 cm). E. Vein containing coarsely crystalline quartz, sphalerite, and galena (Pachuca-Real del Monte, Mexico; scale bar = 1.25 cm). F. Brecciated vein material in gold-silver–bearing ore (Golden Cross, New Zealand; scale bar = 4 cm).

3. Low-sulfidation tin-silver-base metal deposits

- *They* form at **shallow depth** and are related to **rhyolite** or quartz latite domes.
- The hydrothermal alteration is similar to other low-sulfidation deposits.
- There is a tin-tungsten-bismuth association at greater depths, and lateral zoning to base metal-rich mineralisation (Smirnov *et al, 1983; Nakamura and Hunahashi,*1970).
- The epithermal tin bearing deposits may be of several styles, rather than the one style described here.

Boiling is the critical process to deposit high concentration of Au in LS epithermal deposits

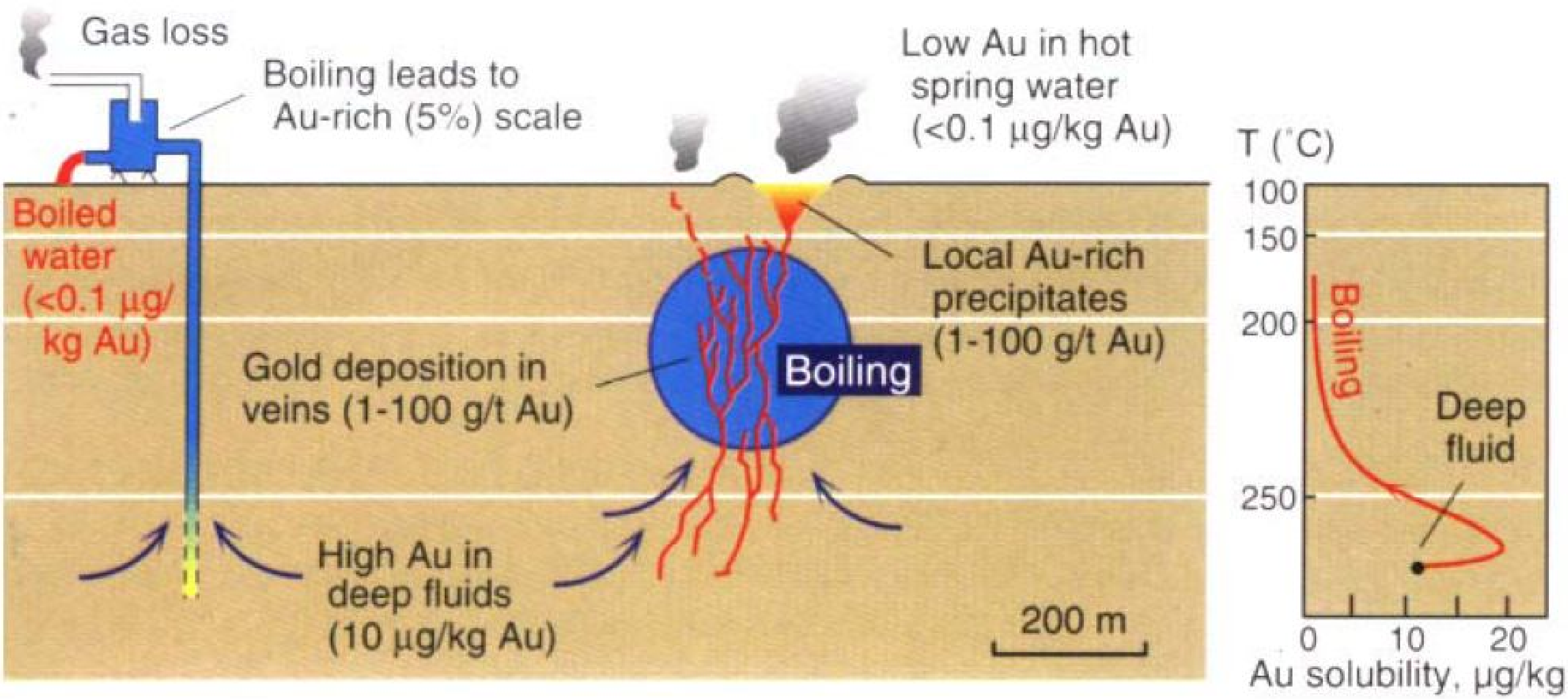

Mechanisms of Au deposition have a profound effect upon Au grade varying from:

- **Cooling** in the case of many coarse sulphides with low grade Au contents.
- **Rapid cooling** promoted by quenched magmatic fluids evidenced by fine sulphides, or by mixing of ore fluids with deep circulating meteoric waters, commonly recognised in high precious metal polymetallic vein deposits where low temperature quartz (opal) is in contact with high temperature sulphides.
- While **boiling** fluids deposit much of the gangue (adularia, quartz pseudomorphing platy calcite and local chalcedony), in epithermal veins and some Au other mechanisms are preferred to account for elevated Au grades.
- **Mixing of oxygenated ground waters with ore fluids** at elevated crustal settings produces elevated Au grades and is evidenced by hypogene haematite in the ore assemblage.
- **Mixing of bicarbonate waters derived** from the condensation of CO^2 volatiles released from cooling intrusions is responsible for the development of higher Au grades as the carbonate-base metal group of low sulphidation Au deposits.
- **Mixing of low pH waters**, developed by the condensation of H^2S volatiles above the water table, and responsible for the development of near surficial acid sulphate caps, provide the highest Au grades and is evidenced by the presence of hypogene kaolin including halloysite within the ore assemblage

High-sulfidation styles

High-sulfidation gold-silver-copper deposits can be separated into two different styles on the basis of the associated hydrothermal alteration. Both are disseminated deposits; with a core of intense acidpH hydrothermal alteration that hosts the economic mineralisation.

a) With vuggy quartz alteration (commonly called Nansatsu-style, see Hedenquist *et al, 1994).*

b) With pyrophyllite-sericite alteration

a) With vuggy quartz alteration (commonly called Nansatsu-style, see Hedenquist *et al, 1994).*

they are characterised by a core of intensely acid-leached residual quartz (vuggy quartz - see Hedenquist *et al,*
1994), typically preserving the texture of the original host-rock. This core is commonly in part quartz flooded, producing a massive quartz zone; it also commonly contains alunite. Around the sharp contacts of this quartz±alunite zone there is commonly a very narrow clay-altered margin, which grades out to propylitic alteration
- the gold is always in the siliceous core.
The amount of gold, silver and copper (and other elements) varies widely, even in one mineralised district or cluster of deposits.

b) With pyrophyllite-sericite alteration

In these deposits the core of vuggy quartz (which characterises the Nansatsu deposits) is poorly developed, or may be absent, and instead the core is dominated by **pyrophyllite**.

Recent work on the Peak Hill deposit in New South Wales (Masterman, 1994), showed that the pyrophyllite-rich core grades out through a **zone** with **kaolinite-alunite to sericite, illite-smectite** and finally **propylitic alteration** zones.

The **gold** principally occurs on the margin of the pyrophyllite core.

Strato-volcano and epithermal mineralization

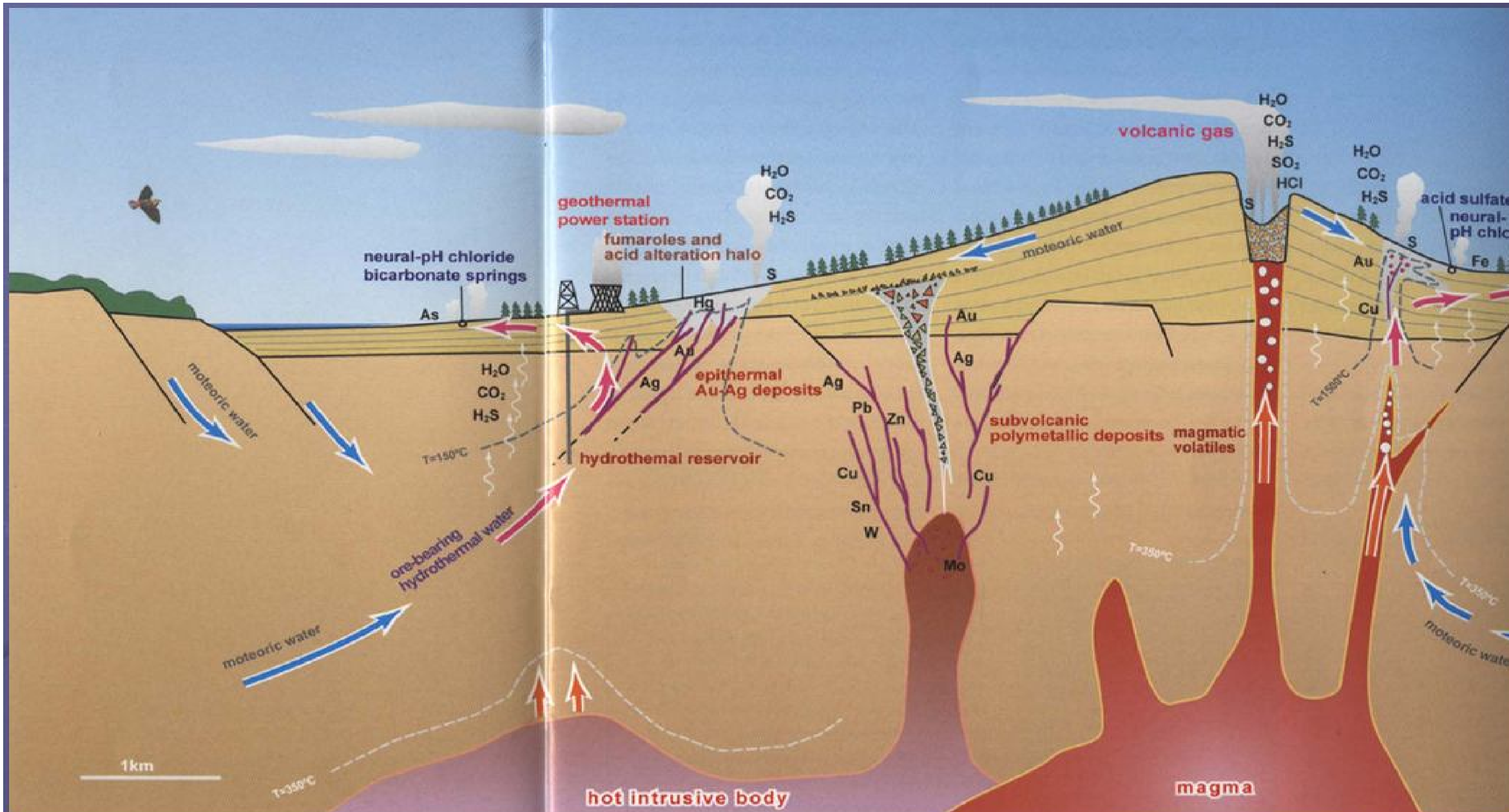

Reduced neutral pH fluids

High oxidation state of acidic hypogene fluids

Typical paragenetic opaque mineral evolution in Quartz-alunite / high sulfidation epithermal deposits

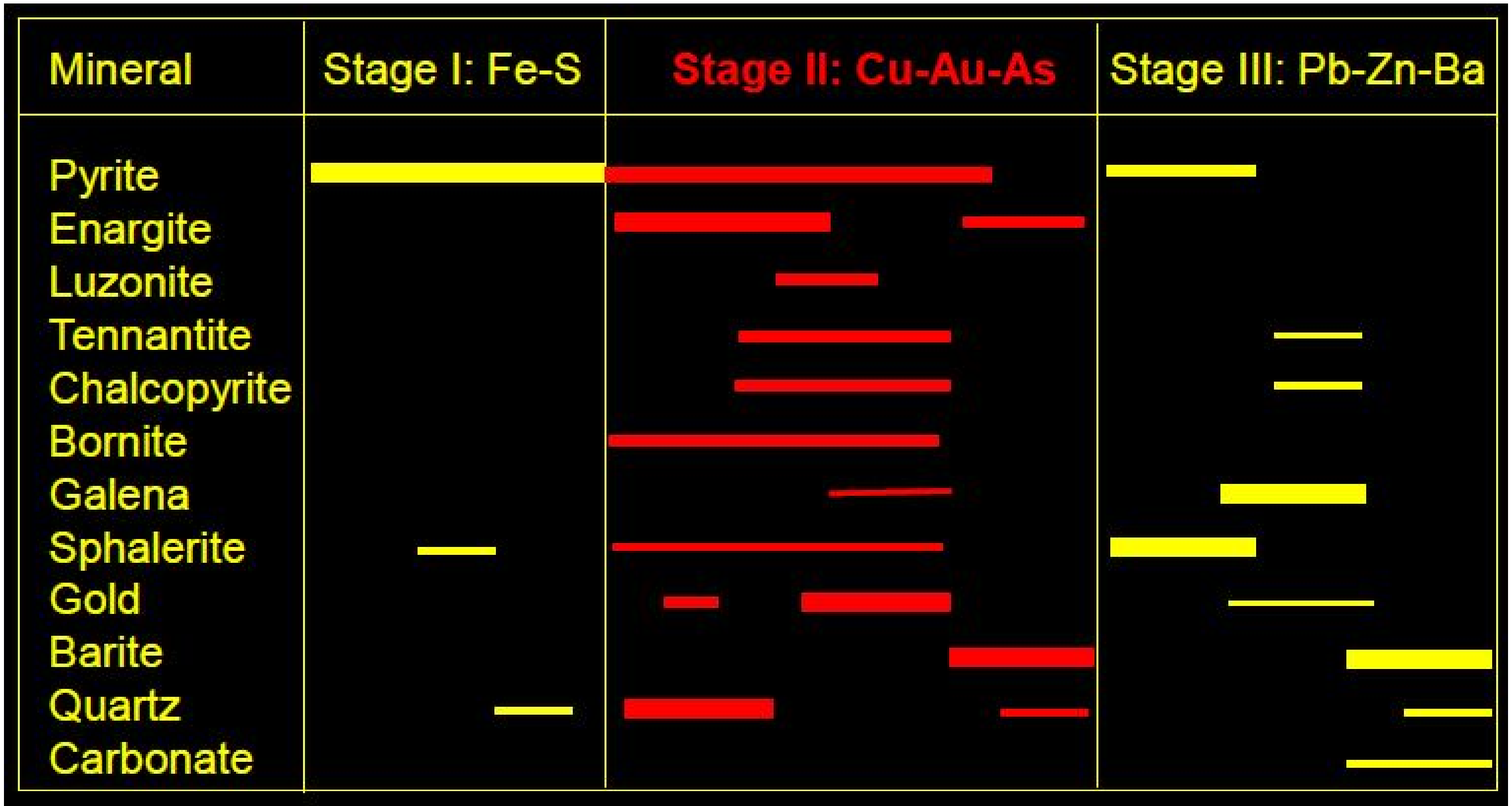

Example of the Chelopech deposit, Bulgaria

(Petrunov, 1989, 1994, 1995; Jacquat, 2003)

Alteration zones in high sulfidation epithermal deposits

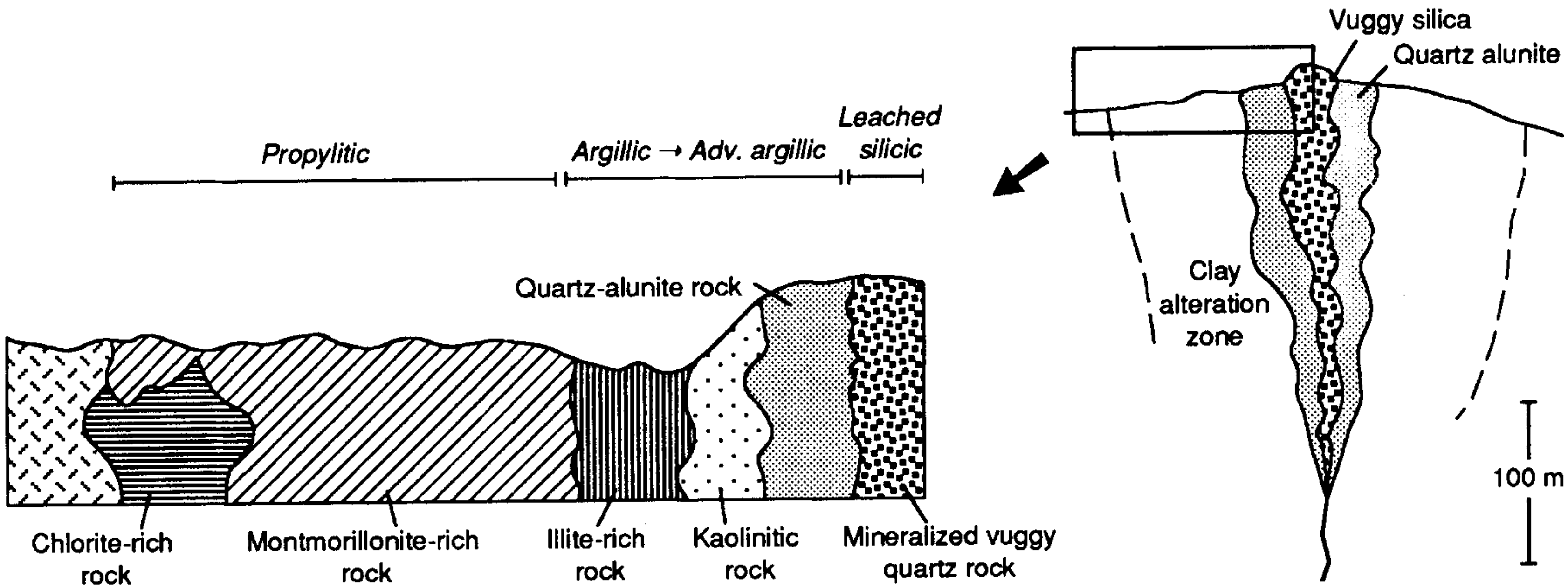

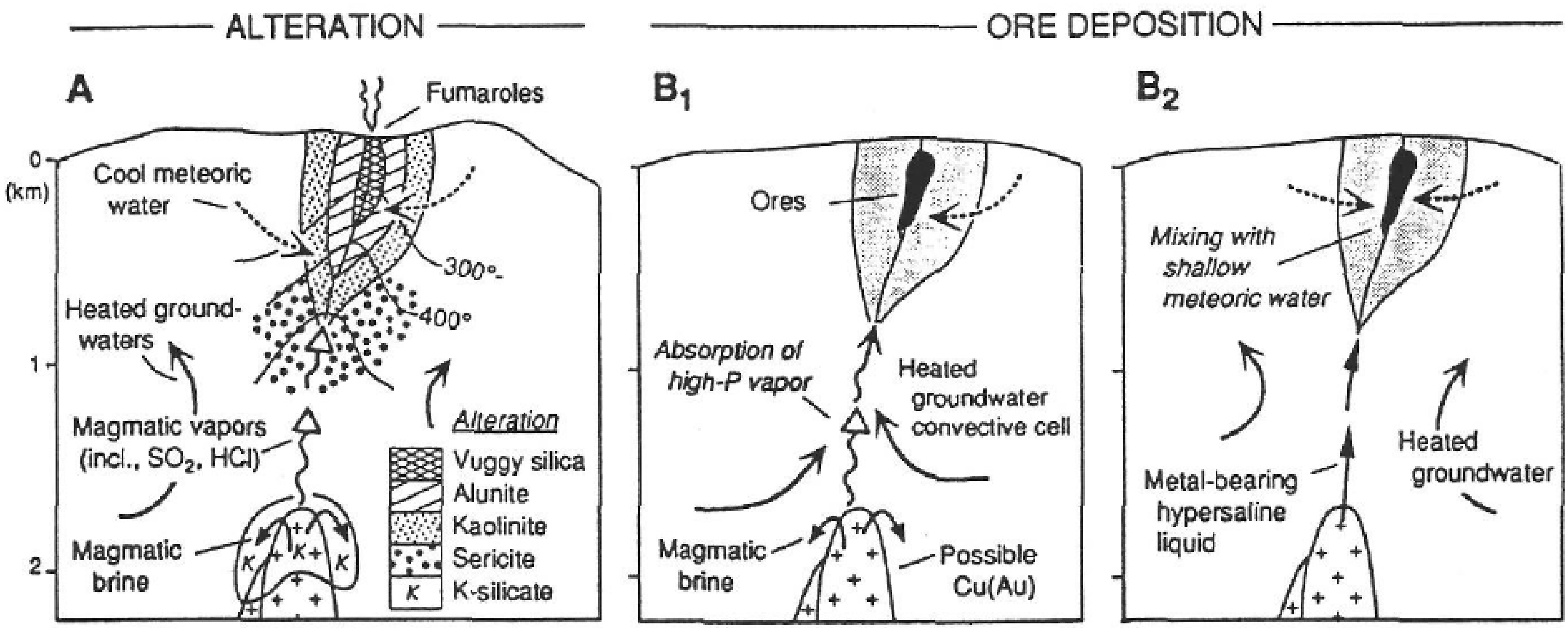

Figure 9. Model showing the two main stages of evolution of HS deposits. **A:** Early stage of advanced argillic alteration dominated by magmatic vapor. **B_1** and **B_2**: Two genetic hypotheses proposed for the stage of ore formation. B_1 = absorption of high-pressure vapor by entrainment in meteoric water cell at depth to explain low-salinity, mixed magmatic–meteoric ore fluid (Hedenquist this volume). B_2 = ascending metal-bearing magmatic brine with shallow cooler meteoric waters to explain high-salinity, mixed magmatic–meteoric ore fluid (White 1991; Rye 1993; Hedenquist *et al.* 1994a).

Acid waters in epithermal systems:
Three environments of advanced argillic alteration

(a) Magmatic-hydrothermal:
>200°C
quartz-tabular alunite-dickite-pyrophyllite-diaspore-zunyite
Cuts across stratigraphy, follows high-angle structures (epigenetic)
Below water table
Magmatic-derived acidic waters

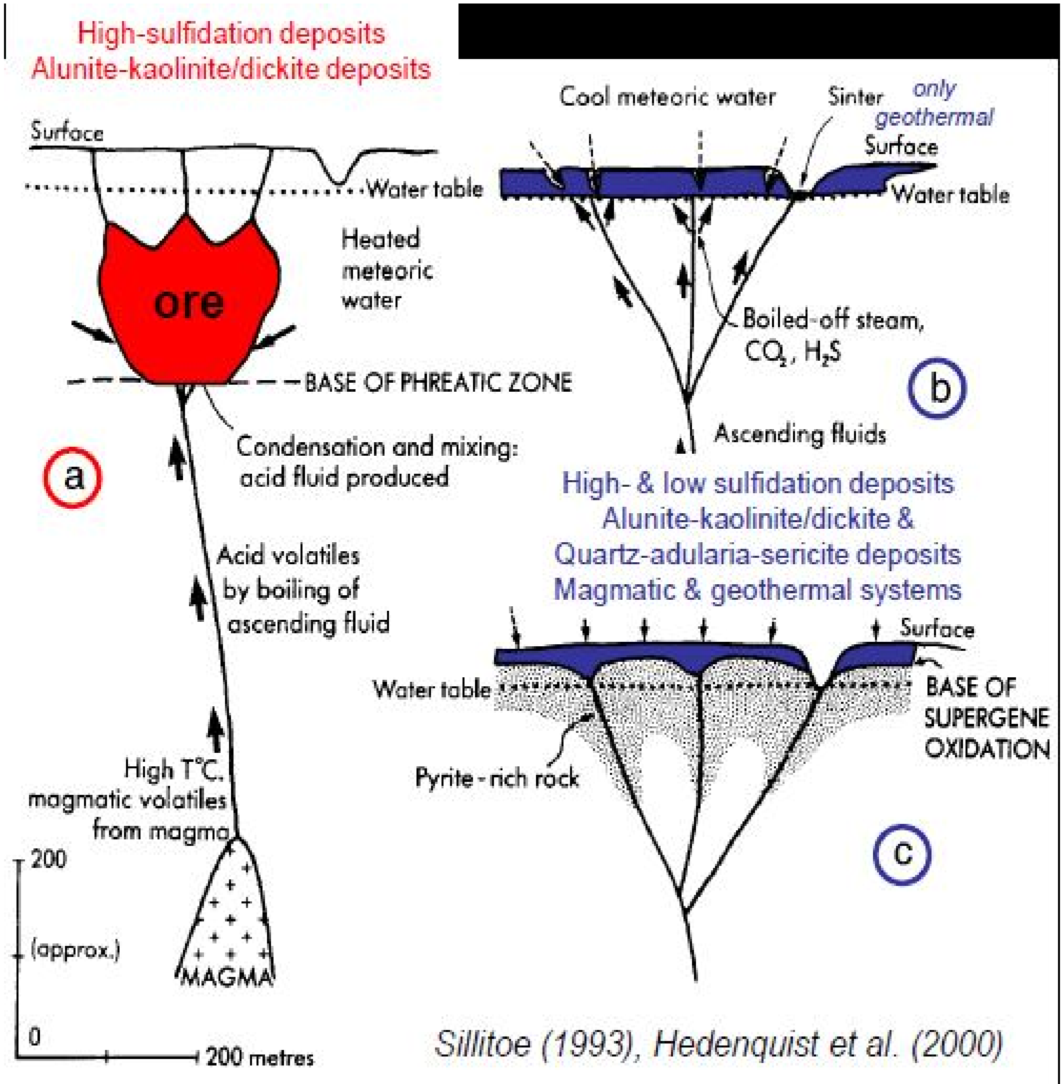

(b) Steam-heated:
Steam-heated:
<120°C
opal-fine grained alunite-kaolinite-pyrite-marcasite
Forms above water table, shallowest environment. Sinter deposits only in geothermal systems.

(c) Supergene:
<40°C
alunite-kaolinite-halloysite-jarosite-Fe oxides
Weathering & oxidation of sulfide-bearing rocks, within vadose zone.

Acid waters in epithermal systems:

Alunite in magmatic-hydrothermal environment of AAA

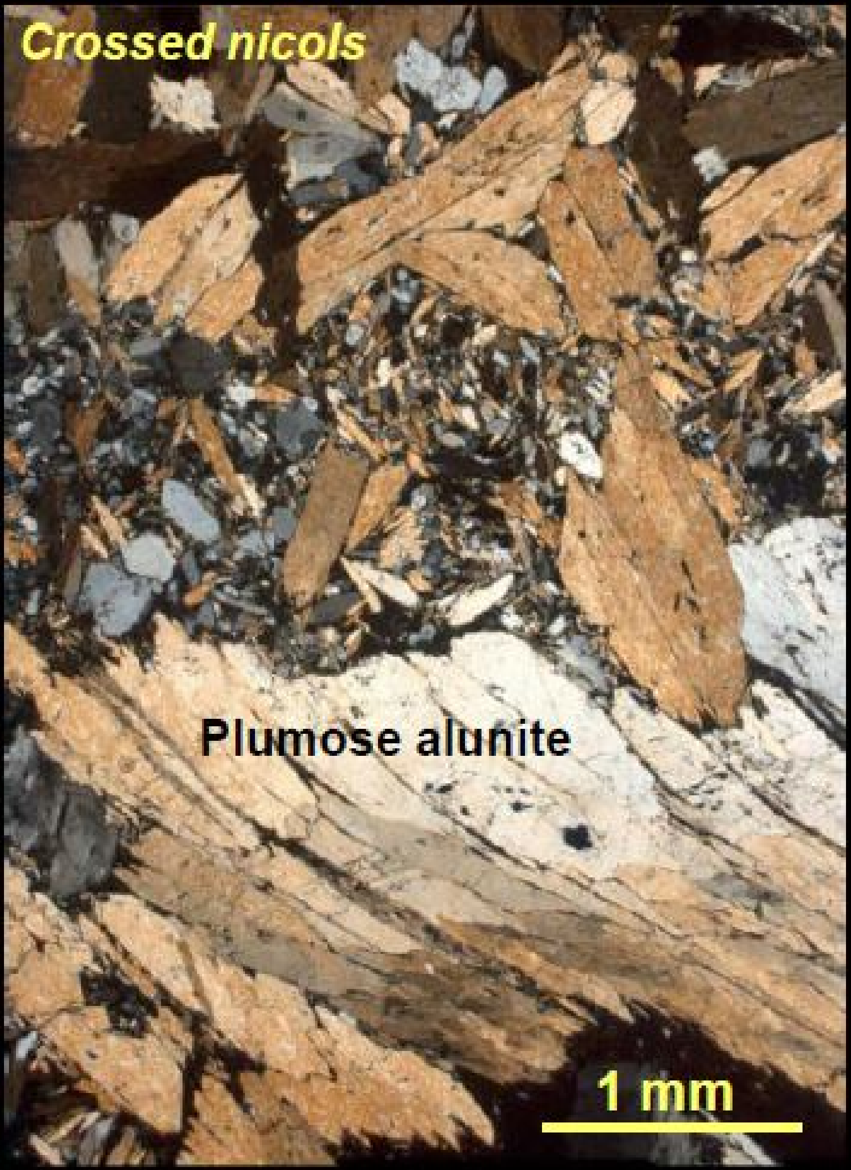

Acid waters in epithermal systems:

Alunite in steam-heated environment of AAA

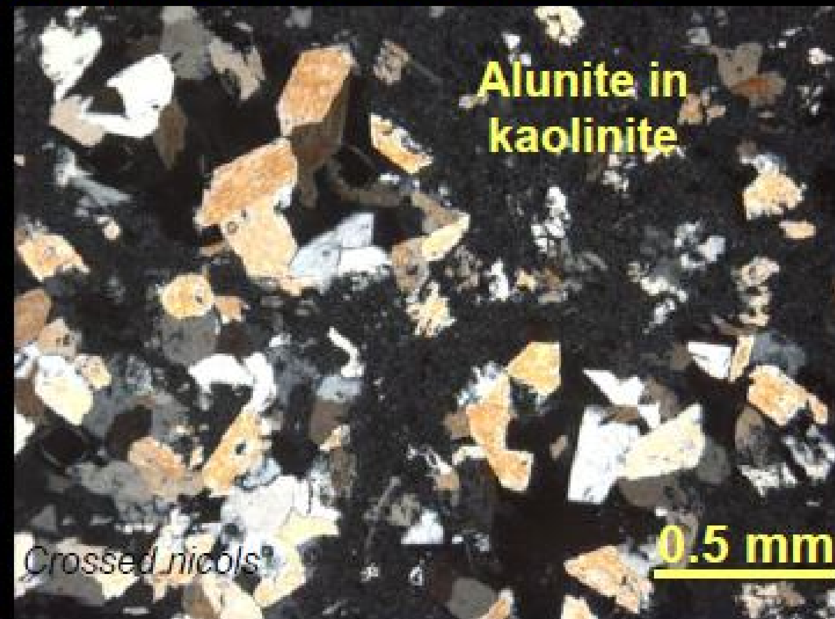

White alunite & kaolinite in a steam-heated zone affecting rhyolite tuff above the water table (Kirally Hill, HUNGARY)

Acid waters in epithermal systems:

Jarosite & alunite in supergene environment of AAA

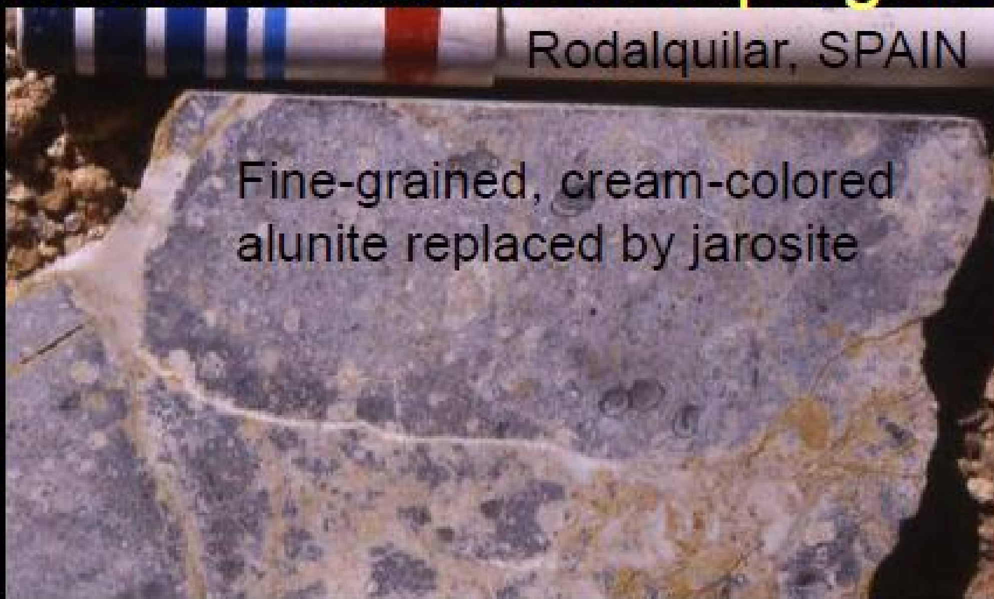

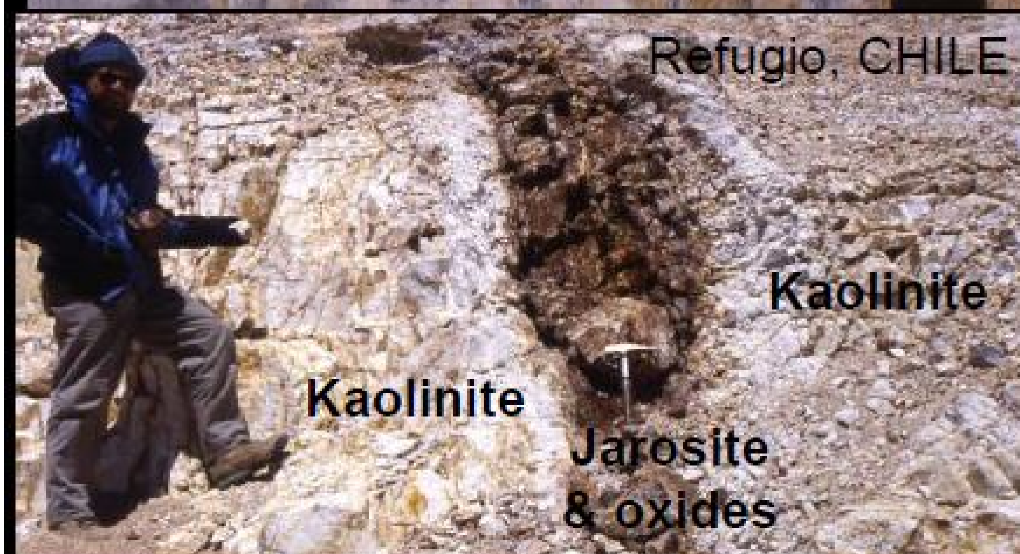

Alteration zones in high sulfidation epithermal deposits

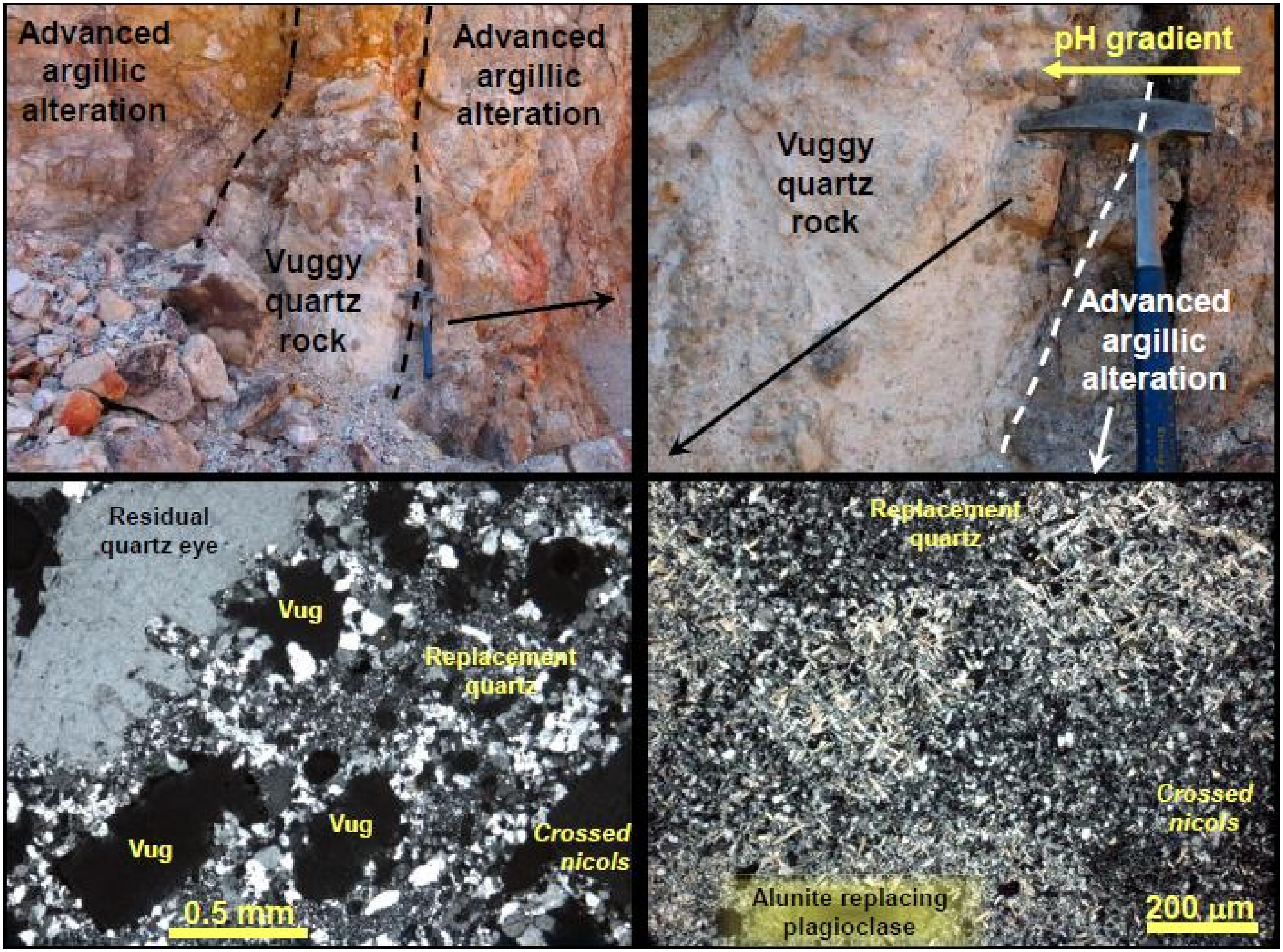

Types of silicic alteration & veining in epithermal deposits

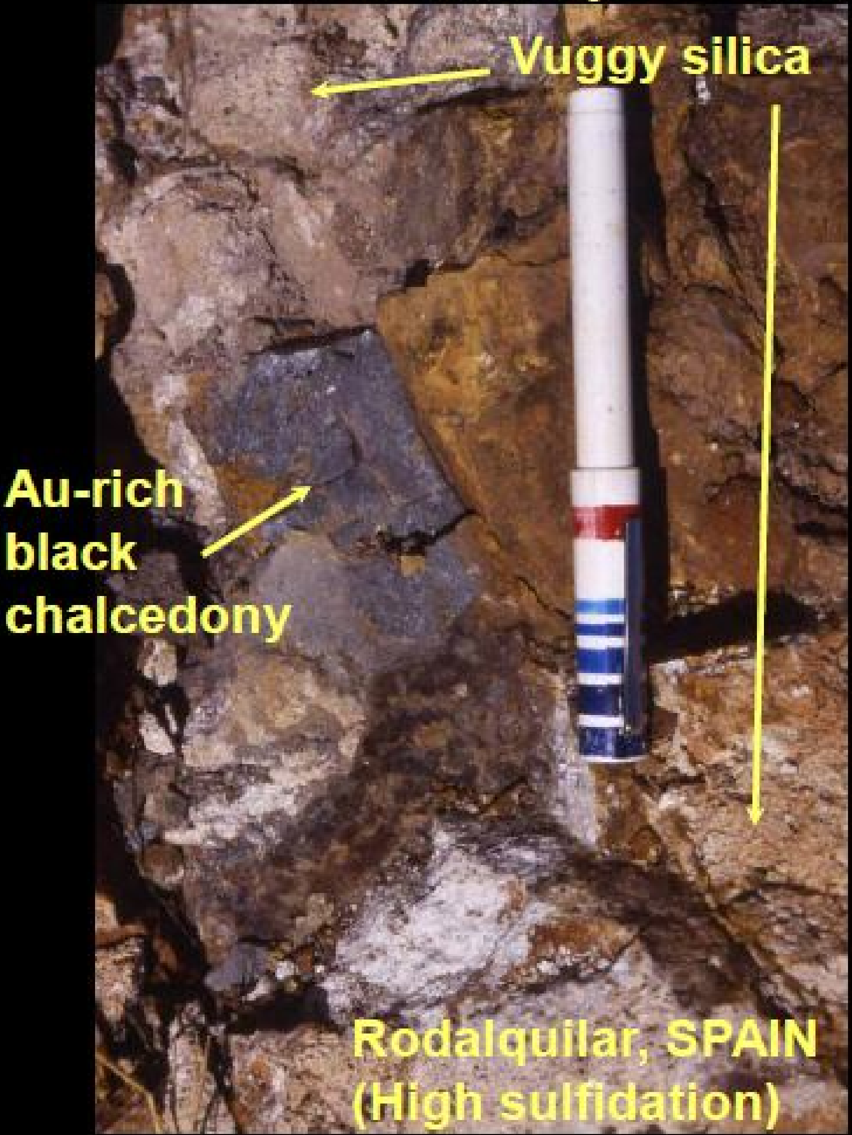

Model for the evolution of HS epithermal ore system ore system

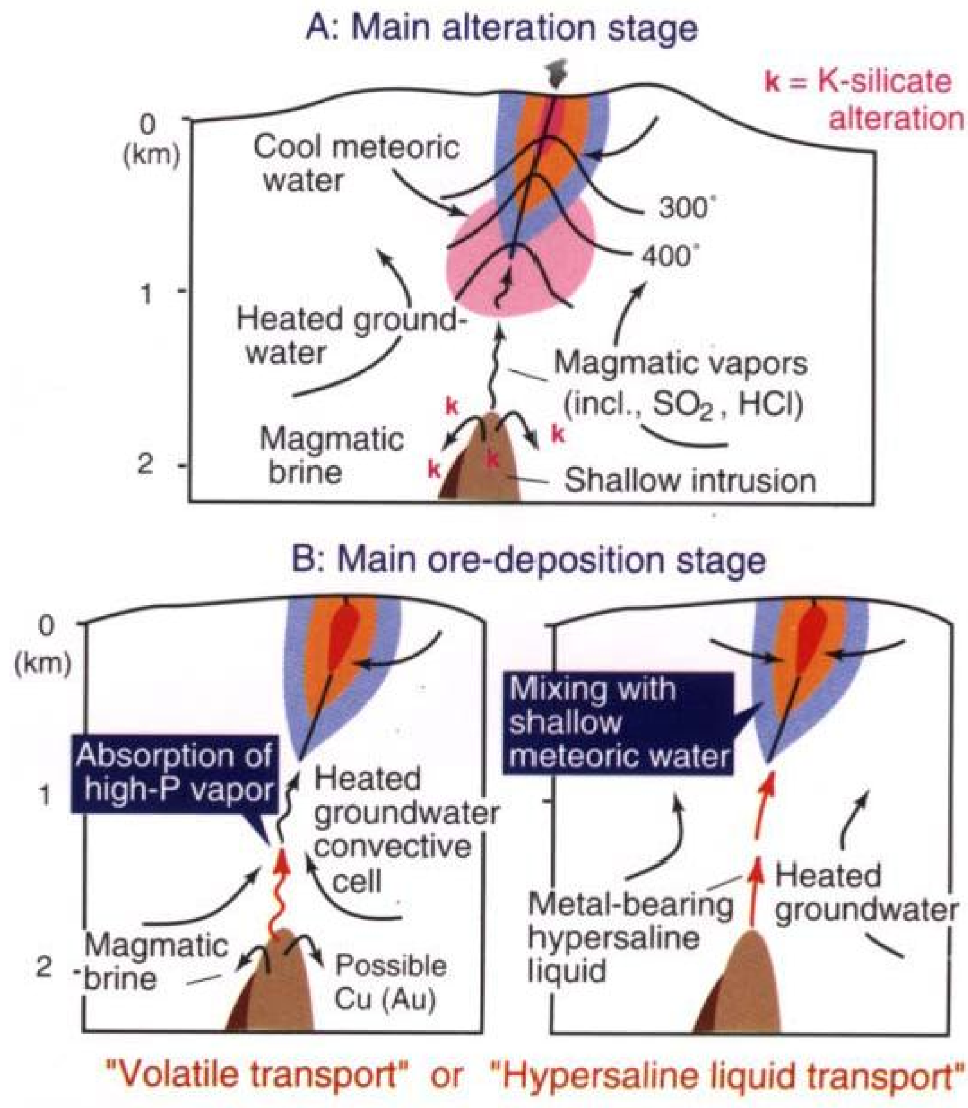

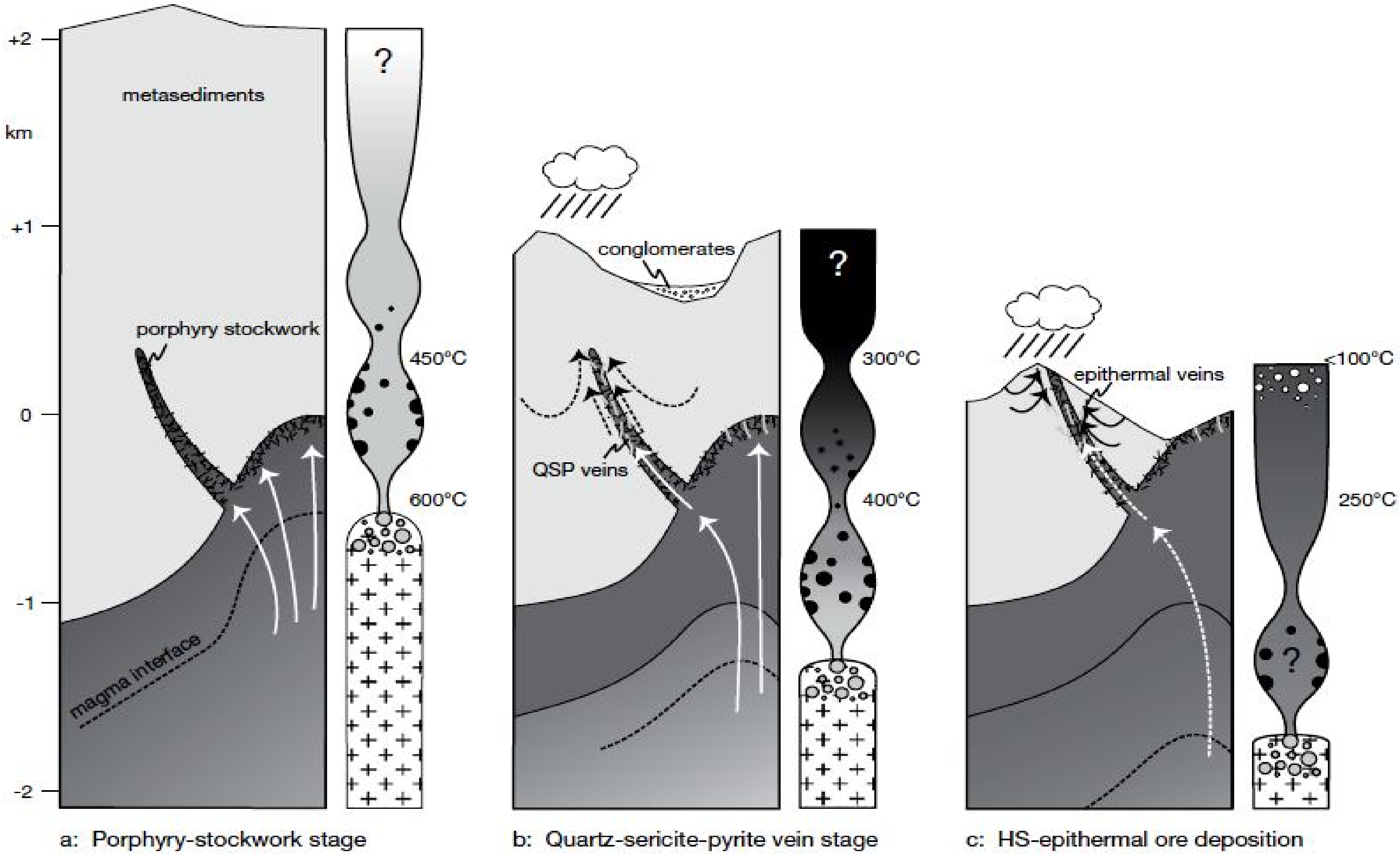

FIG. 11. Schematic cross sections through the Famatina Cu-Mo-Au system, illustrating the inferred fluid evolution paths from the deep porphyry setting (a) through the transitional QSP stage (b) to the shallow high-sulfidation epithermal environment (c), based on continued ascent of magmatic-hydrothermal fluid in a progressively cooling and eroding hydrothermal system. White arrows indicate the source fluid exsolving from a crystallizing magma at progressively greater depth. Black arrows highlight the progressive input of meteoric water. Fluid columns ("chimneys") to the right of each cartoon section schematically illustrate the evolving phase state of the single- and two-phase fluids along their upflow path. Fluids are shaded to denote the fluid density, varying between low-density vapor (white) and dense liquids of various salinities (black). Note that the vaporlike fluid in b and c evolves, through contraction, to become more dense on ascent and cooling, and thus liquid-like at epithermal depths (in contrast to the high-temperature vapor discharge at the surface in a). Constrictions denote confined permeability, which are likely to lead to pressure fluctuations between lithostatic conditions at the magmatic interface, and pressures that are increasingly controlled by the density of the fluid phase where veins are open to the eroding surface, i.e., hydrostatic (or vaporstatic) conditions.

Generalised model of Porphyry and epithermal deposits associated with shallow sub-volcanic intrusions and strato-volcano

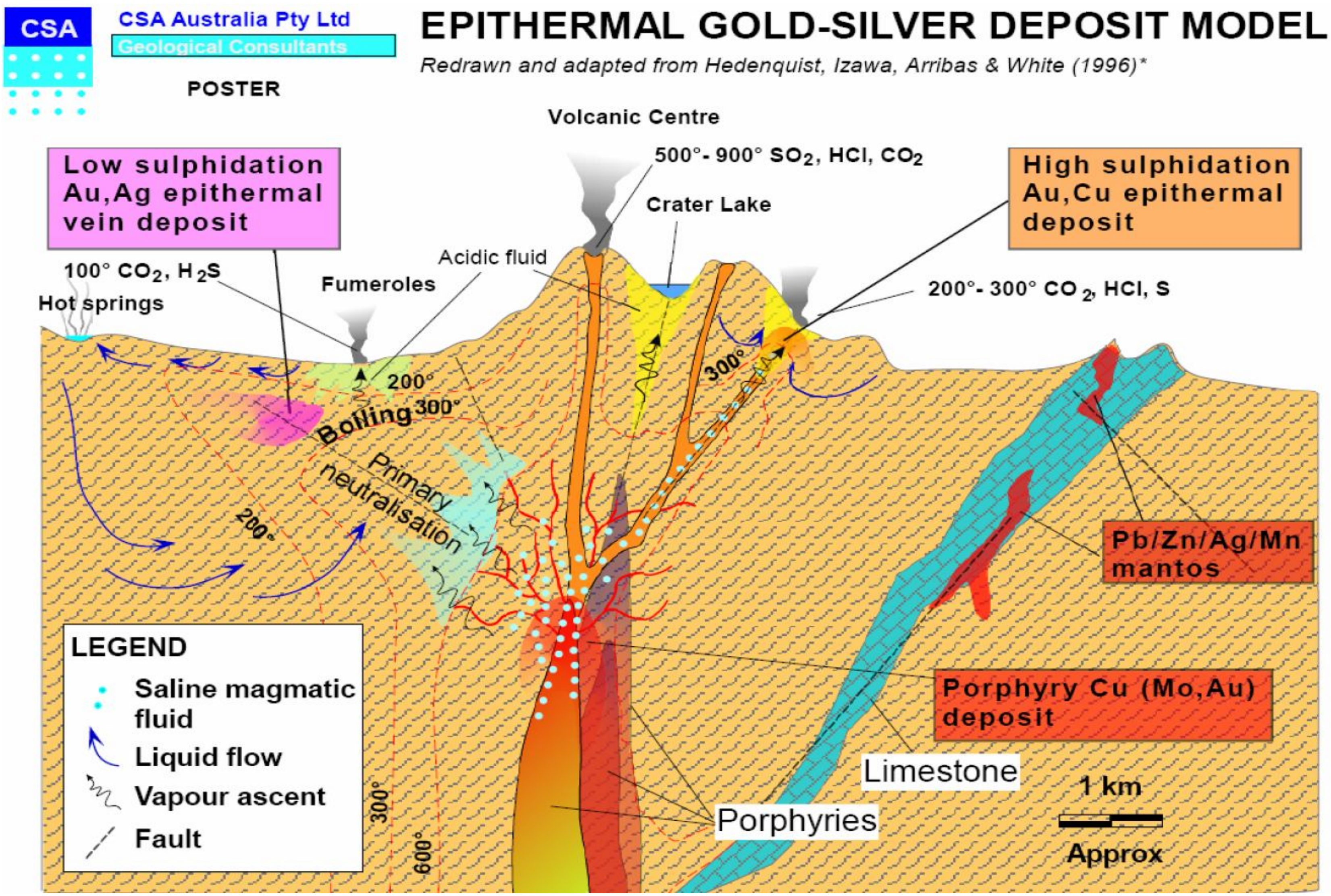

Active volcanic-hydrothermal systemsextends from degassing magma to fumaroles and acidic springs, and incorporate **porphyry and/or high-sulfidationore environments**

Epithermal Au deposits may be found in association with volcanic activity in numerous tectonic settings, including **island-arc volcanoes** (e.g. Papua New Guinea: Sillitoe, 1989), and **continental-based arcs** and **volcanic centres** (e.g. Silverton caldera, Colorado).

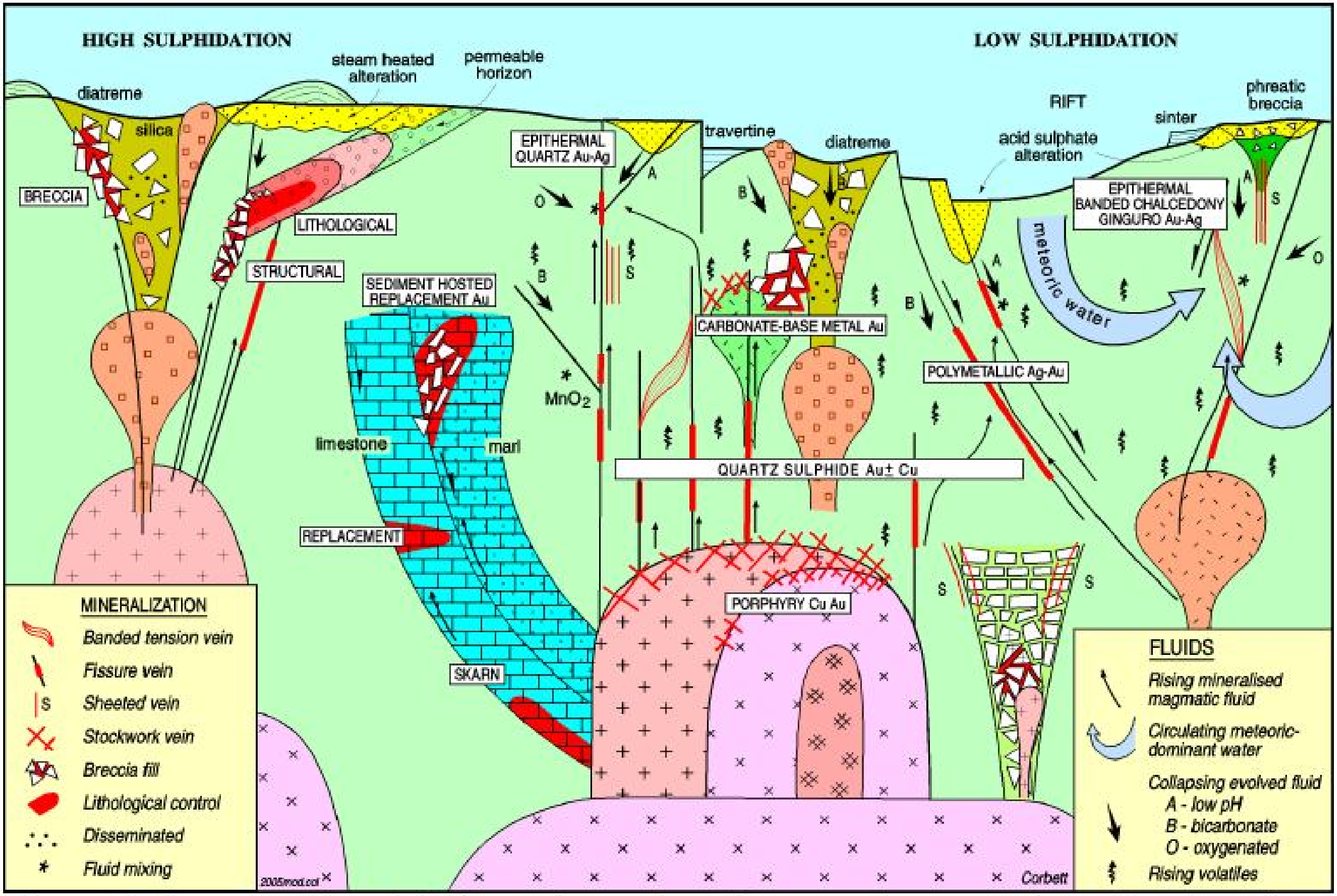

Figure 3. Conceptual model illustrating styles of magmatic arc porphyry Cu-Au and epithermal Au-Ag mineralisation. Geoscience Australia, 2004

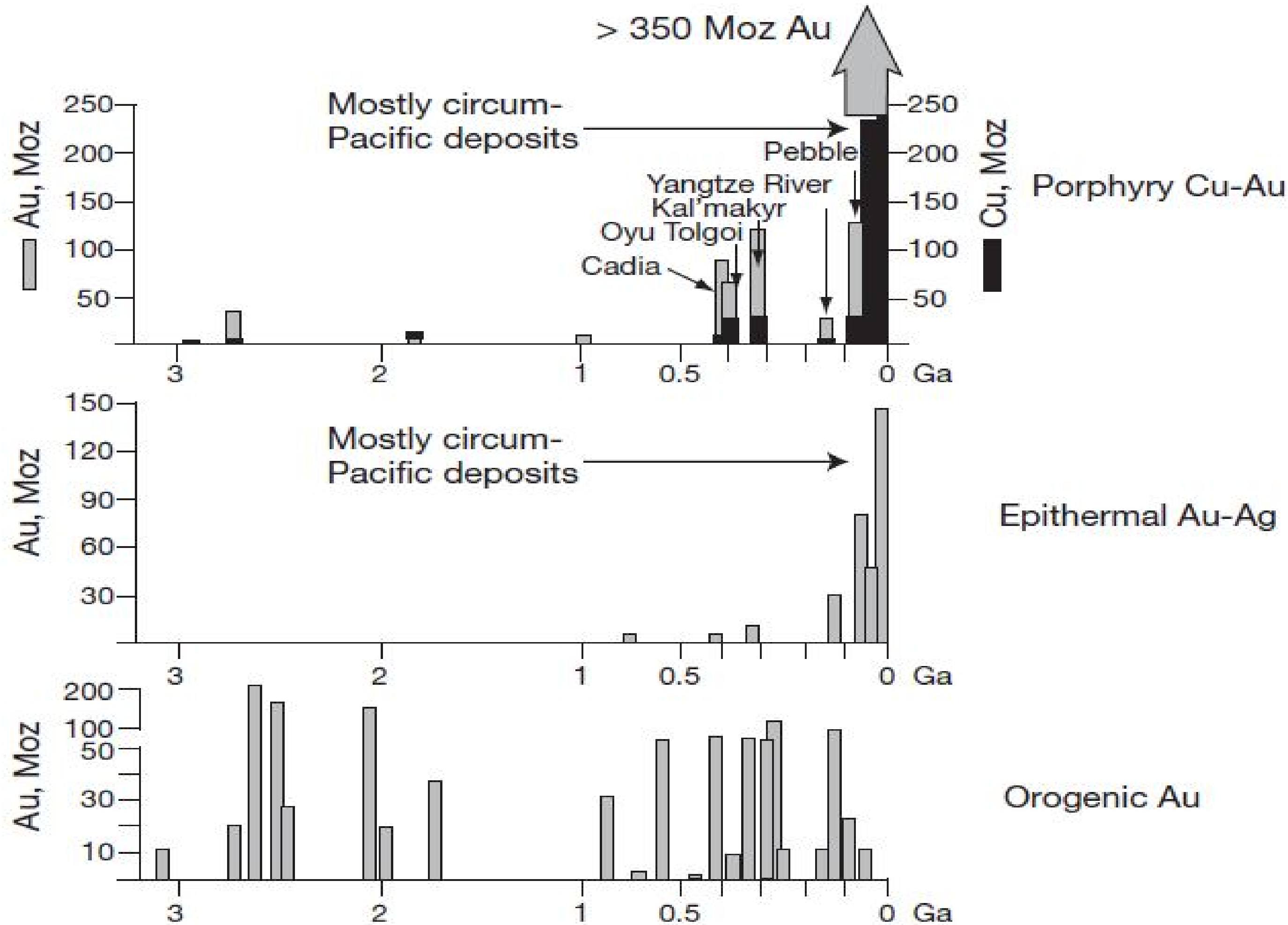

FIG. 2. Secular distribution of porphyry Cu-Au, epithermal Au, and orogenic Au deposits, after Groves et al. (2005b).

The former two deposit types, formed at relatively shallow levels, have been typically eroded from the geologic record beyond about 20 to 30 Ma, although particularly the porphyry deposits have some giant exceptions that have been preserved since the Mesozoic and earlier times.

The orogenic gold deposits have a much broader temporal distribution, reflecting their deeper levels of formation and thus greater likelihood to be preserved in older orogenic belts. (**Goldfarb et al., 2010)**

Summary of Geological Setting, Definitive Characteristics[1] and Several Examples of Typical Epithermal Au Deposit SubTypes

	HIGH-SULPHIDATION subtype	LOW-SULPHIDATION subtype	
	Hosted in volcanic rocks	**Hosted in volcanic and plutonic rocks**	**Hosted in sedimentary and mixed host rocks**
Geological Setting	**volcanic terrane**, often in caldera-filling volcaniclastic rocks; **hot spring** deposits and **acid lakes** may be associated	Spatially related to **instrusive centre**; veins in **major faults**, locally **ring fracture** type faults**; hot springs** may be present	In **calcareous to clastic sedimentary** rocks; may be intruded at depth by magma; can form at variety of depths
Ore Mineralogy	native gold, electrum, tellurides; magmatic-hydrothermal: py (+bn), en, tennantite, cv, sp, gn; Cu typically > Zn, Pb; Au-stage may be distinct, base-metal poor; steam-heated: base-metal poor; gangue: quartz **(vuggy silica), barite**	electrum (lower Au/Ag with depth), gold; sulphides include: py, sp, gn, cpy, ss); sulphosalts; gangue: quartz, adularia, sericite, calcite, chlorite; ± barite, anhydrite in deeper deposits variable base metal content, high sulphide veins closer to intrusions	gold (micrometre): within or on sulphides (e.g. pyrite unoxidized ore), native (in oxidized ore), electrum, Hg-Sb-As sulphides, pyrite, minor base metals; gangue: **quartz, calcite**
Alteration mineralogy	**advanced argillic + alunite, kaolintie, pyrophyllite (deeper);** ± sericite (illite); adularia, **carbonate absent;** chlorite and Mn-minerals rare; no selenides; barite with Au; steam-heated: vertical zoning	sericitic replaces argillic facies (**adularia ± sericite ± kaolinite**); Fe-chlorite, Mn-minerals, selenides present; **carbonate** (calcite and/or rhodochrosite) may be abundant, lamellar if boiling occurred; quartz-kaolinite-alunite-subtype minerals possible in steam-heated zone; clays	silicification, decalcification, sericitization, sulphidation; alteration zones may be controlled by stratigraphic permeability rather than by faults and fractures; quartz (may be chalcedonic)-sericite (illite)-montmorillonite
Host rocks	**silicic to intermediate (andesite)**	**intermediate to silicic intrusive/extrusive rocks**	**felsic intrusions**; most sedimentary rocks **except massive carbonates** (hosts to mantos and skarns)
Ore fluids (examples from fluid inclusion studies)	**160-240ºC; ≤1 wt.% NaCl (late fluids);** possibly to 30 wt.% NaCl in early fluids; **boiling common**; (Nansatsu district, Japan; Hedenquist et al., 1994)	**<u>sulphide-poor</u>: 180-31ºC, ≤1 wt.% NaCl,** about 1.0 molal CO_2 (Mt. Skukum: McDonald, 1987) **<u>sulphide-rich:</u> ave. 25ºC, <1 to 4 wt.% NaCl** (Silbak-Premier: McDonald, 1990)	**bimodal: 150-160 (most); 270-280ºC, ≤15 wt.% NaCl; nonboiling**: (Cinola: Shen et al., 1982); 230-250ºC, ≤1 wt.% NaCl; nonboiling (Dusty Mac: Zhang et al., 1989)
Age of mineralization and host rocks	host rocks and mineralization of **similar age**	mineralization variably **younger (>1 Ma)** than host rocks	mineralization variably **younger (>1 Ma)** than host rocks.
Deposit size	**small** areal extent (e.g. 1 km^2) and size (e.g. 2500-3500 kg Au)	may occur over large area (e.g. several tens of km^2); may be **large** (e.g. 100 000 kg Au).	may have **large** areal extent (e.g. >>1 km^2), large size (e.g. 58 000 kg Au), low grades (e.g. 2.5 g/t)
Modern analogues:	Matsukawa, Japan[2]	Broadlands, New Zealand[3]	Salton Sea geothermal field, California[4]

Mechanisms of Au deposition

- More efficient mechanisms of Au deposition provide higher Au grades
- Several mechanisms to consider
  - Boiling
  - Cooling
  - Rapid cooling
  - Sulphidation reactions
  - Carbon reactions
  - Mixing with oxygenated groundwaters
  - Mixing with bicarbonate waters
  - Mixing with low pH waters

Boiling textures

Banded chalcedony-ginguro Au-Ag vein

Banded quartz vein - Golden Cross

Quartz pseudomorphing platy carbonate

Adularia

Vera Nancy

Hishikari

Slow cooling

- low Au grades, good metallurgy in quartz-sulphide Au

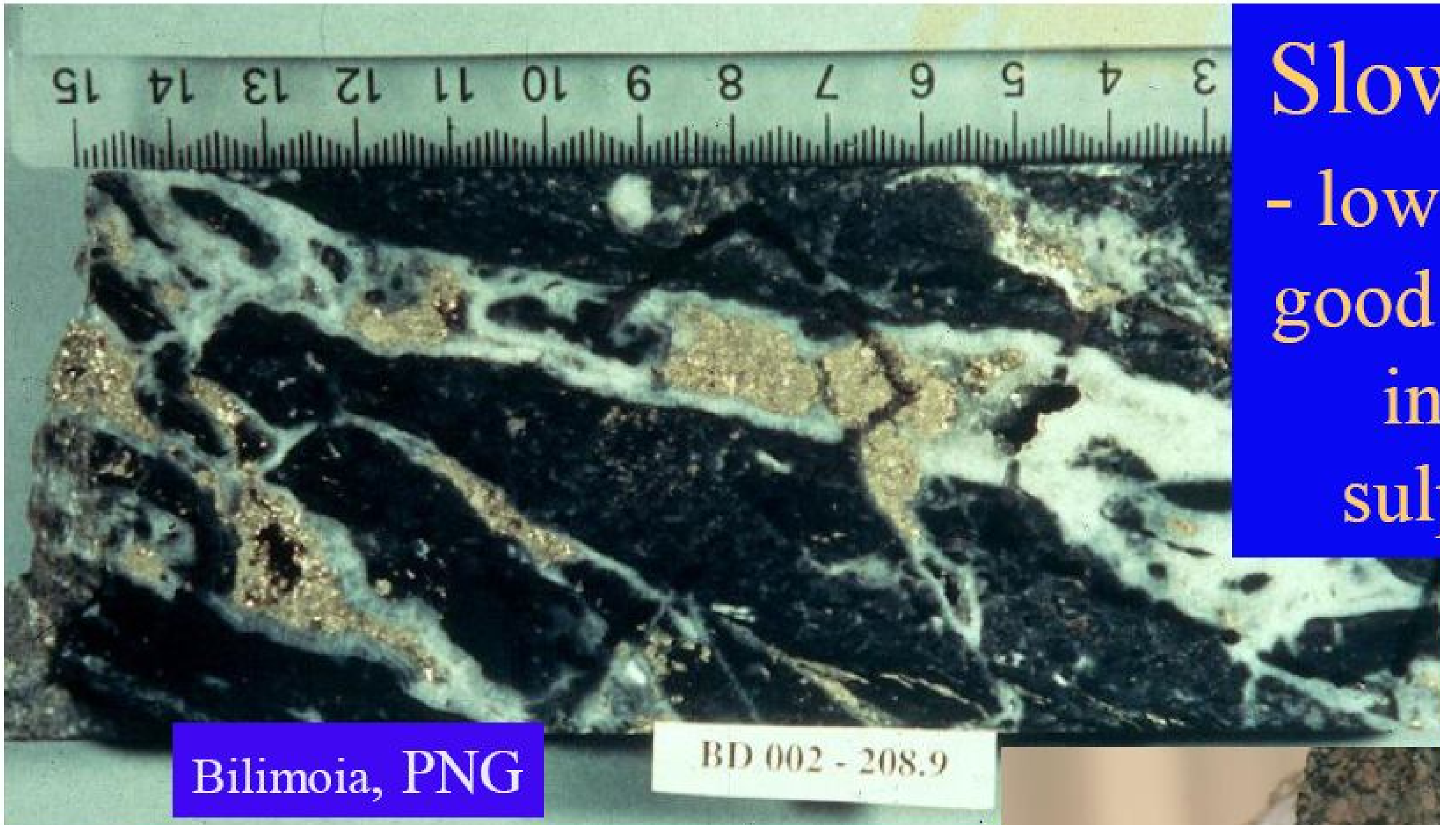

Cowal

Rapid cooling – opal in contact with sulphides

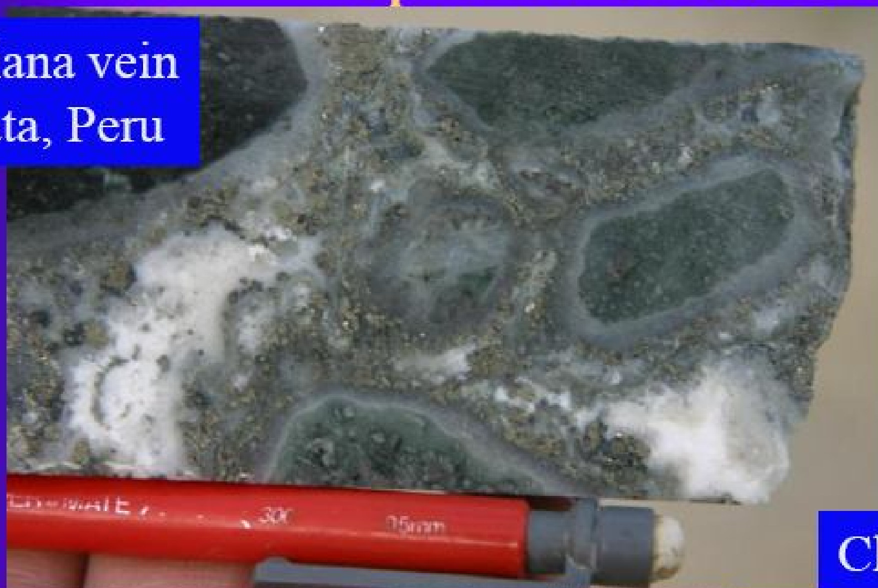

Mariana vein
Arcata, Peru

Chatree, Thailand

Fresnillo

Huevos Verde,
Patagonia

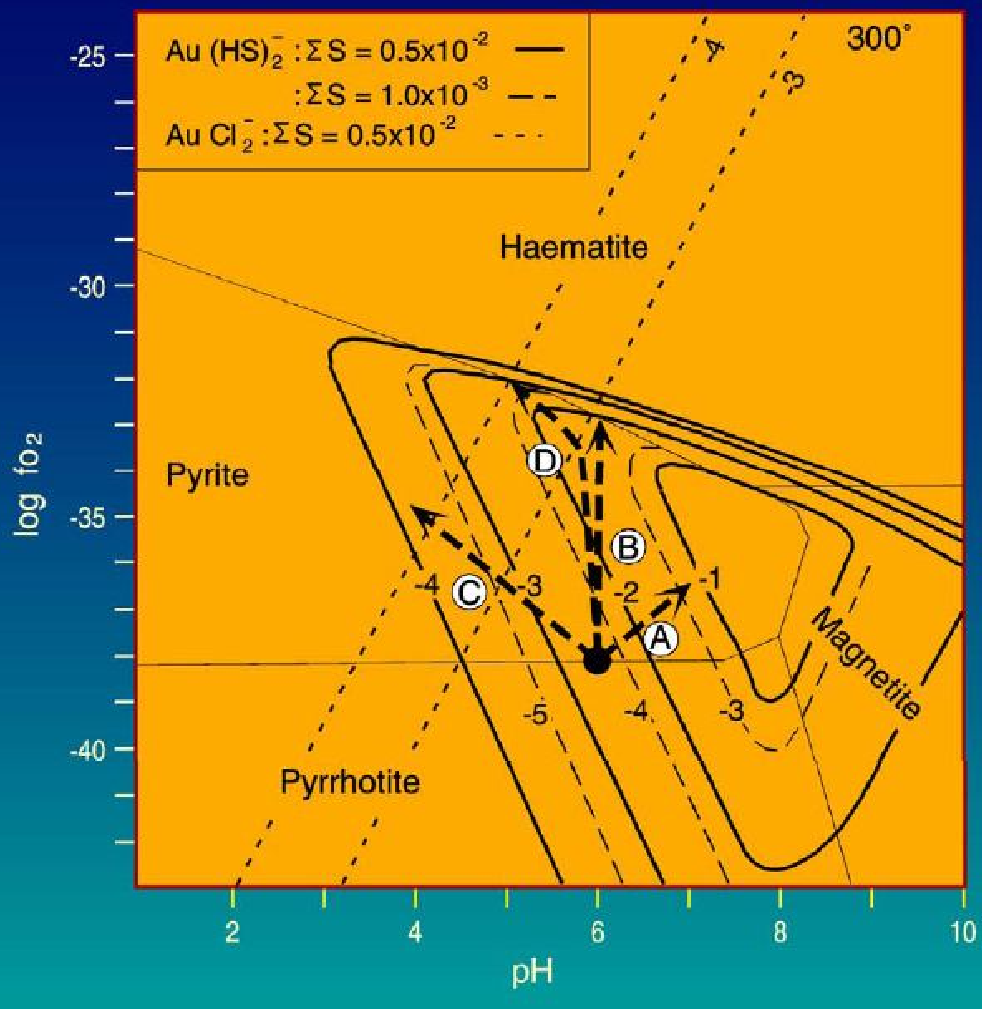

Gold Solubility

Gold solubility as HS^- and Cl^- complexes as a function of pH, fo_2 and ΣS (modified from Seward 1982; Brown 1986).

A: boiling
B: Mixing with oxygenated fluids
C: Mixing with low pH fluids
D: Mixing with bicarbonate-sulphate water

A - C Leach in Corbett & Leach 1998
D by D. Cooke May 1998 & Leach 2008

Leach
94487LIT

Mixing with oxygenated waters – hypogene haematite

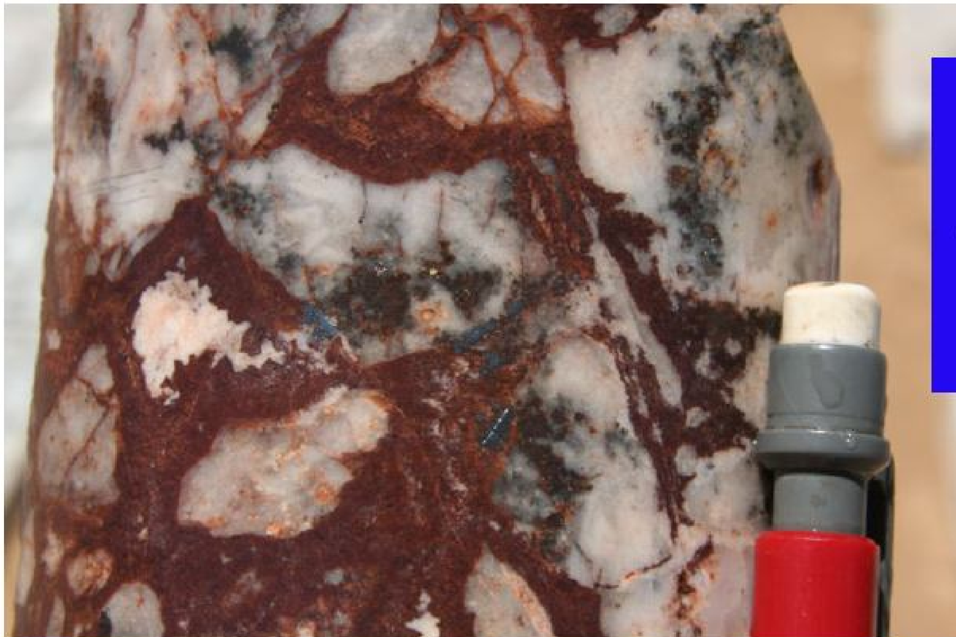

Palmarejo Mexico

Kupol, Russia
86 g/t Au 1370 g/t Ag

Fresnillo, Mexico

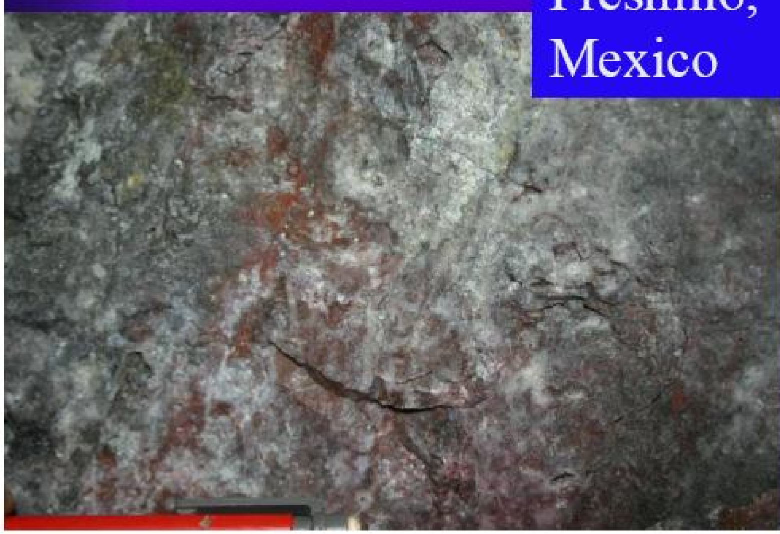

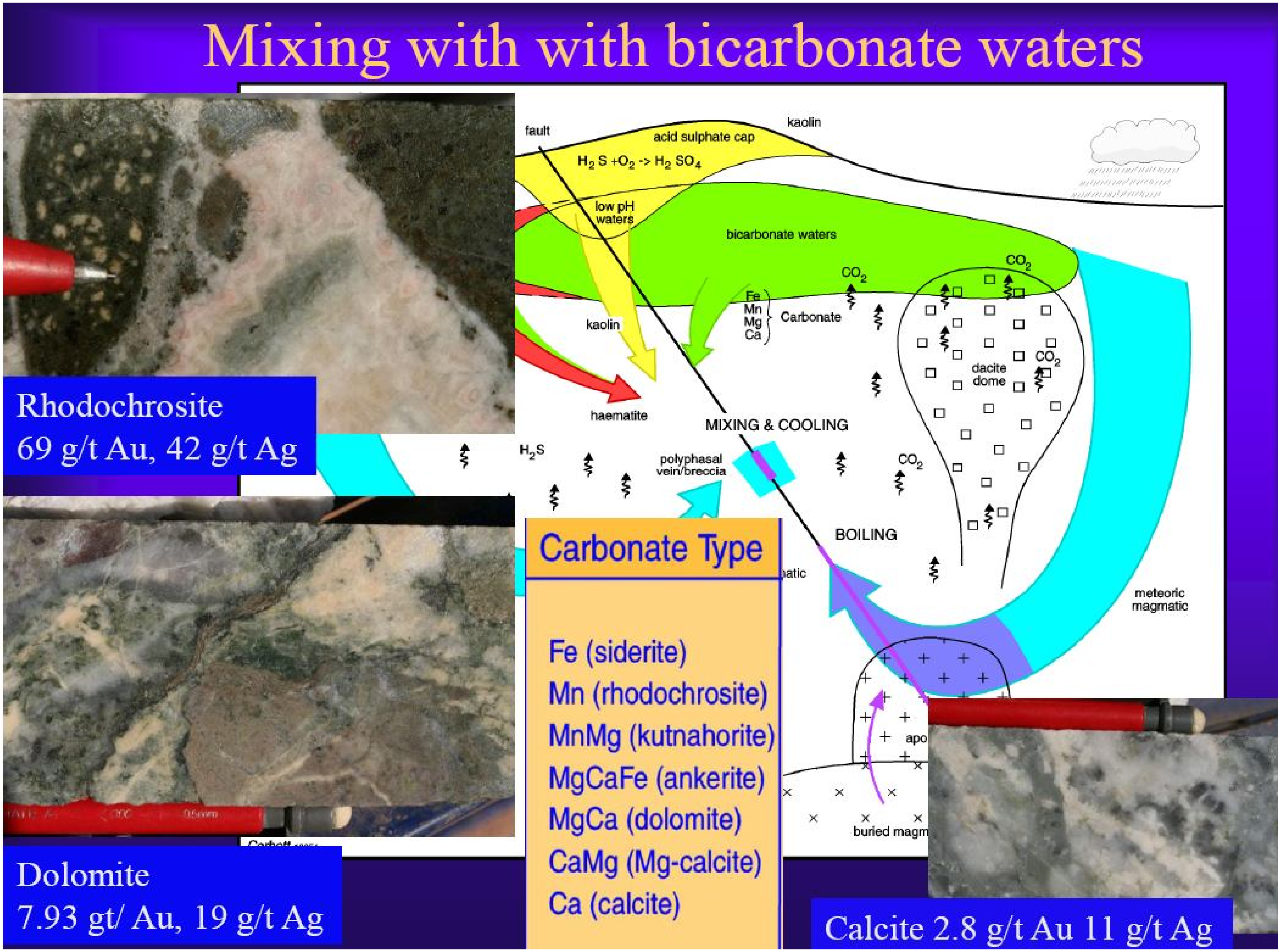

Mixing with with bicarbonate waters
Rhodochrosite
69 g/t Au, 42 g/t Ag
Dolomite
7.93 gt/ Au, 19 g/t Ag
Calcite 2.8 g/t Au 11 g/t Ag
fault
acid sulphate cap
kaolin
$H_2S + O_2 \rightarrow H_2SO_4$
low pH waters
bicarbonate waters
CO_2
Fe
Mn
Mg
Ca
Carbonate
kaolin
dacite dome
haematite
MIXING & COOLING
H_2S
polyphasal vein/breccia
BOILING
meteoric magmatic
Carbonate Type
Fe (siderite)
Mn (rhodochrosite)
MnMg (kutnahorite)
MgCaFe (ankerite)
MgCa (dolomite)
CaMg (Mg-calcite)
Ca (calcite)

Champagne Pool, Waitapu, New Zealand

Orange precipitate in ppm or %
Au 80, Ag 170, 170 Hg, 2% As, 2% Sb

- Several mechanisms may account for the deposition of Au in low sulphidation epithermal Au systems
- While boiling does deposit Au, this is not always the case
- Several different mixing reactions may account for elevated Au grades with increased efficiency and hence higher Au grade involving:
  - Oxygenated groundwaters
  - Bicarbonate waters
  - Low pH acid sulphate waters

Photo 1. Quartz-sulphide gold $\pm$ copper style mineralization from Bilimoia (Corbett et al 1994) containing early quartz and later coarse crystalline pyrite.

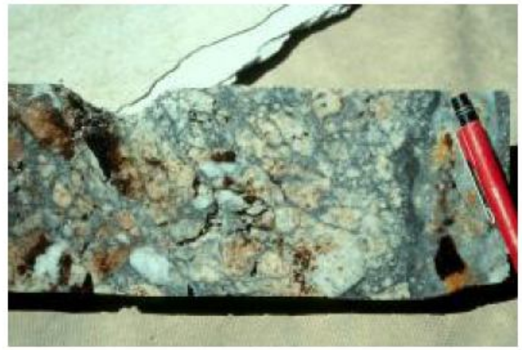

Photo 2. Kerimenge sulphide fill breccia typically comprising arsenopyrite-pyrite-marcasite-quartz

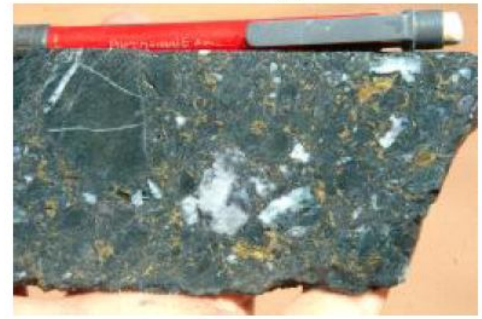

Photo 5. High temperature quartz-sulphide gold ± copper mineralization from Mineral Hill comprising chalcopyrite rich breccia mined for in Cu-Au-Bi

Photo 3. Low temperature quartz-sulphide gold ± copper mineralization from Rawas containing opaline silica and marcasite-pyrite

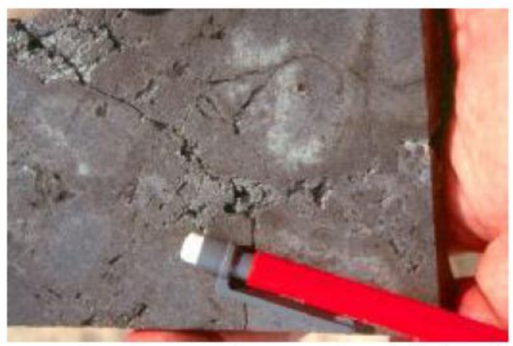

Photo 4. Low temperature quartz-sulphide gold ± copper mineralization from Lihir composing flooding of arsenean pyrite

Photo 6. Telescoped low sulphidation mineralization with pyrite, base metal sulphides and opal from Tavatu

Photo 13. Carbonate-base metal gold vein cuts quartz-sulphide gold ± copper mineralization, Mt Kare

Photo 14. Rio del Medio, El Indio district carbonate-base metal gold mineralization showing rhodochrosite

Photo 15. Transitional quartz-sulphide gold ± copper to carbonate-base metal gold vein showing early quartz and later pyrite, dark sphalerite, lesser galena and minor later carbonate from Kidston.

Photo 16. Carbonate-base metal gold mineralization as a breccia matrix, Mt Leyshon.

Photo 17. Bonanza epithermal quartz gold-silver mineralization from Porgera Zone VII containing wire gold, quartz and roscoelite.

Photo 18. Bonanza gold grade epithermal quartz gold-silver style mineralization comprising gold fill of an open quartz vein, Edie Creek.

Photo 19. Banded adularia-sericite epithermal gold-silver fissure vein showing marginal floating clast breccias, Hishikari

Photo 20. Banded adularia-sericite epithermal gold-silver mineralization showing well developed banded quartz and ginguro ore from Golden Cross.

Photo 21. Adularia-sericite epithermal gold-silver mineralization showing well developed quartz pseudomorphing platy calcite from Vera Nancy.

Photo 22. Banded banded vein with chalcedony, ginguro band and pink adularia, Cracow.

Photo 23. High grade (948 g/t Au, 3720 g/t Ag) adularia-sericite epithermal gold-silver vein with abundant mineralised ginguro material, Hishikari.

Photo 24. Toka Tindung eruption breccia with sinter and wood fragments in a strongly silicified matrix

Photo 31. Diatreme breccia showing silicification of the within the finely comminuted breccia matrix and vughy silica alteration of porphyritic, interpreted intrusion, fragments, Veladero.

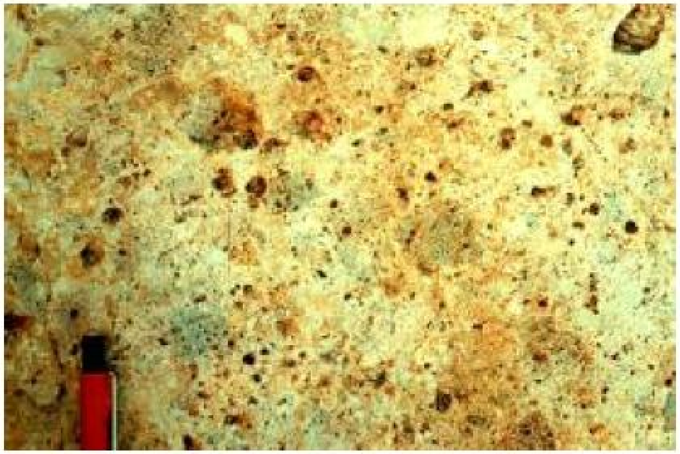

Photo 32. Vughy silica alteration of a lapilli tuff, Del Carmen.

Photo 33. Vughy silica alteration of porphyry intrusion, El Indio district.

Knowledge Gaps

Upon comparison of many features, both regional and local, of 16 bonanza (>30 tonnes Au) and giant (>200 tonnes Au) epithermal Au deposits, Sillitoe (1992) concluded that, although complex arc environments and unusual igneous rock types seemed more prospective, no single feature could be isolated as an apparent cause or explanation.

Either an unusually rich source of Au or an unusually effective depositional process was necessary to effect such concentrations of Au. This ‘chicken or egg’ conclusion remains as a principal enigma, a key question in the knowledge gap.

A firmer understanding of links between porphyries and epithermal systems is evolving, and an understanding of the temporal differences in magmatic and hydrothermal evolution that explains the lack of direct linkages (e.g. low-sulphidation and porphyry Cu-Au deposits).

A sufficient number of ancient epithermal Au deposits, both low- and high-sulphidation subtypes, are now known to raise the level of understanding needed regarding the likelihood of preservation and rates of destruction of the epithermal regime of the crust. Clearly very old examples have survived.

Economic Geology, v. 104, pp. 623–633

Resources of Gold in Phanerozoic Epithermal Deposits

STEPHEN E. KESLER[1,†] AND BRUCE H. WILKINSON[2]

[1] *Department of Geological Sciences, University of Michigan, Ann Arbor, Michigan 48109-1005*

[2] *Department of Earth Sciences, Syracuse University, Syracuse, New York 13244-1070*

Tectonic-diffusion model

Age-frequency distributions for mineral deposits at convergent margins are log-normal (skewed) in form and there is a direct relation between the mode (most common value) in these distributions and the depth at which the deposits form (Kesler and Wilkinson, 2006). Deposits that form at great depth require more time to reach the surface than deposits that form at shallow levels, and their age frequency distribution defines an older modal age.

Using preliminary compilations of isotopic ages, Kesler and Wilkinson (2006) showed that epithermal deposits, which form largely in the upper kilometer of the crust, have a modal age of ~3 Ma, whereas porphyry copper deposits, which originate at average depths of ~2 km, have a modal age of ~12 Ma, and orogenic gold deposits that form largely at average depths closer to 10 km have a modal age of ~160 Ma. This relation between depths of emplacement and modal ages makes ore deposits an excellent indicator of uplift and denudation (erosion) rates, and provides the basis for the tectonic-diffusion model.

Tectonic-diffusion model

The basic function of the tectonic-diffusion model is to produce a theoretical (computational) age-frequency distribution that comes as close as possible to matching the actual (real-Earth) age-frequency distribution for a specific group or type of deposits (Wilkinson and Kesler, 2007).

For the estimate of epithermal gold resources, we have compiled a global database that is discussed below and that yields an age-frequency distribution (Fig. 1) very similar to that from our preliminary compilation (Kesler and Wilkinson, 2006). The important point to resource estimates is that in generating the theoretical age-frequency distribution, the model calculation determines the number and vertical distribution of deposits in the crust. The calculation does this by emplacing deposits at a fixed rate and crustal depth, and then allowing each one to move randomly (tectonic diffusion) upward (uplift and erosion), downward (subsidence and burial) or sideways (stasis) during each interval of model time (Fig. 2). In the calculation, some migration paths bring deposits upward to a position above the Earth's surface, where they are "eroded" (Fig. 2A, B). Many other deposits undergo amounts of subsidence that equal or exceed rates of uplift and therefore remain in the subsurface, never reaching the computational surface; these constitute Earth's crustal endowment of ore deposits (Fig. 2C).

We have estimated Earth’s endowment of gold in Phanerozoic epithermal deposits using a tectonic-diffusion model, which simulates the emplacement of deposits at a shallow crustal depth and their subsequent vertical tectonic migration in the crust. The calculation was calibrated by least-squares comparison of a calculated age-frequency distribution to the age-frequency distribution for 448 epithermal deposits of Phanerozoic age.

Results indicate that ~17 percent of the epithermal deposits that formed through Phanerozoic time remain in the crust today whereas ~83 percent have been removed by erosion. Assuming a similar age distribution for all 1,181 epithermal deposits in our compilation indicates that ~307,000 deposits formed throughout Phanerozoic time, that ~63,000 of these remain in the crust, and that ~244,000 have been eroded. Grade and tonnage data of gold in 757 epithermal deposits in the compilation have an arithmetic average of 34.7 t and yield an estimate of 2.2 × 106 t of gold for epithermal deposits remaining in the crust.

all of the epithermal deposits that formed through Phanerozoic time represent only about 0.03 percent of the gold in the crust. Only about 0.007 percent of crustal gold remains in epithermal deposits; the rest has been eroded and recycled.

Finally, we are consuming gold from epithermal deposits about 17,000 times faster than Earth is replenishing the supply.

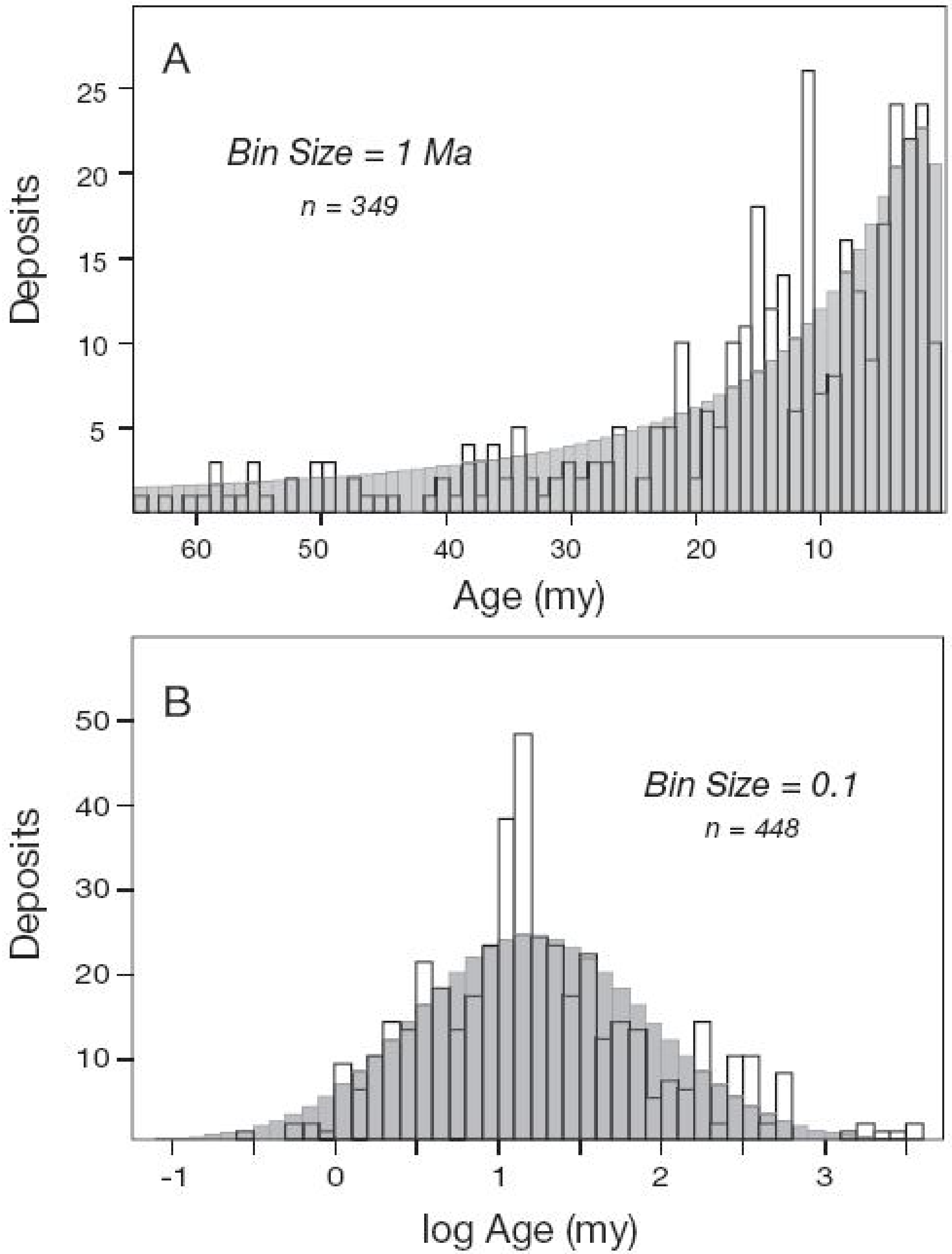

Ages of epithermal gold-bearing deposits.

A. Age-frequency distribution plotted on an arithmetic scale. Open bars show the actual agefrequency distribution for all deposits of Cenozoic age. Shaded bars are the age-frequency distribution that would result if ore formation proceeded at a Phanerozoic average rate.

B. Age-frequency distribution (open bars) plotted on a log scale showing the approximate log-normal distribution of all deposit ages. Shaded bars are the normal age-frequency distribution to the log data (mean = 1.25, standard deviation = 0.71).

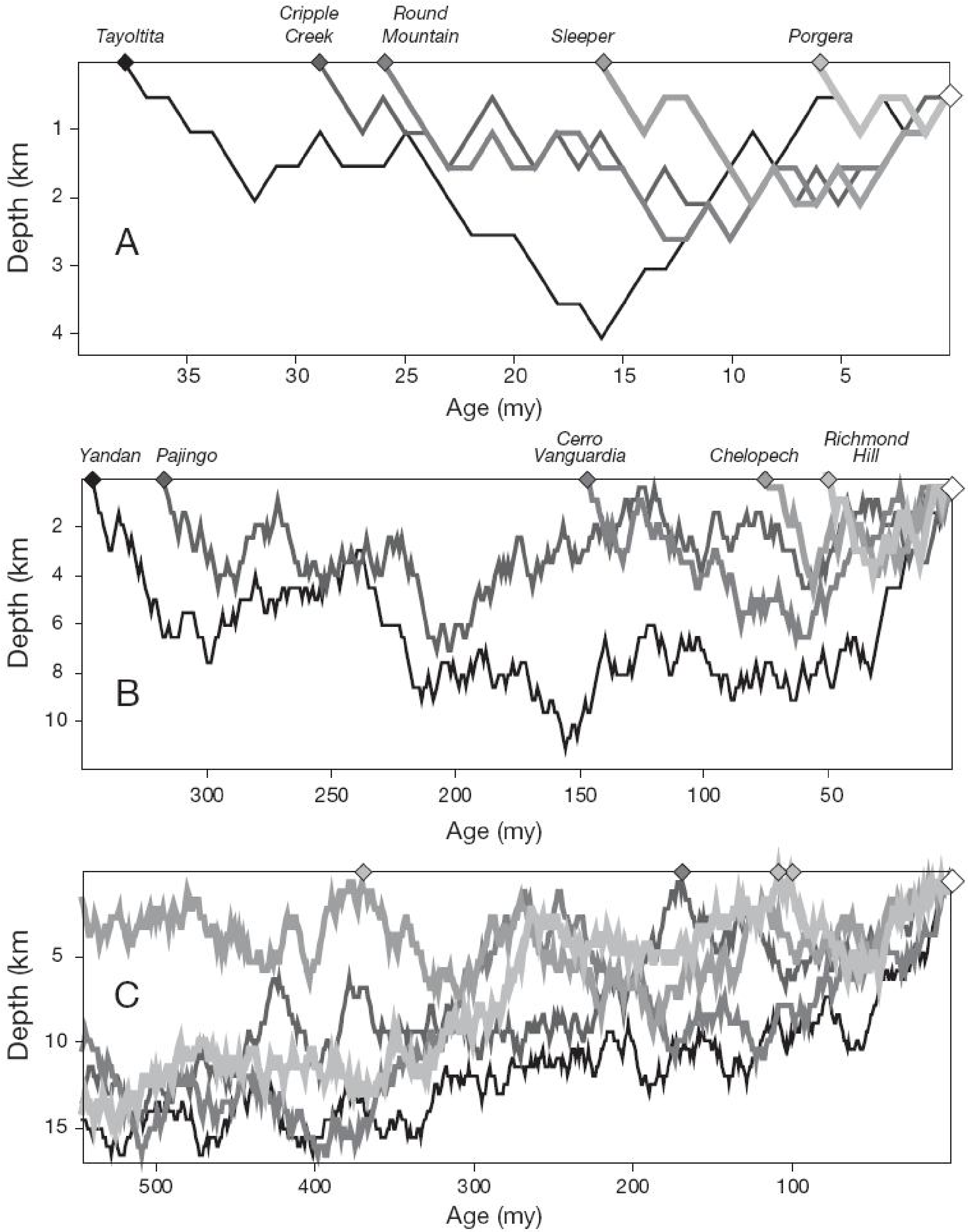

Time-depth random-walk paths defined by the tectonic-diffusion model calculation showing how some known deposits (shaded diamonds) might have moved through crustal time-depth prior to exposure. All deposits were formed at a depth of 0.5 km (large open diamonds to right).

Panels A and B show several different spans of time since formation (deposit ages): corresponding deposit ages are as follows: ~6 Ma (Porgera, PNG) to 38 Ma (Tayoltita, Mexico), B) ~50 Ma (Richmond Hill, South Dakota) to 345 Ma (Yandan, Australia).

Panel C shows hypothetical depth-time paths of five deposits that were not exposed during Phanerozoic time. Note that several of these (still buried) deposits nearly reached the surface (shaded diamonds) but were buried again and did not reemerge during the remainder of Phanerozoic time. If paths were continued into Precambrian, several paths might emerge as older deposits, such as Hope Brook, with an age of 576 Ma (Dubé et al., 1998). Although duration of burial in these diagrams matches actual data, actual depths could have been greater or lesser.

TABLE 1. Results of the Model Calculation and Adjusted Amounts Based on the Ratio of Dated Phanerozoic Deposits (448) Used in the Model Calculation to All Deposits (1181) in the Database

	Model result	Unit	Adjusted for all deposits in database
Emplacement depth[1,2]	0.50 ± 0.3	km	
Emplacement rate[1]	213	/Ma	562
Modal age[1,2]	2	My	
Tectonic step[1]	295	m/ Ma	
Modal exhumation rate[1]	250	m/ Ma	
Modal deposit depth[1]	0.88	km	
Up-stasis-down[1]	32-36-32	%	
Total deposits[1]	116,000	100%	307,000
Extant deposits[1]	24,000	17%	63,000
Eroded deposits[1]	92,000	83%	244,000
Model exposed deposits[1]	519		
Actual exposed deposits[2]	448		
Average gold content[2]		t	34.7
Gold in total deposits[1]		t	10.6×10^6
Gold in eroded deposits[1]		t	8.5×10^6
Gold in extant deposits[1]		t	2.2×10^6

The tectonic step, which is 295 m thick, represents the average vertical distance moved by deposits during each million years of the calculation; it is therefore the thickness of the "surface" layer in the model calculation

[1]Model-derived parameters

[2]Data-derived parameters

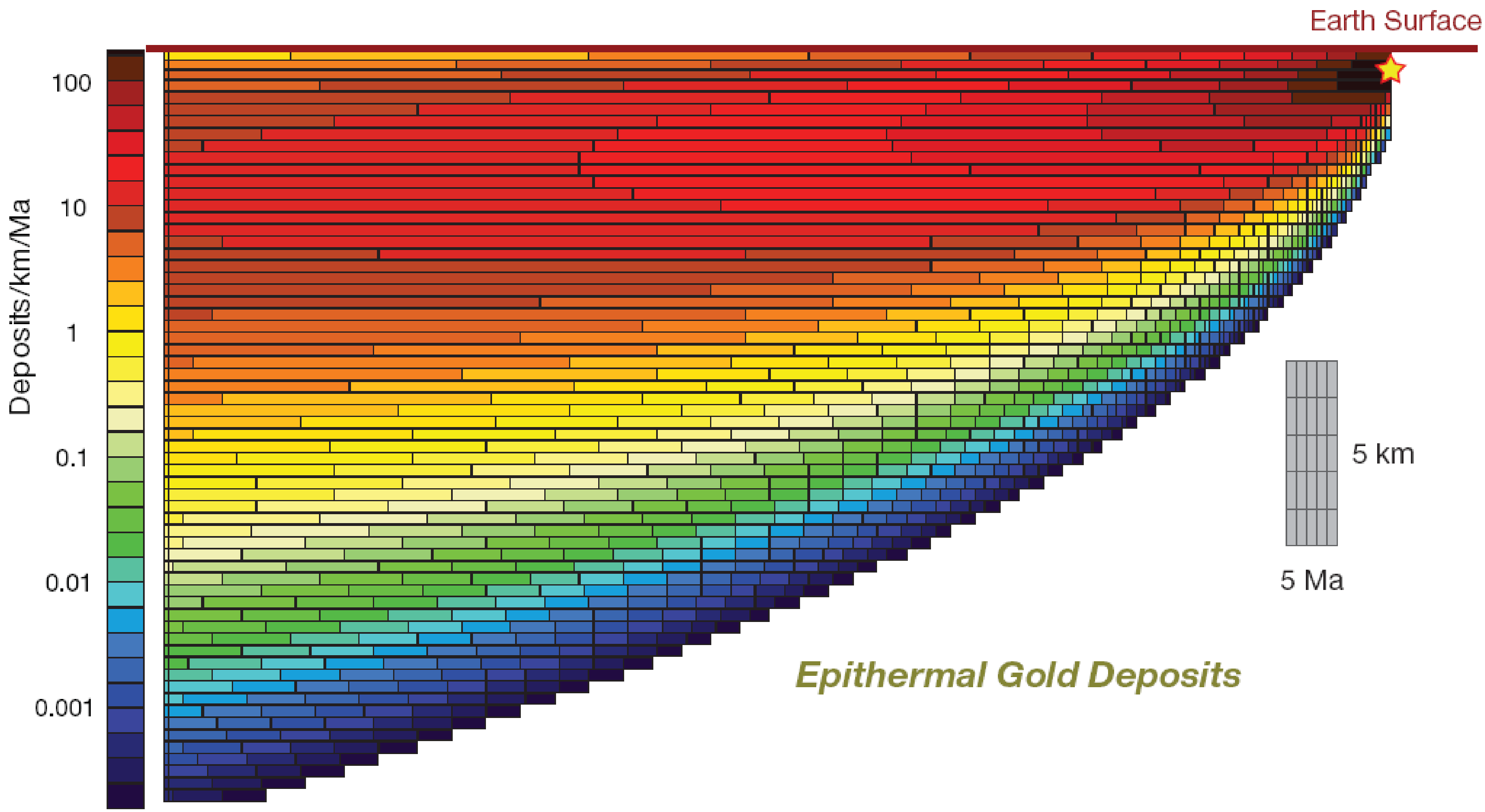

FIG. 4. Model distribution of epithermal gold deposits in age-depth space for the last 250 m.y. of Earth history (age is on the X-axis, maximum = 250 Ma; depth is on the Y-axis, maximum = 20 km) assuming that the number of discovered deposits in our database (1,164) approximately represents all such deposits now exposed at the Earth's surface. Color shades are log-scaled (left column) as the number of deposits that exist in each 1 Ma × 1 km time-depth "area" (a 5 km × 5 Ma grid is shown as the gray reference rectangles). Deposits enter the diagram at the upper right source region (star) at the rate of 562 deposits per m.y. and migrate (diffuse) across the diagram through time. Of the ~307,000 deposits that formed over Phanerozoic time, about 20 percent (63,000) are preserved in the crust (42,700 of those <250 Ma in age are represented here), while 83 percent have been removed by uplift and erosion. The gradual deepening of the maximum number of deposits with increasing time results from the loss of large numbers of deposits to erosion.

Economic Geology
Vol. 97, 2002, pp. 3–9

Relationship of Epithermal Gold Deposits to Large-Scale Fractures in Northern Nevada

D. A. PONCE AND J. M. G. GLEN
U.S. Geological Survey, MS 989, 345 Middlefield Rd., Menlo Park, California 94025

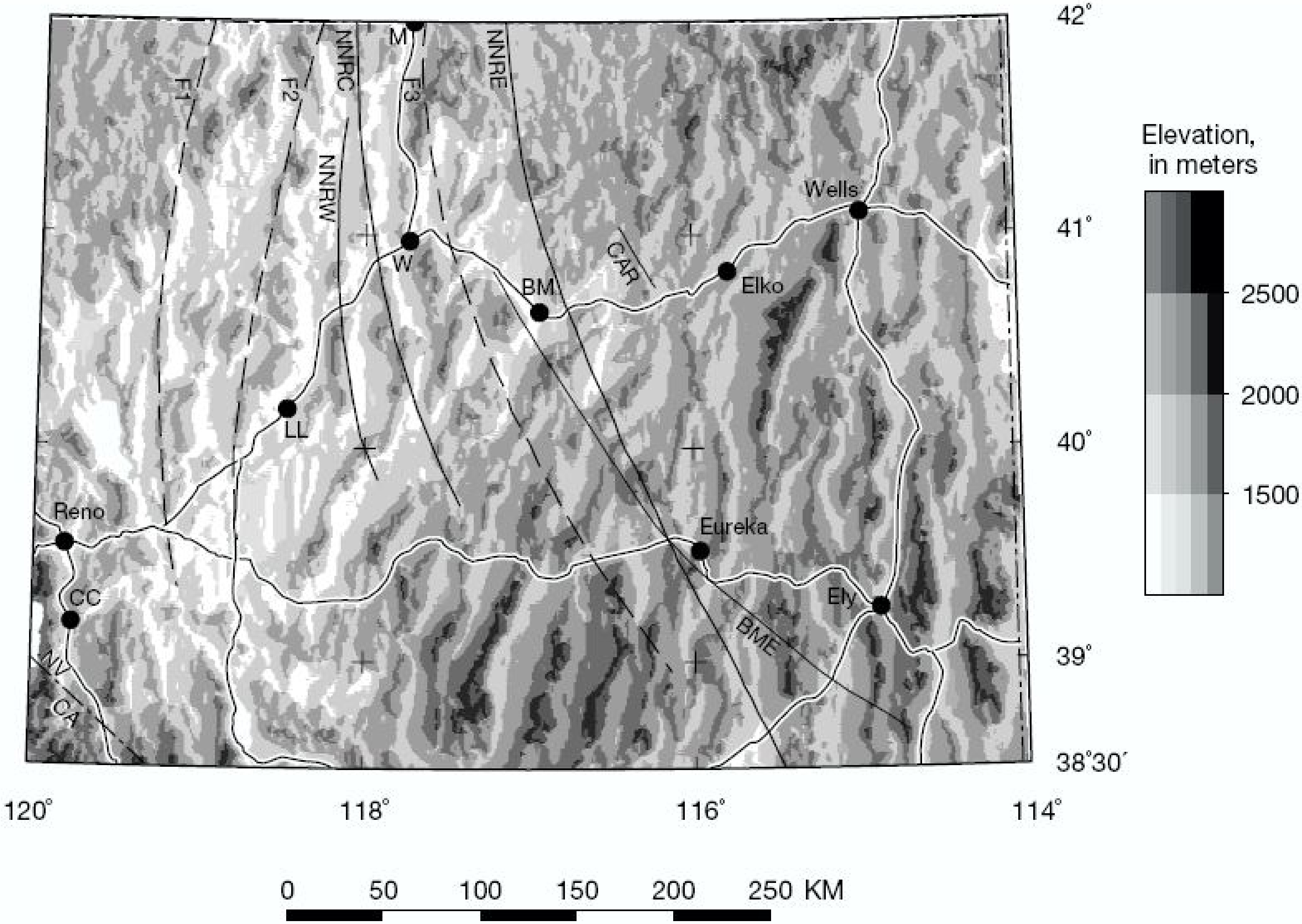

FIG. 1. Shaded-relief terrain map of northern Nevada showing location of the northern Nevada rift-east (NNRE), two parallel features to the west (northern Nevada rift-west [NNRW], northern Nevada rift-central [NNRC]), and other less prominent large-scale features (F1–F3) derived primarily from magnetic data. BM = Battle Mountain; BME = Battle Mountain-Eureka mineral trend; CA = California; CC = Carson City; CAR = Carlin mineral tend; LL = Lovelock; M = McDermitt; NV = Nevada; W = Winnemucca.

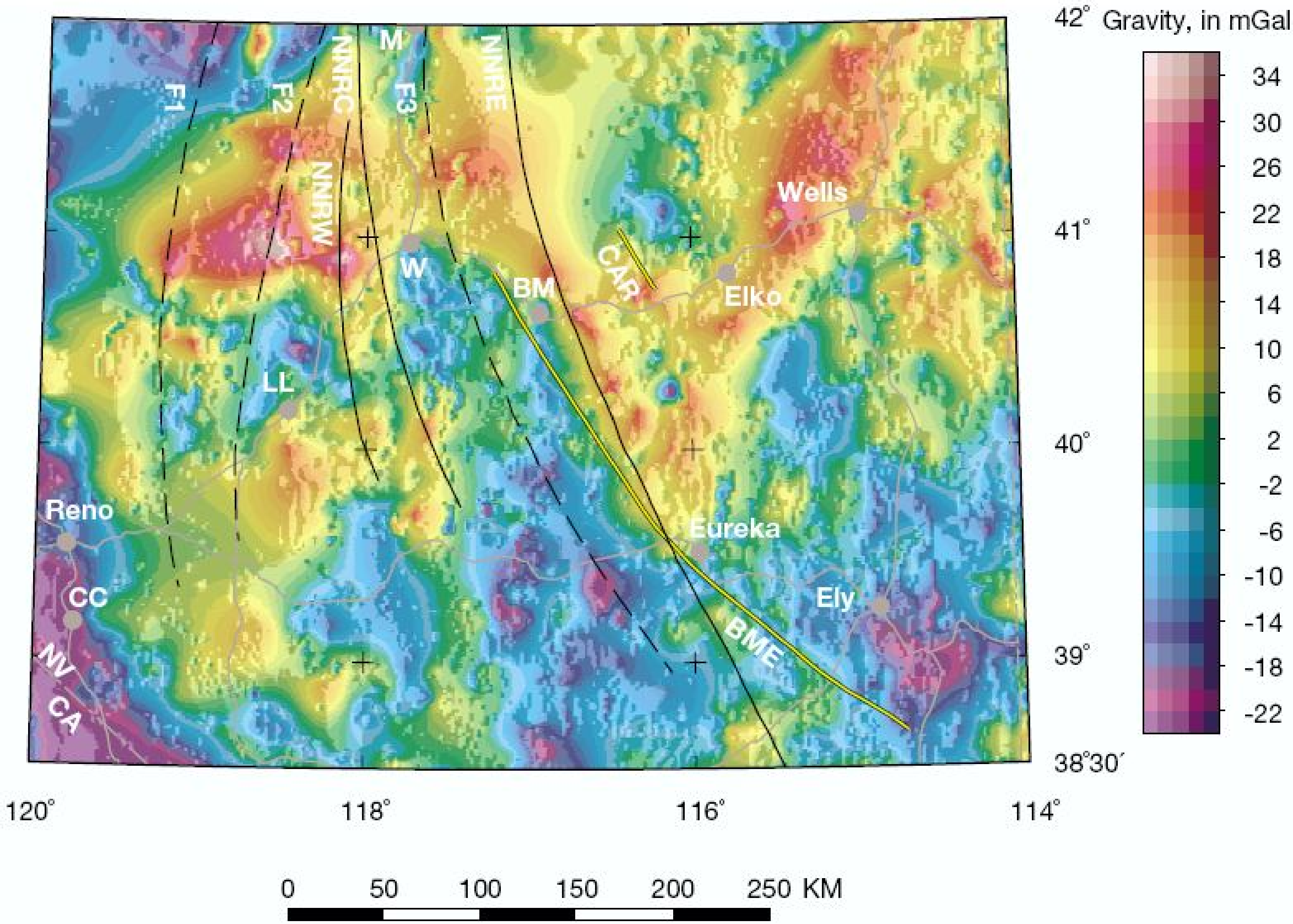

FIG. 3. Basement gravity map of northern Nevada derived by removing the gravity effect of Cenozoic basins from isostatic gravity anomalies. Prominent V-shaped basement gravity anomaly transects northern Nevada. Explanation as in Figure 1.

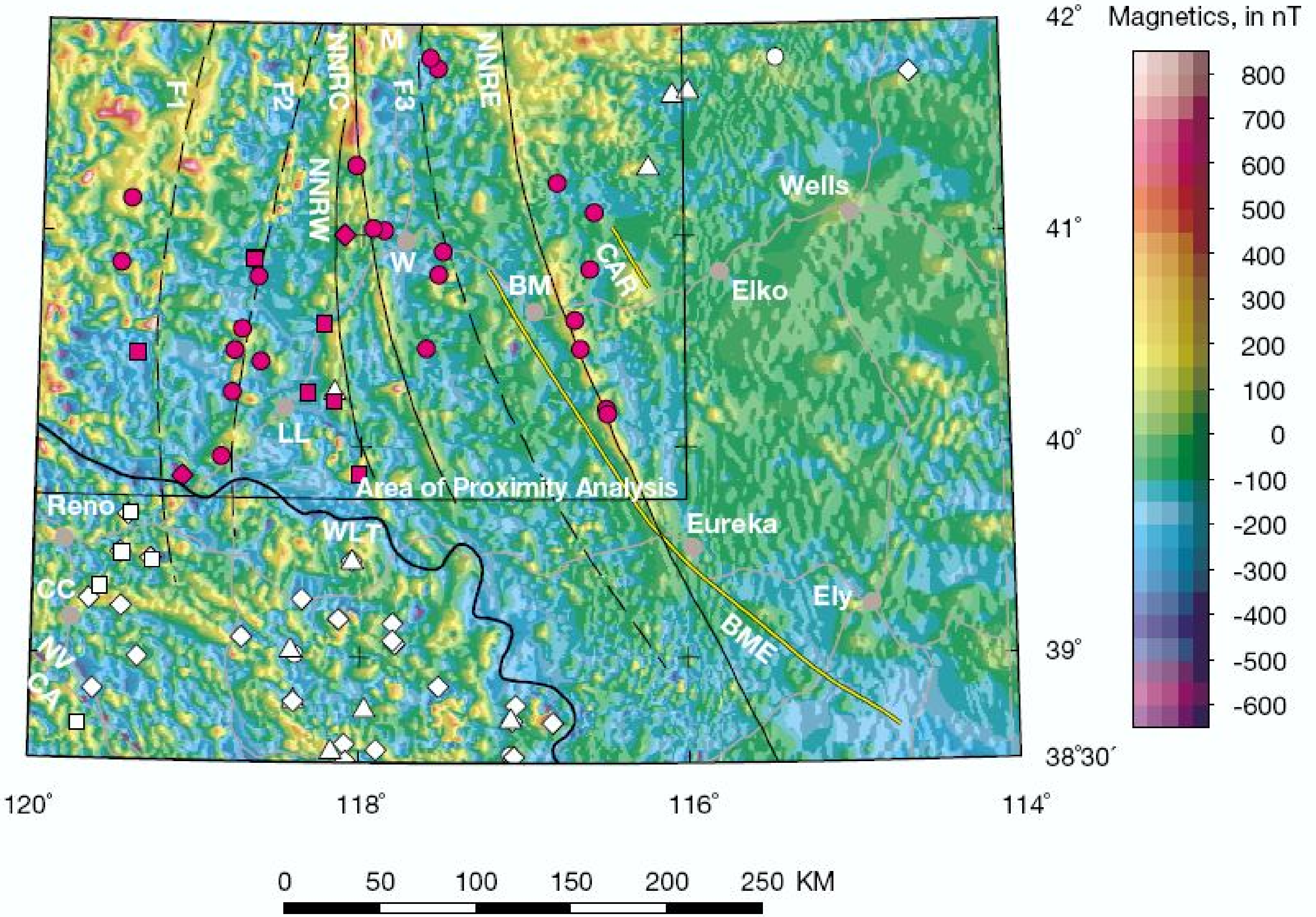

FIG. 4. Aeromagnetic map of northern Nevada showing the magnetic expression of large-scale features. Especially prominent are the northern Nevada rift-east (NNRE) and two parallel features to the west (northern Nevada rift-west [NNRW], northern Nevada rift-central [NNRC]). Bold black line (Walker Lane terrane [WLT]) northeast boundary of the Walker Lane geophysical terrane; black rectangle, area of proximity analysis. Deposits: triangle, epithermal deposits older than mid-Miocene; circle, mid-Miocene epithermal deposits; square, epithermal deposits younger than mid-Miocene; diamond, epithermal deposits of uncertain age or age range that spans across Mid-Miocene; red, epithermal deposits used in the proximity analysis (modified from Seedorff, 1991; John et al., 2000; Wallace et al., 2001). Explanation as in Figure 1.

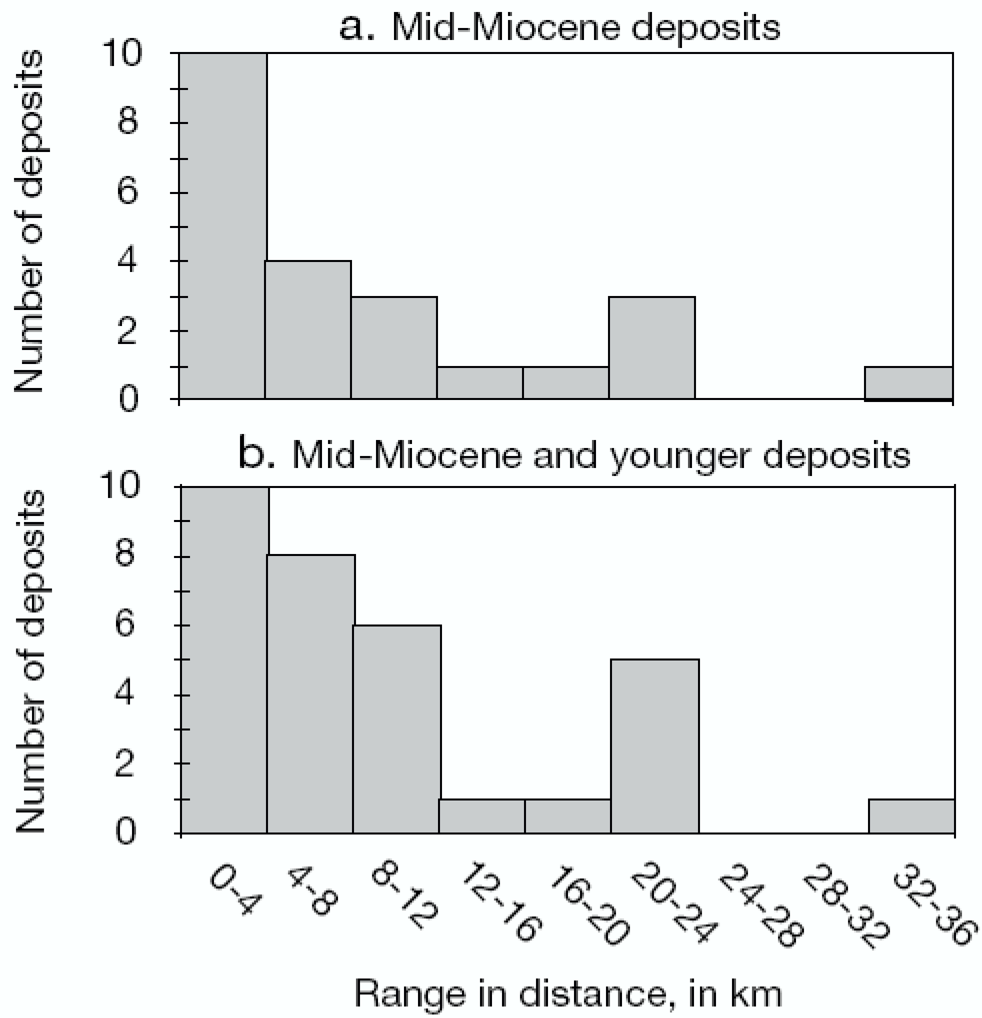

FIG. 6. Histogram showing number of epithermal gold deposits and their distances from large-scale features derived from geophysical data. a. Mid-Miocene deposits (n = 23). b. Mid-Miocene and younger deposits (n = 32).

Epithermal Gold and Base Metal Mineralization at Gandy Deposit, North of Central Iran and the Role of Rhyolitic Intrusions

M. Fard, E. Rastad,* and M. Ghaderi

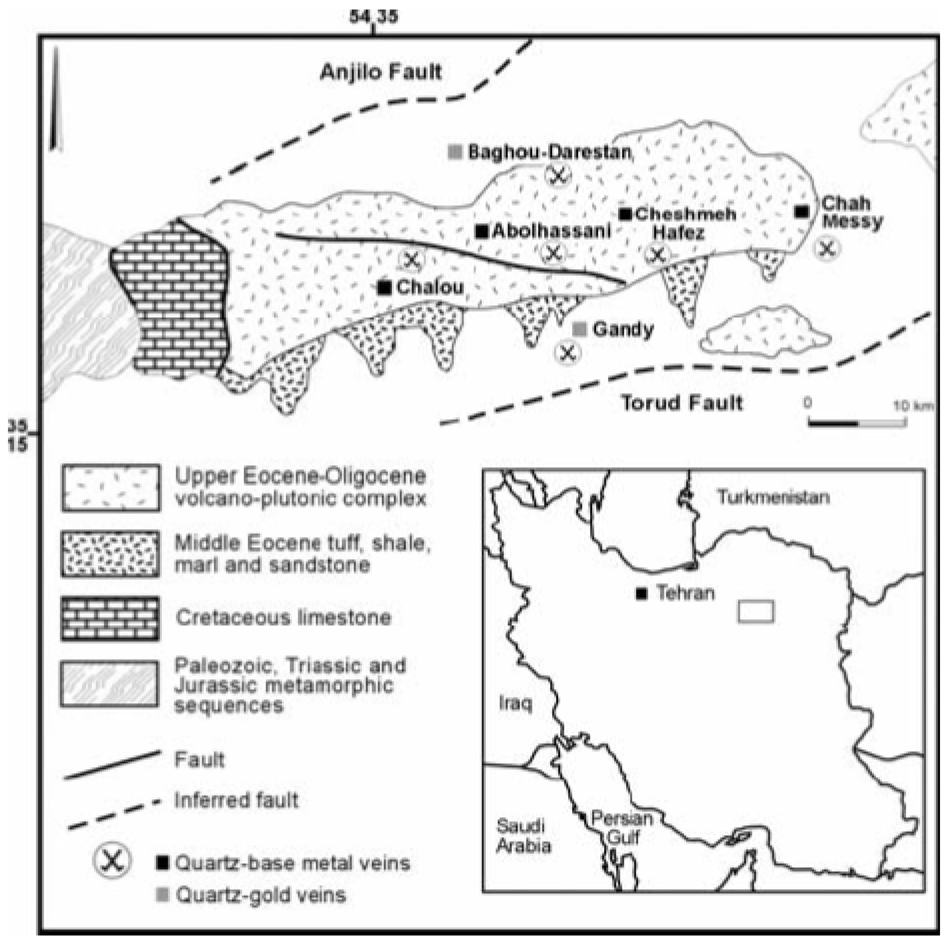

Figure 1. Simplified geological map of the Torud-Chahshirin range showing the location of quartz-base metal veins; Gandy Au (Ag+Pb+Zn+Cu), Chalou Cu (Au), Baghou-Darestan Au (Cu), Abolhassani Pb+Zn+Cu (Au), Cheshmeh Hafez Pb+Zn+Cu (Au) and Chah Messy Cu.

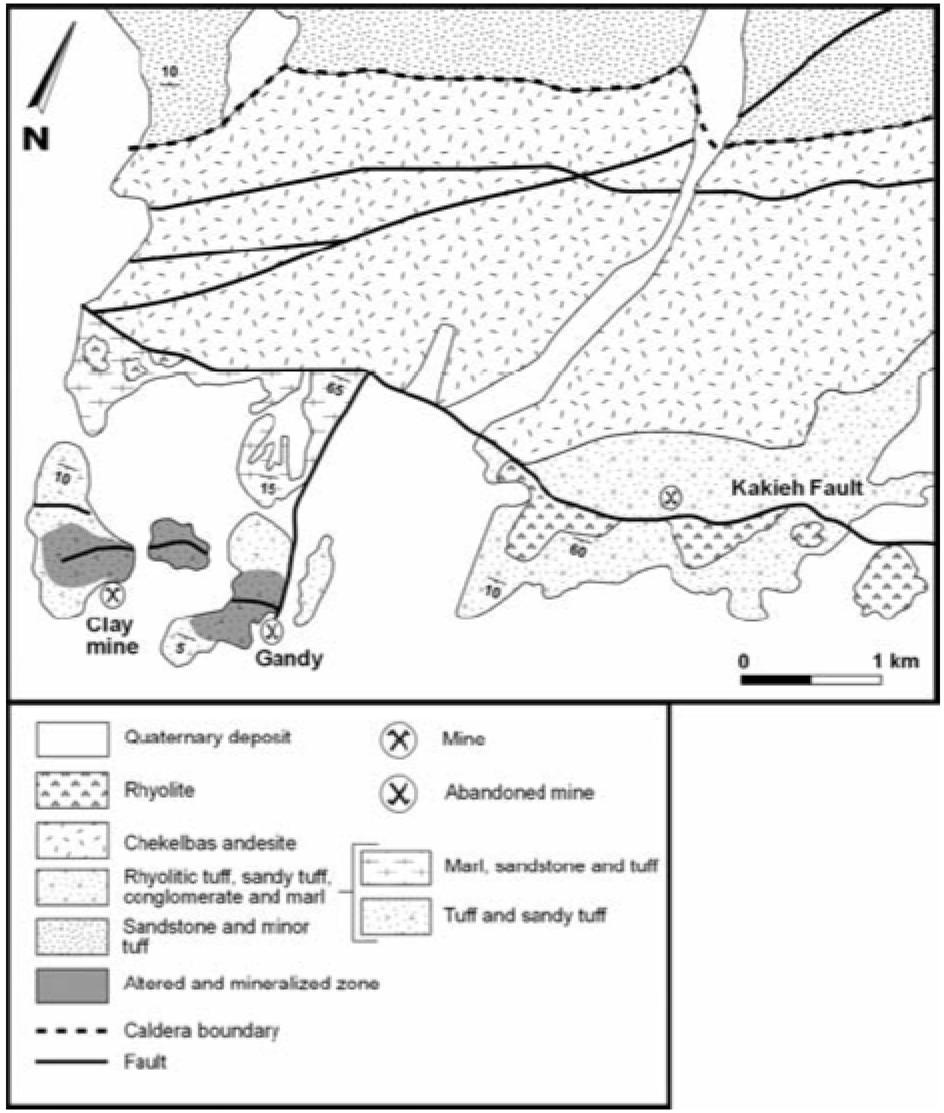

Figure 2. Geological map of the Gandy deposit showing the mineralized area located south of Kakieh normal fault.

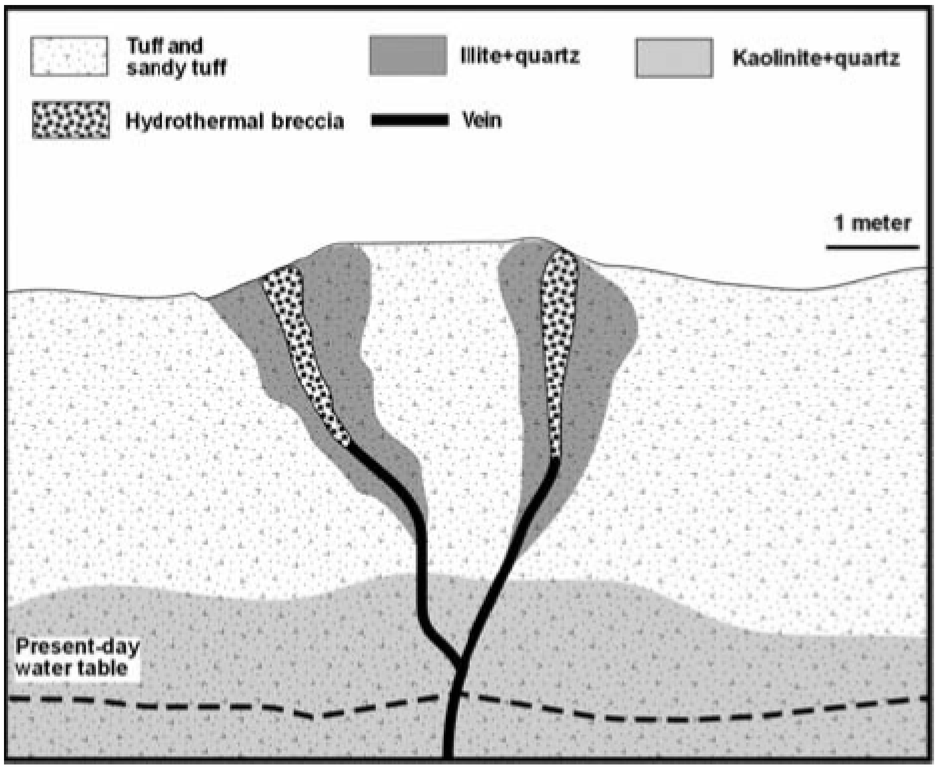

Figure 4. Illustration of two styles of alteration at the Gandy deposit; pervasive advanced argillic alteration (kaolinite + quartz) and vein-controlled illite + quartz assemblage.

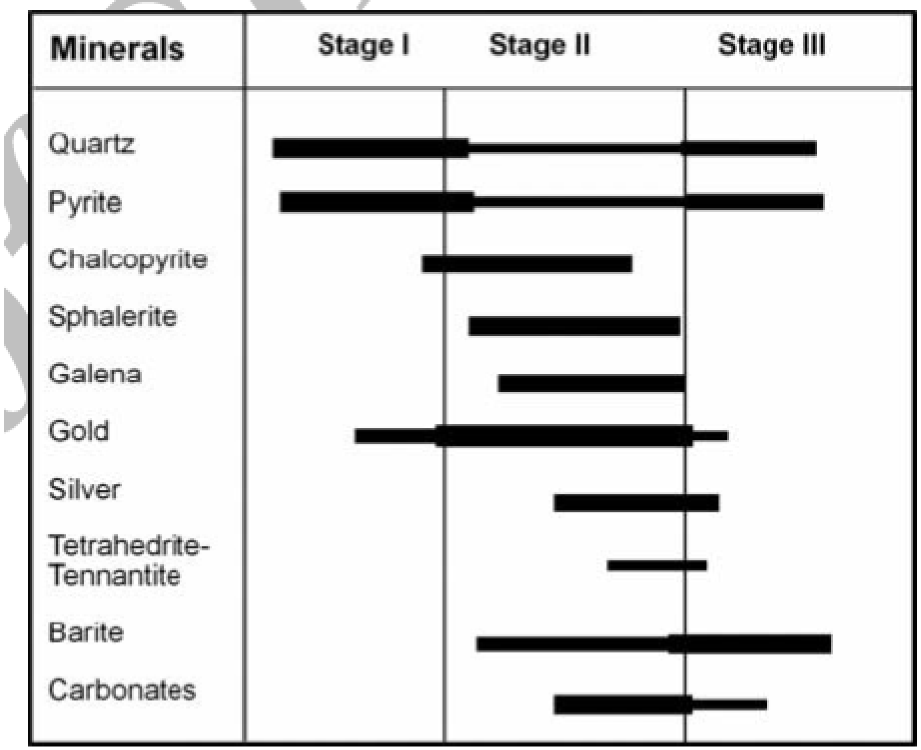

Figure 6. Diagram showing three stages of mineralization and mineral paragenesis at the Gandy deposit; gold mainly occurs in stage II base metal sulfides.

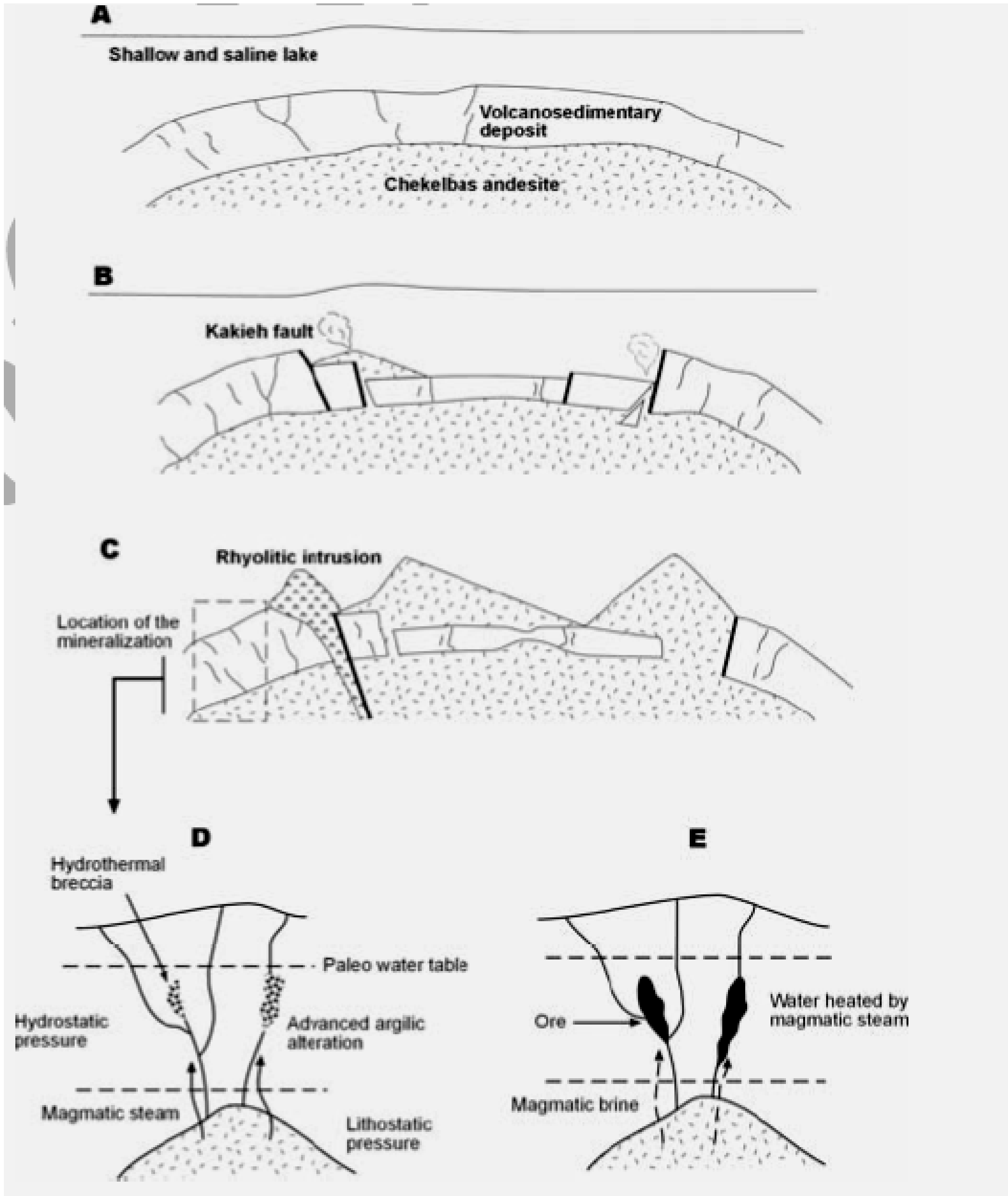

Geological events that have led to mineralization at Gandy,

A. Emplacement of Chekelbas andesite has resulted in doming of volcanosedimentary layers in a shallow lake.

B. Eruption of Chekelbas andesite has resulted in collapse of volcanosedimentary layers, formation of a caldera and developing a series of normal faults including Kakieh fault.

C. Emplacement of rhyolitic intrusions along caldera related normal faults and subsequent mineralization.

D and E. Emplacement of rhyolitic intrusions results in increase in local strain rate resulting in breaching of sealed zone dividing lithostatic from hydrostatic domain and allows brine and gas to be expelled quickly to the epithermal environment and cause the observed mineralization.

Geology of the Sari Gunay Epithermal Gold Deposit, Northwest Iran*

JEREMY P. RICHARDS,

DAMIEN WILKINSON,

HOMAS ULLRICH

Richards JP, Wilkinson D, Ullrich T (2006) Geology of the Sari Gunay epithermal gold deposit northwest Iran. Economic Geology 101:1455–1496.

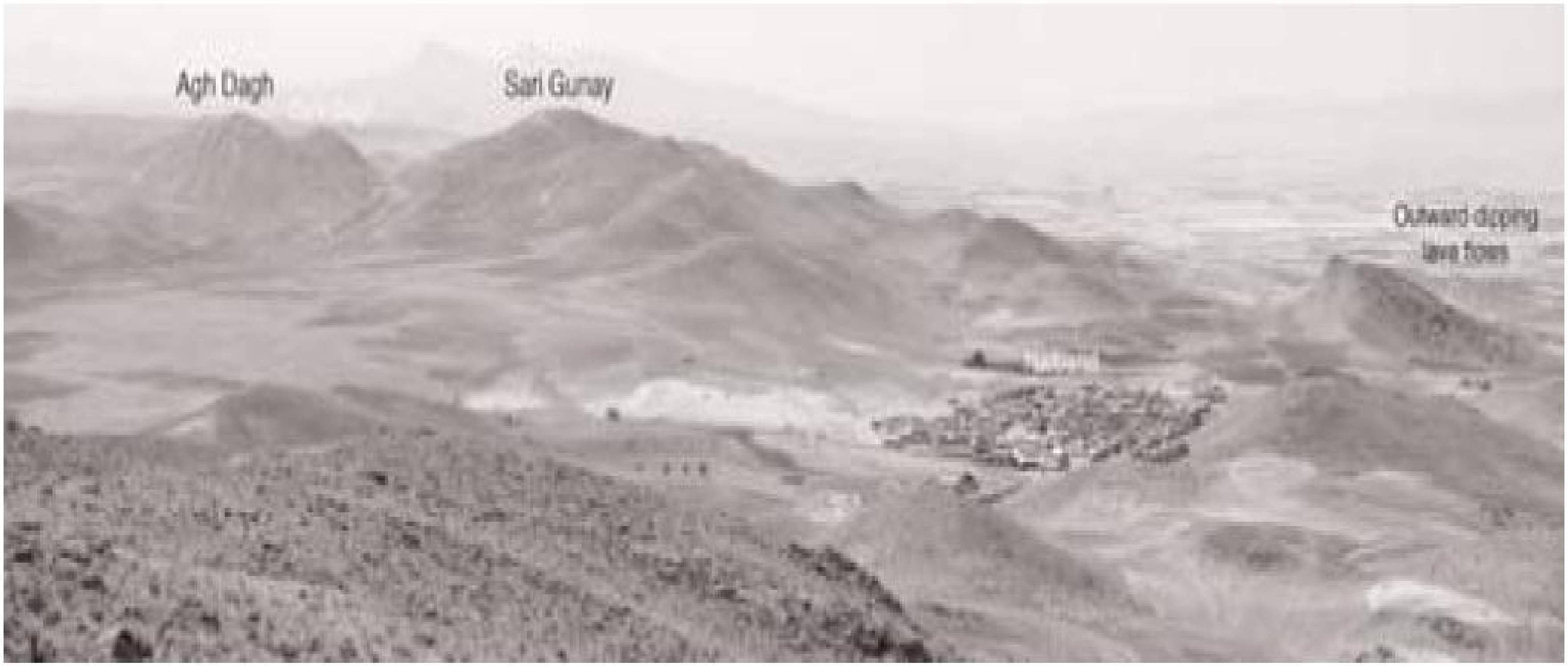

FIG. 5. Composite photograph of the Sari Gunay (center) and Agh Dagh (left) hills, looking south; strong hydrothermal silicification has rendered these hills resistant to erosion. Lavas exposed in the small hill on the right (west) dip away from Sari Gunay, and suggest the preerosional profile of the central volcano; however, a fault runs through the valley between these hills, so vertical correlation across the fault may be invalid. Peaks in the distance are formed by Mesozoic granitic and metamorphic rocks of the Sanandaj-Sirjan zone.

- The Sari Gunay epithermal gold deposit is located within a mildly **alkaline latitic** to **trachytic** volcanic complex in central-northwest Iran.
- Intrusive and volcanic rocks that host the deposit have been dated at between **11.7 and 11.0 Ma**,
- whereas sericitic alteration associated with an early stage of hydrothermal activity occurred between ~10.8 and~10.3 Ma.

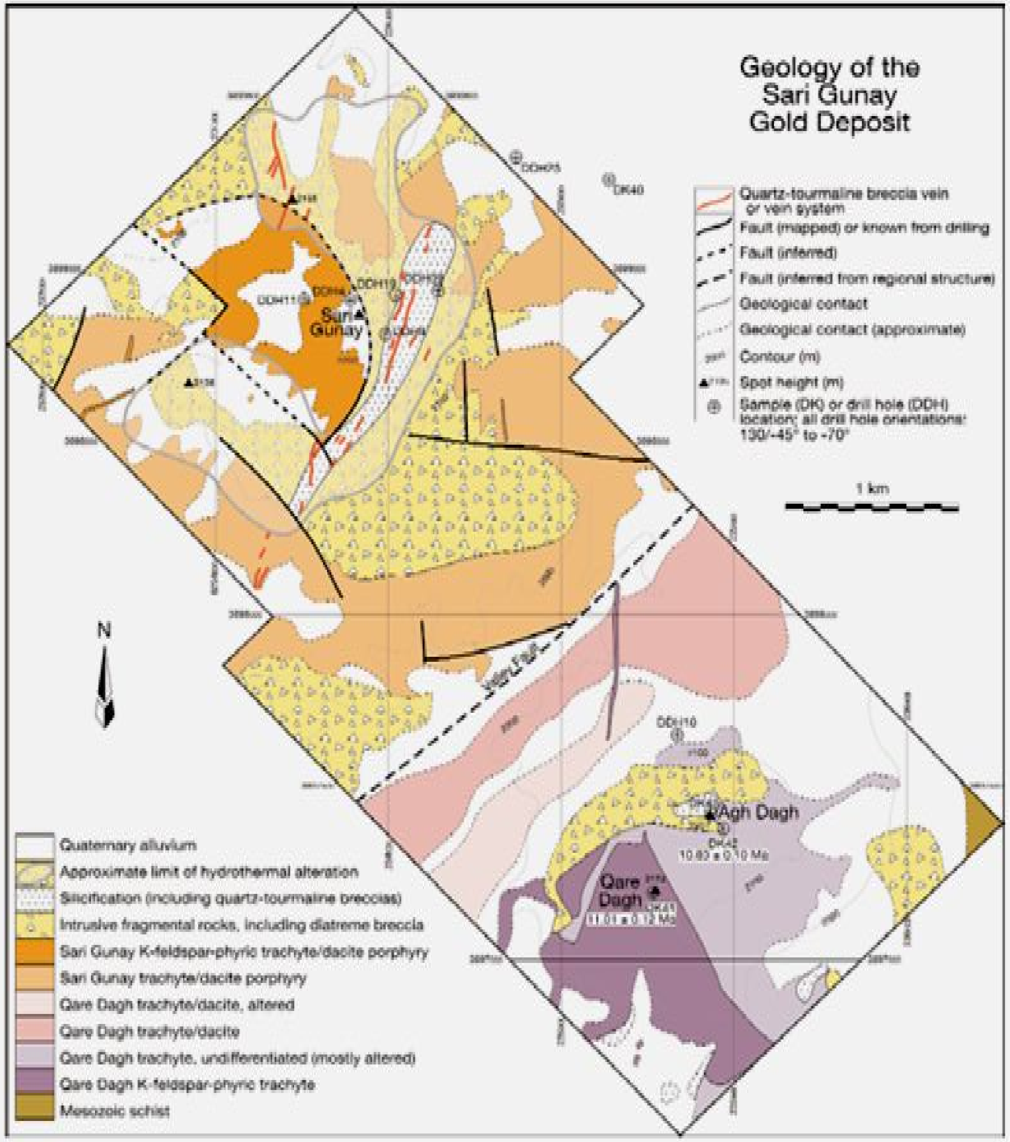

FIG. 14. Geologic map of the Sari Gunay and Agh Dagh subvolcanic and hydrothermal centers, compiled and simplified from company maps by D. Wilkinson and M. Namin (Zar Kuh Mining Company; UTM zone 39S).

- Early hydrothermal activity produced weak porphyry-like **quartz-sulfide-magnetite veining** and **potassic** alteration but with low grades of copper and gold mineralization (~**0.25 wt % Cu, ≤0.5 ppm Au**).

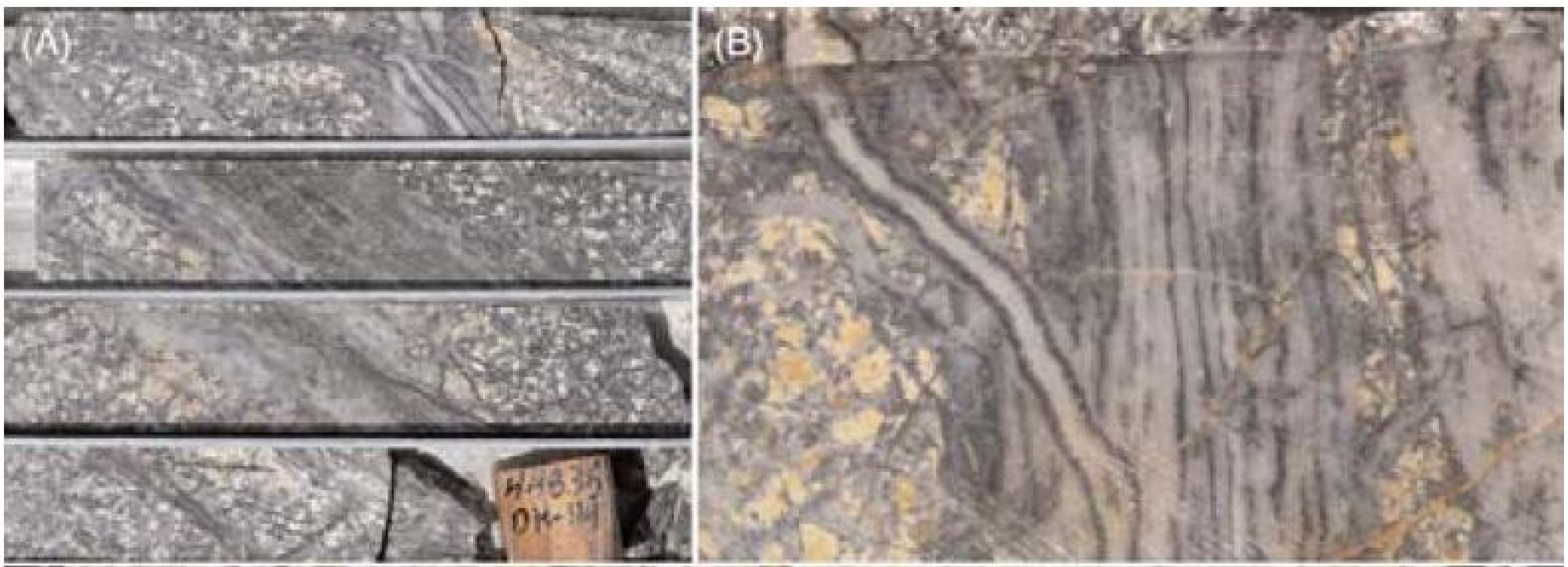

(A, B). Banded and sheeted quartz-magnetite veins cutting sericitized (white alteration) porphyry wall rocks.

Fluid Inclusion of quartz-sulfide-magnetite veins

- Fluid inclusions indicate temperatures of 246° to 360°C and salinities of **34.4 to 46.1** wt percent NaCl equiv in hypersaline inclusions coexisting with low-density, **CO_2-bearing vapor-phase** inclusions.

- Later quartz-tourmaline veins and **breccias** similarly introduced little gold but provided a structurally prepared pathway for the passage of later epithermal fluids.

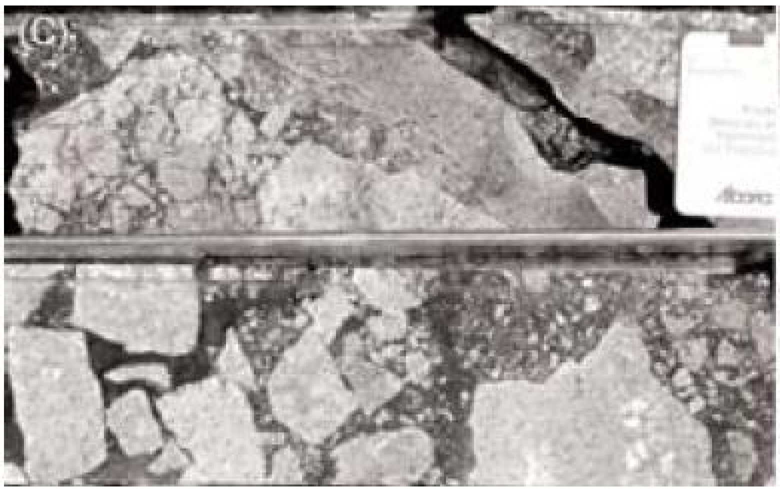

Quartz-tourmaline–cemented hydrothermal breccia.

Quartz tourmaline breccia vein crosscutting and then following an earlier quartz-sulfide-magnetite vein.

- The main stage of gold deposition occurred early in the paragenesis of quartz-pyrite-stibnite-realgar-orpiment veins, with the deposition of fine-grained, auriferous, sooty arsenical pyrite and minor arsenopyrite.

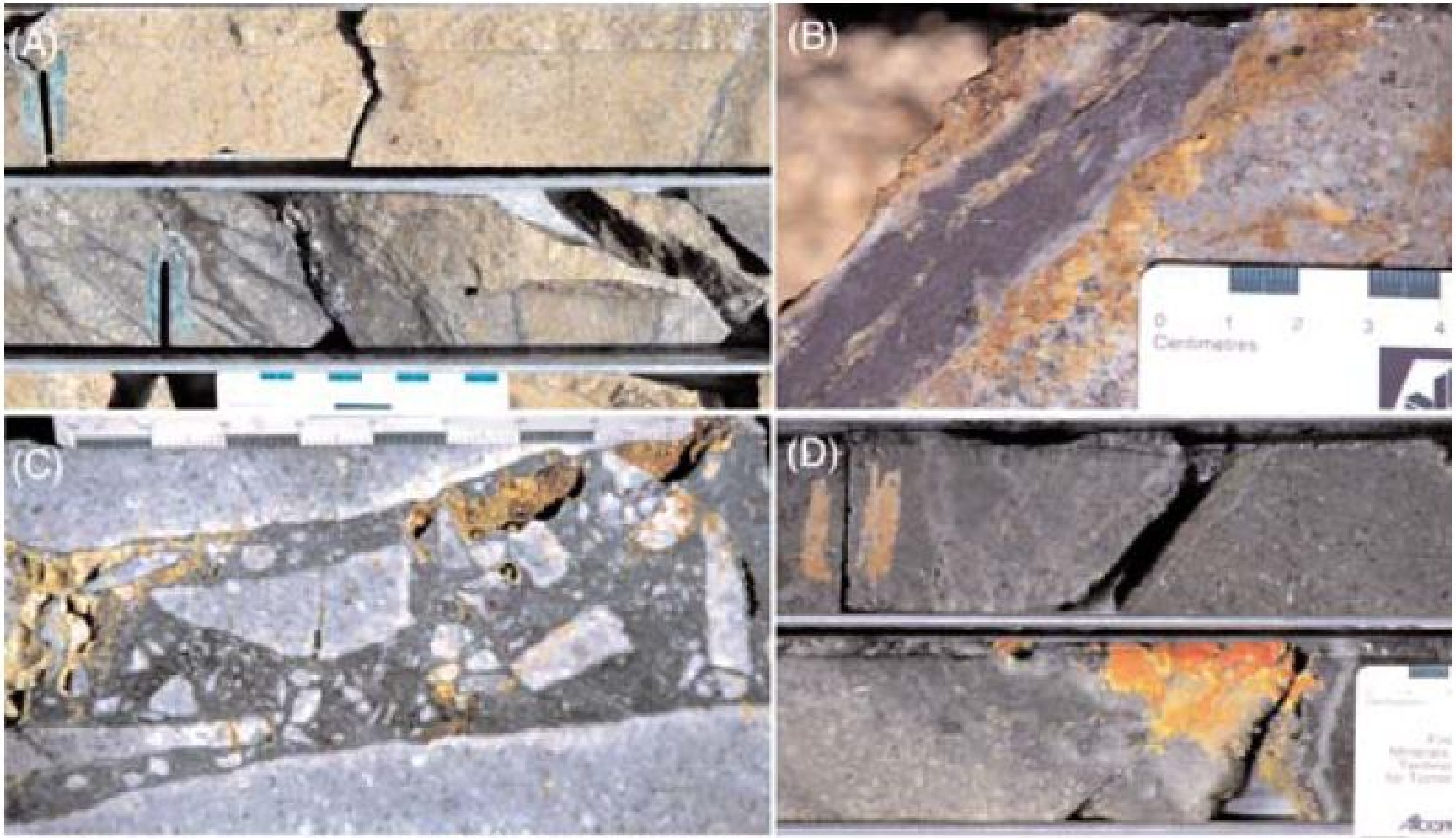

(A). Quartz-sooty pyrite-stibnite vein cutting earlier quartz-sulfide-magnetite veins and sericitic Alteration .(B) Quartz-stibnite vein with orpiment impregnations in wall rock. (C). Quartz-tourmaline breccia vein, with vuggy cavities infilling by late orpiment. (D). Realgar and acicular orpiment overgrown by late chalcedony in a vug in a quartz-sooty pyrite vein.

Mineralization

- Invisible gold occurs in solid solution in fine-grained arsenical pyrite and minor arsenopyrite, deposited in the early stages of quartz-adularia-pyrite-stibnite veins.
- Liquid-rich fluid inclusions in these veins have an average homogenization temperature (trapping temperature) of 199° ± 24°C, salinities of 3.6 ± 1.1 wt percent NaCl equiv, and coexist with low-density CO2-bearing vapor-phase inclusions, suggesting low-pressure conditions.

Genetic Model

- The Sari Gunay deposit may thus be classified as a collision-related alkalic-type epithermal system, although it is less alkaline than classic deposits of this group such as Porgera,Emperor, or Cripple Creek.

The Gandy and Abolhassani Epithermal Prospects in

the

Alborz Magmatic Arc, Semnan Province, Northern Iran

GHOLAM HOSSEIN SHAMANIAN,

JEFFREY W. HEDENQUIST, KIKO H. HATTORI,

JAMSHID HASSANZADEH

Shamanian, G. H., Hedenquist, J. W., Hattori, K. H. & Hassanzadeh, J. 2004.
The Gandy and Abolhassani epithermal prospects in the Alborz magmatic
arc, Semnan province, Northern Iran. Economic Geology,.712–691 ,99

- The Gandy and Abolhassani epithermal precious and base metal deposits occur in the **Torud-Chah Shirin** mountain range in the **Alborz magmatic belt** of northern Iran.
- The mountain range is considered to be part of the **Paleogene Alborz volcanic arc.**
- The Gandy and Abolhassani areas are about 3 km apart, and each contains a small abandoned Pb- Zn mine.
- Mineralization at Gandy occurs in **quartz sulfide veins** and **breccias** and is accompanied by alteration halos of **quartz, illite, and calcite** up to 2 m wide.

- The average homogenization temperatures (Th) and salinities of fluid inclusion assemblages from Gandy range from 234° to 285°C, with a peak at about 250°C and **4.2 to 5.4 wt** percent NaCl equiv.
- The temperature and salinity values in fluid inclusion assemblages from the Abolhassani deposit range from 234° to 340°C and 6.7 to 18.7 wt percent NaCl equiv.

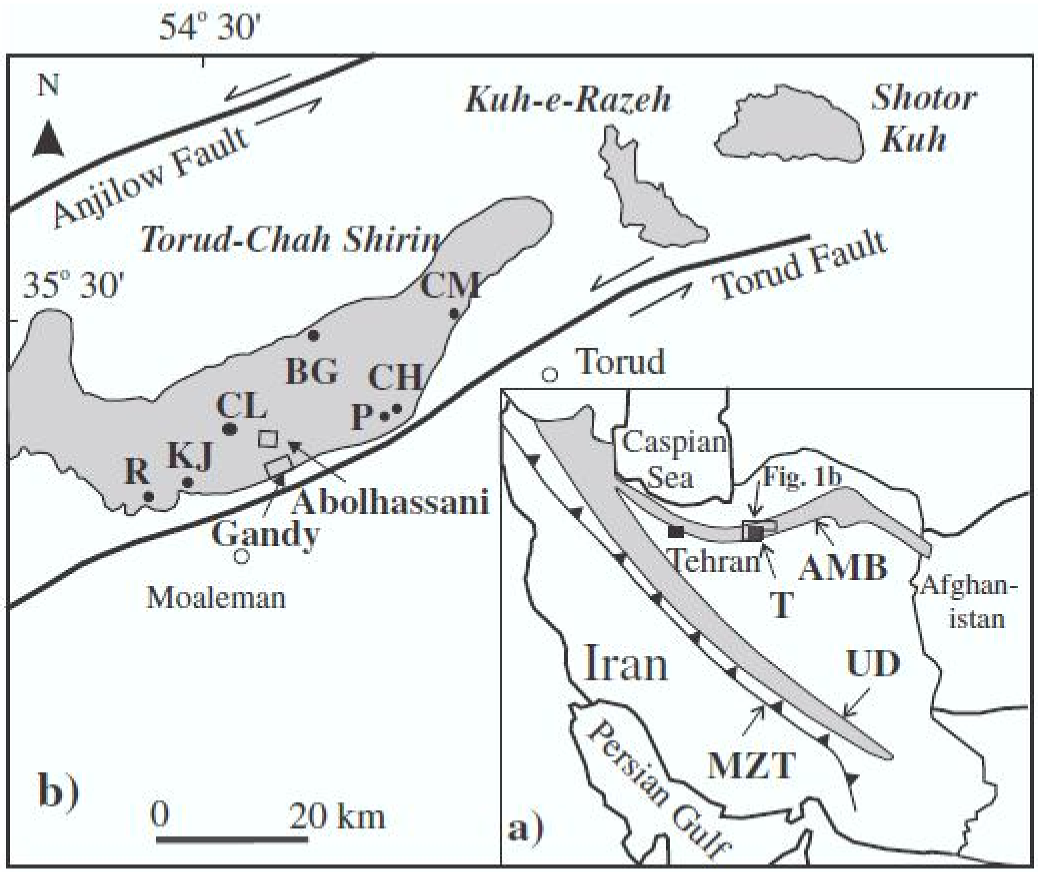

FIG. 1. Location of two main Tertiary volcanic belts in Iran: the NW-trending Urumieh-Dokhtar (UD) zone, which runs parallel to the main Zagros thrust (MZT) cutting central Iran, and the Alborz magmatic belt (AMB) in northern Iran. The Central Iranian Eocene volcanic zone, also called Lut volcanic rocks, is located between the AMB and the MZT in eastern Iran and not shown in the diagram. The exposed rock units of the Torud (T) area include the Paleozoic Shotor-Kuh range, the Mesozoic Kuh-e-Reza range, and the Paleogene Torud-Chah Shirin range. A variety of epithermal and other deposit types occur in the Torud-Chah Shirin mountain range in addition to those in the Gandy and Abolhassani prospects. District names: BG = Baghu, CH = Cheshmeh Hafez, CL = Chalul, CM = Chahmessi, KJ = Khanjar, P = Pousideh, R = Reshm. Modified from Hushmandzadeh et al. (1978).

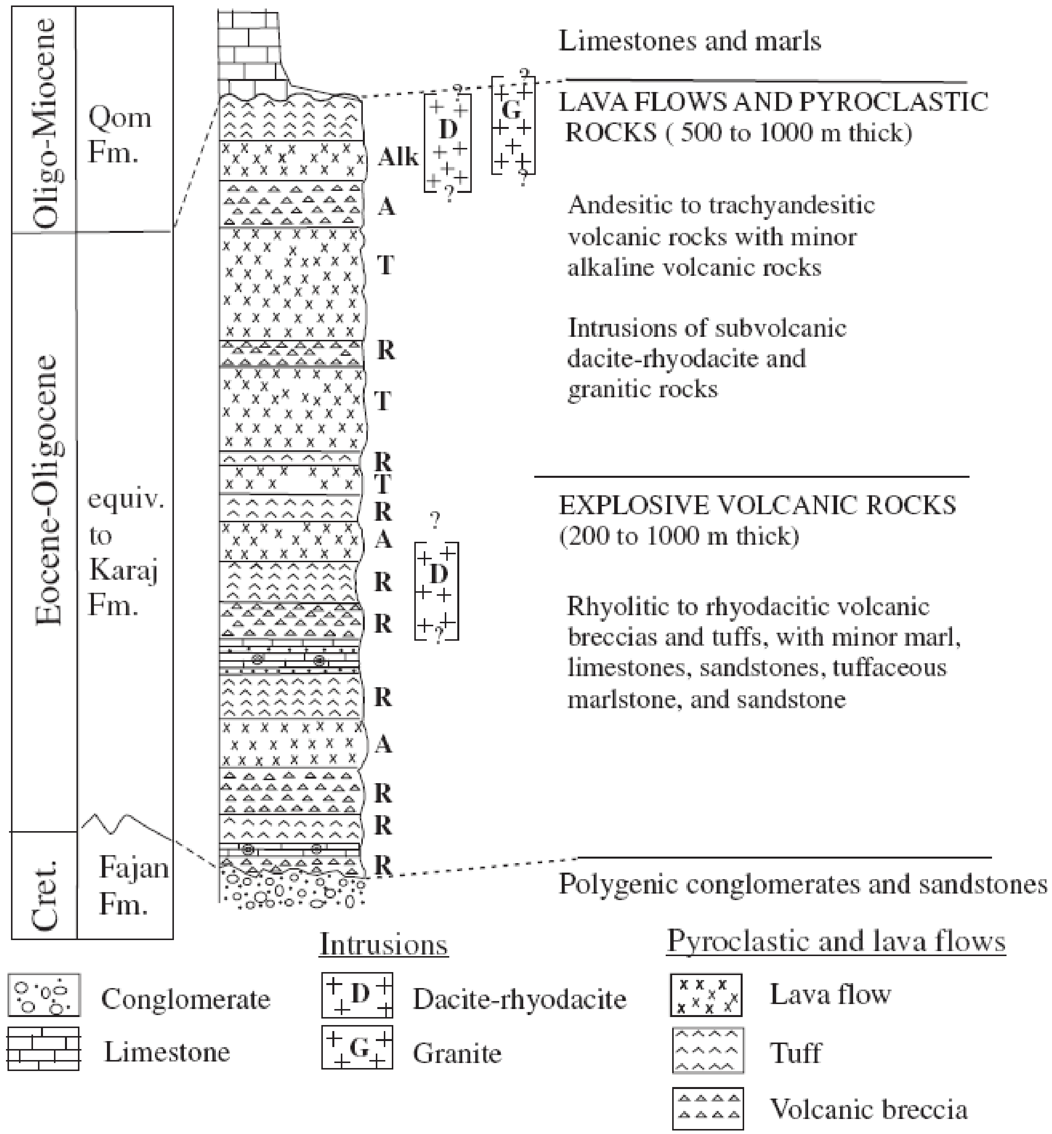

FIG. 2. Tertiary magmatic events in Torud-Chah Shirin mountain range (modified from Hushmandzadeh et al., 1978). A = andesitic, R = rhyolitic to rhyodacitic compositions, T = trachyandesitic.

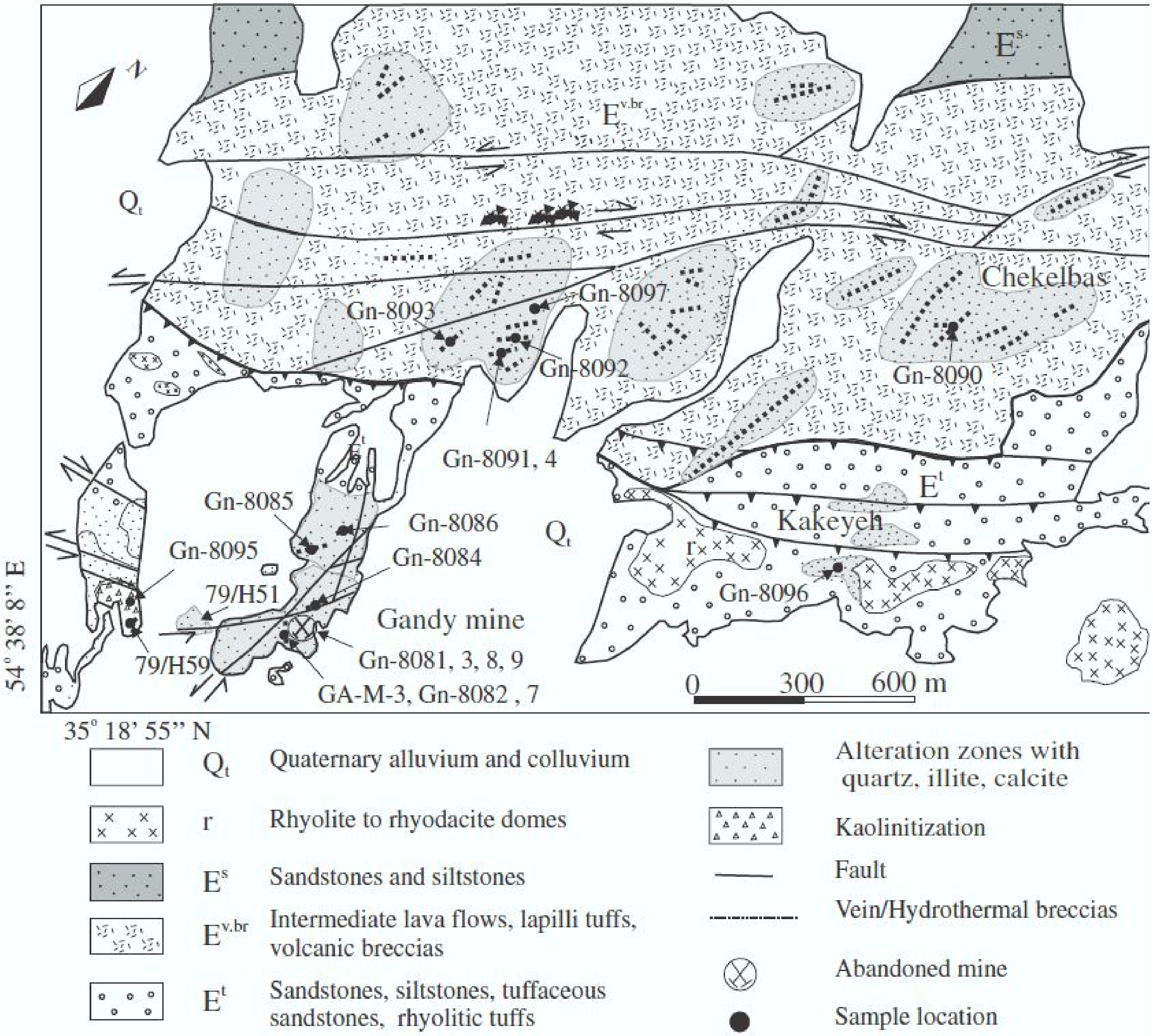

FIG. 4. Geologic map of the Gandy prospect. Latitude and longitude of the southwestern corner is shown.

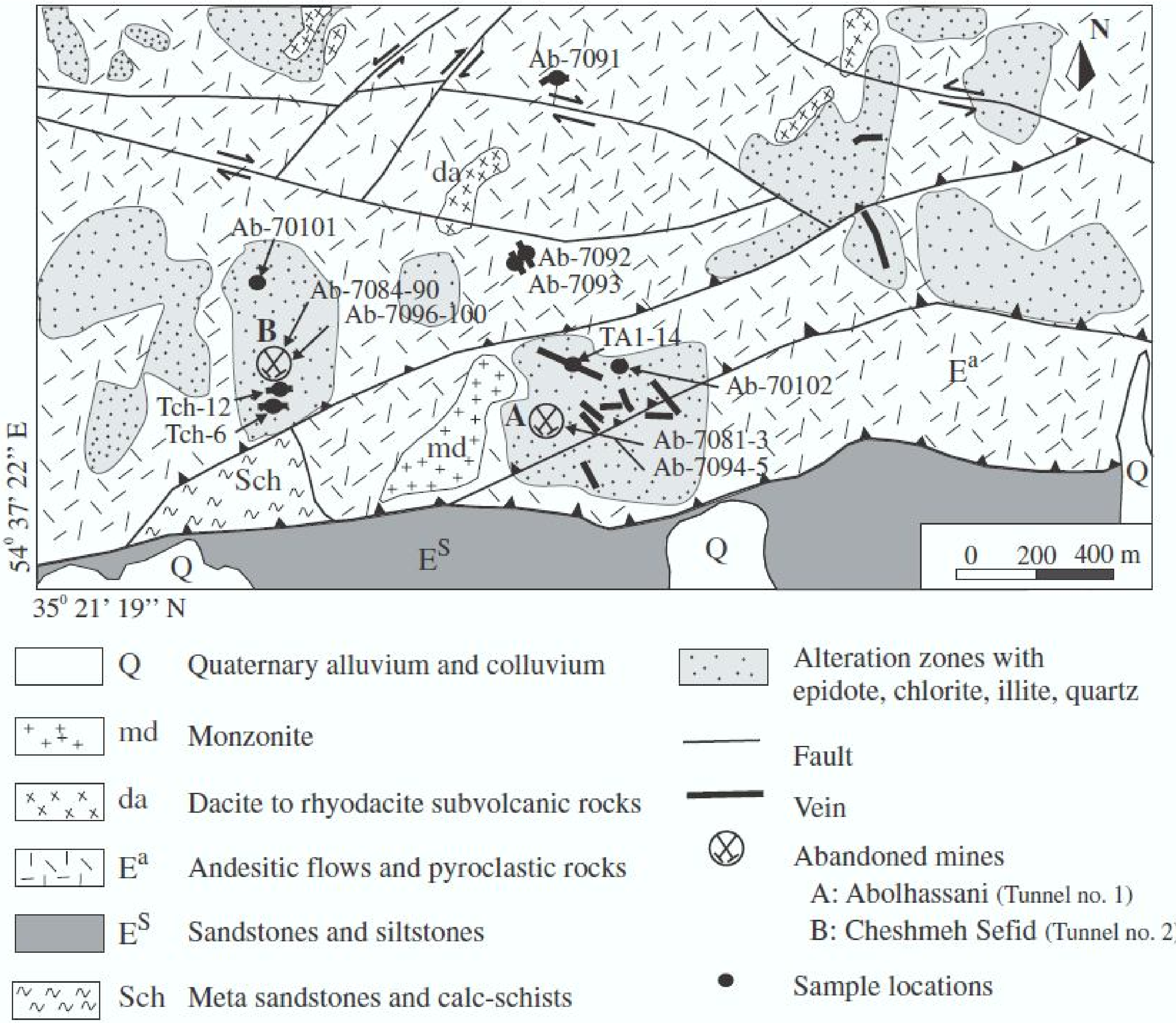

FIG. 5. Geologic map of the Abolhassani prospect. Latitude and longitude of the southwestern corner is shown.

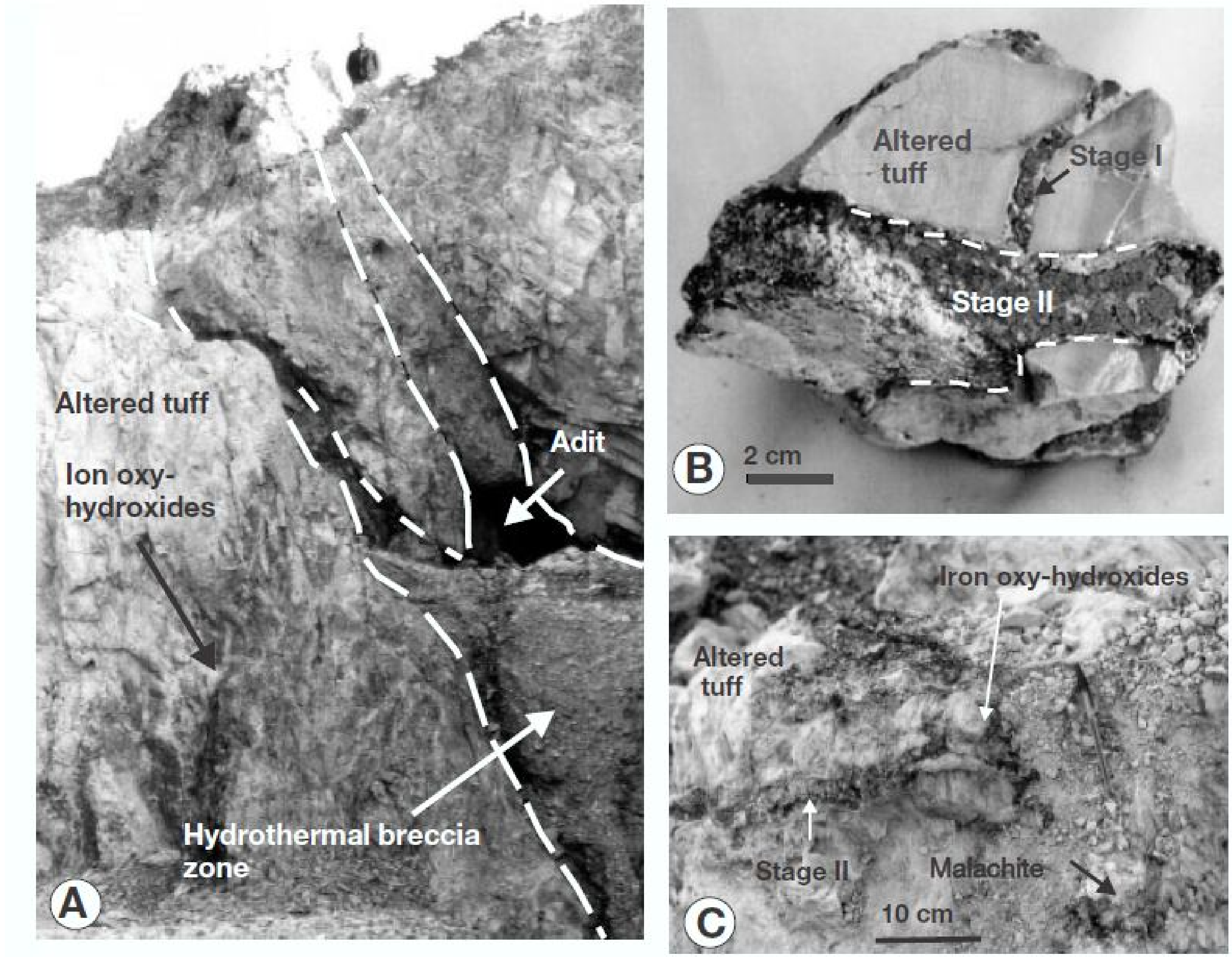

A. Hydrothermal brecciated zones of stage I with fragments of host tuff breccia that have been kaolinitized.

B. B. Hydrothermal breccia of stage I, consisting of brecciated fragments of altered tuff that show a jigsaw-puzzle texture.

C. Narrow veins of base metal sulfides, barite, and quartz of stage II.

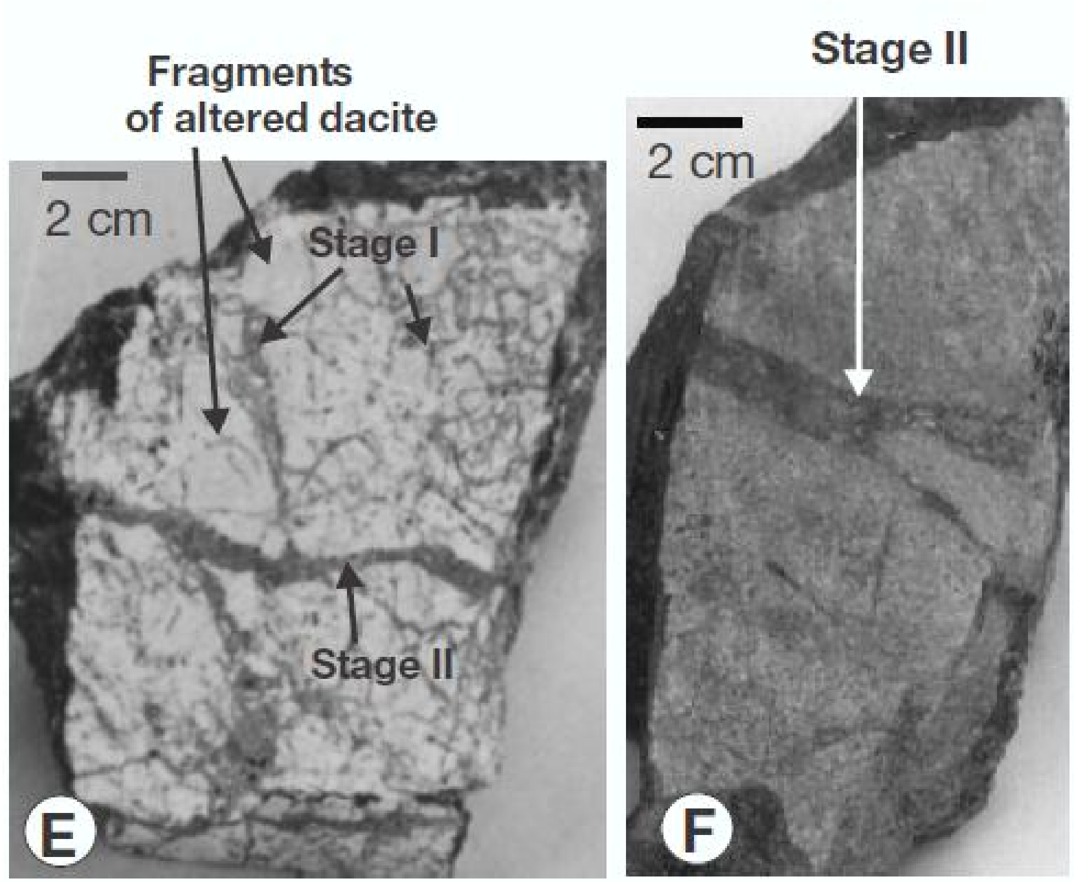

E. Hydrothermal breccias of stage I mineralization in the Abolhassani prospect, consisting of brecciated fragments of altered dacite.

F. Andesite cut by veinlets of galena, sphalerite, and quartz, which represent the second stage of mineralization.

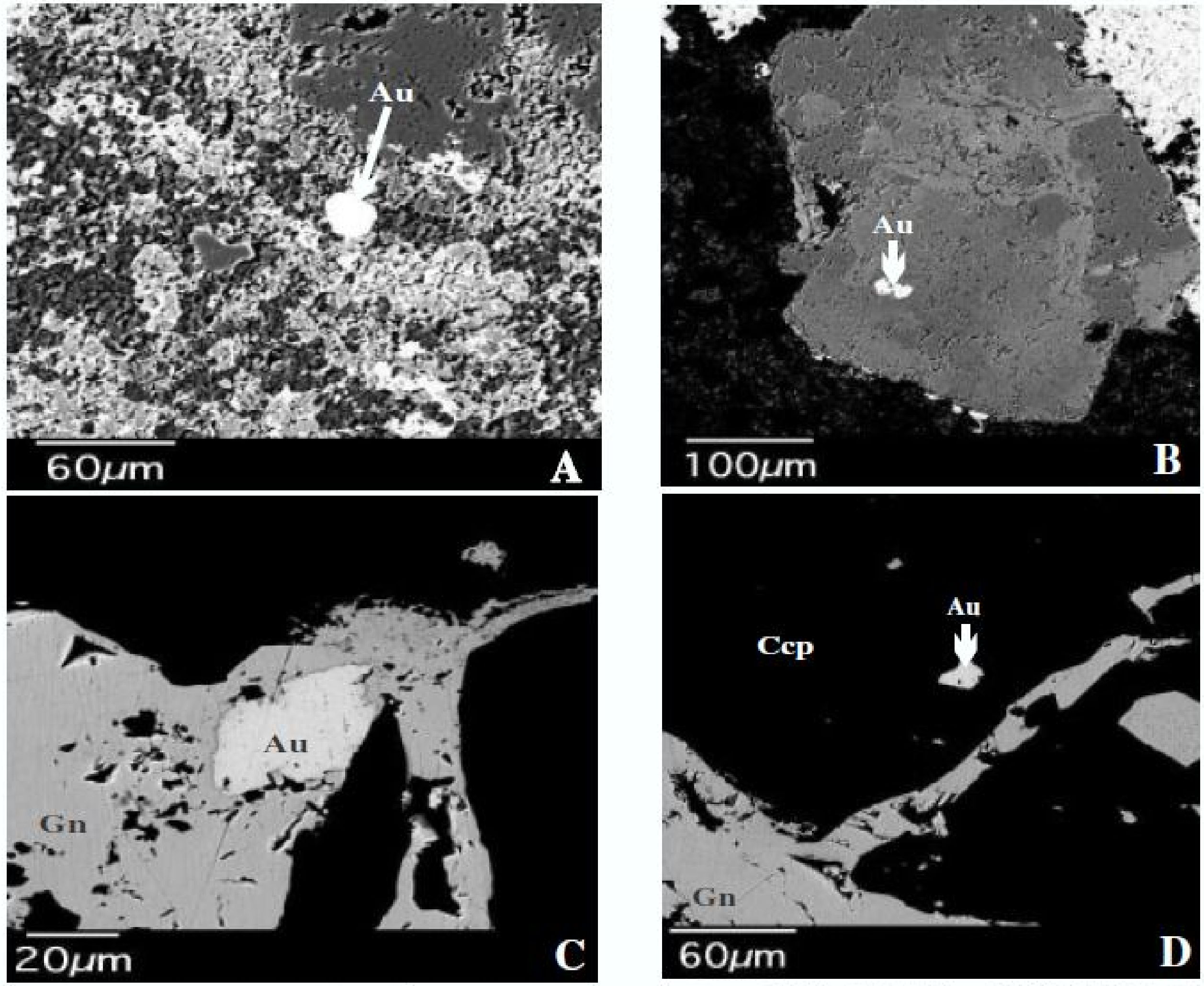

Backscattered electron images of minerals from the Gandy and Abolhassani prospects. A. and B. Gold grains (Au) in secondary iron oxides of stage I (Gandy prospect). C. and D. Gold within galena (Gn) and chalcopyrite (Ccp) of stage II (Gandy prospect).

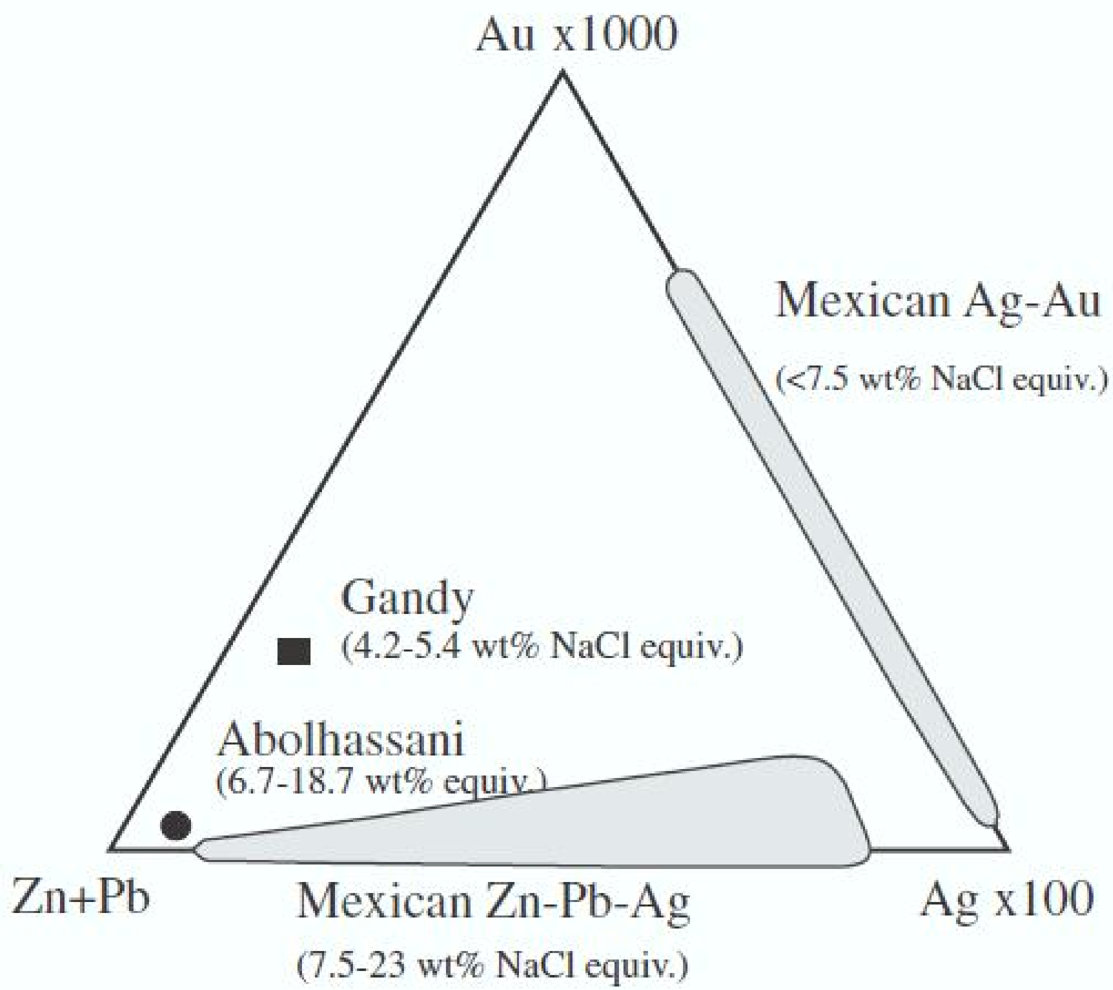

FIG. 13. Ternary diagram of relative precious and base metal contents of the Gandy and Abolhassani deposits (averages of veins from Tables 2 and 3, respectively). Ranges for Mexican epithermal deposits are shown for comparison (fields from Albinson et al., 2001).

Genetic Model

The mineralogy of ore, gangue, and alteration products, combined with fluid inclusion data from both areas, indicate that these are intermediate-sulfidation epithermal veins that share characteristics with those of major districts in Mexico, western United States, Peru, and elsewhere.

Geological setting and timing of the Chah Zard breccia-hosted epithermal gold–silver deposit in the Tethyan belt of Iran

Hossein Kouhestani

Majid Ghaderi

Khin Zaw

Sebastien Meffre

Mohammad Hashem Emami

- **The breccia-hosted epithermal** g**old–silver** deposit of Chah Zard is located within a high-K, calc-alkaline andesitic to rhyolitic volcanic complex in the central part of the Urumieh-Dokhtar Magmatic Arc (UDMA), west central Iran.
- The total measured resource for Chah Zard is ∼2.5 million tonnes of ore at 12.7 g/t Ag and 1.7 g/t Au (28.6 t Ag, 3.8 t Au).
- LA-ICP–MS U–Pb zircon geochronology yields a mean age of **6.2±0.2** Ma for magmatic activity at Chah Zard.

- Precious metals occur with **sulfide and sulfosalt minerals** as d**issemination**s, as well as in the **veins and breccia cement**s.
- ore minerals consisting of pyrite, marcasite, arsenian pyrite, arsenopyrite, chalcopyrite, sphalerite, galena, gold (in electrum and native form), and silver sulfosalts.
- Hydrothermal alteration and deposition of gangue minerals progressed from **illite-quartz to quartz-adularia, carbonate**, and finally gypsum-dominated assemblages.

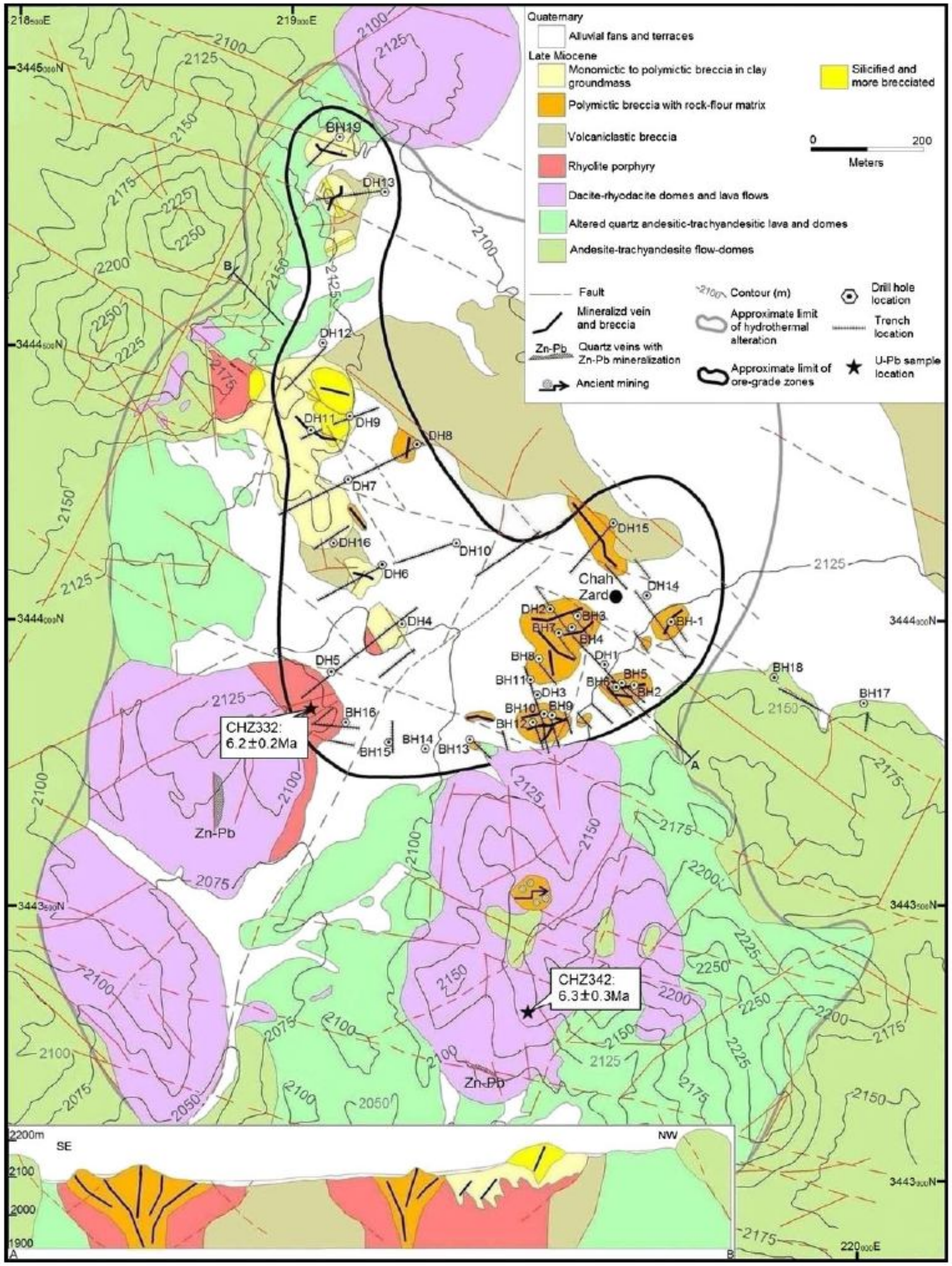
Quaternary
Alluvial fans and terraces
Late Miocene
Monomictic to polymictic breccia in clay groundmass
Silicified and more brecciated
Polymictic breccia with rock-flour matrix
Volcaniclastic breccia
Rhyolite porphyry
Dacite-rhyodacite domes and lava flows
Altered quartz andesitic-trachyandesitic lava and domes
Andesite-trachyandesite flow-domes
0
200
Meters
Fault
Contour (m)
Drill hole location
Mineralizd vein and breccia
Approximate limit of hydrothermal alteration
Trench location
Zn-Pb
Quartz veins with Zn-Pb mineralization
Approximate limit of ore-grade zones
U-Pb sample location
Ancient mining
Chah Zard
CHZ332: 6.2±0.2Ma
CHZ342: 6.3±0.3Ma
SE
NW
2200m
2100
2000
1900
A
B

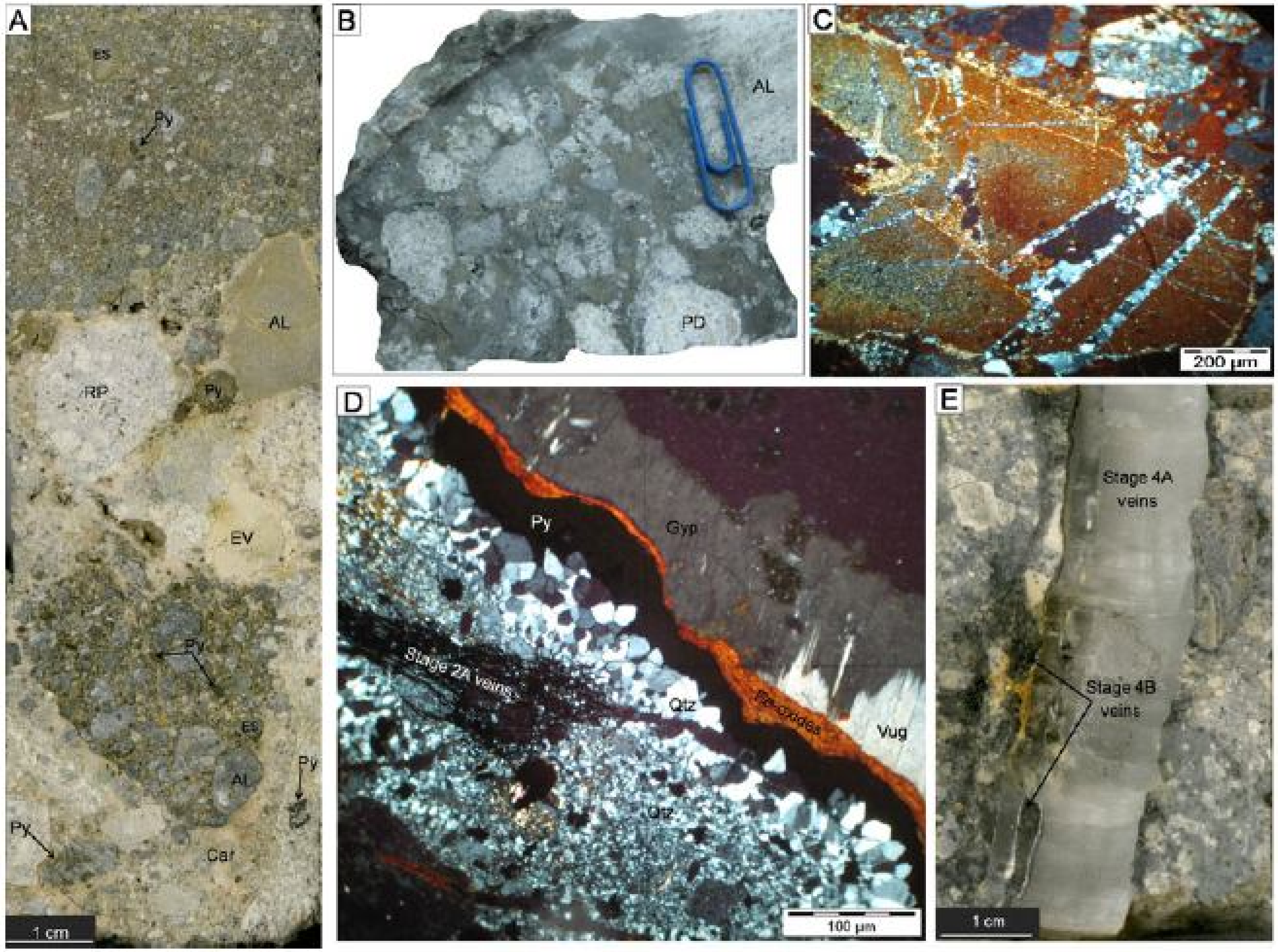

A: Polymictic breccia with carbonate cement, containing pre-brecciationclasts of stage 1 mineralization. B: Clast-rotated polymicticbreccia with stage 2A sulfide (pyrite-arsenian pyrite) cement. C: Photomicrograph of subparallel sheeted stage 2. C :quartz-adularia veins cutting polymictic breccia. D: Photomicrograph of stage 3 veins containing dogtooth quartz and fine-grained aggregates of quartz, and colloform pyrite, cutting stage 2A mineralization. E: Stage 4A quartz–pyrite-base metal sulfide veins overgrown by stage 4B gypsum veins.

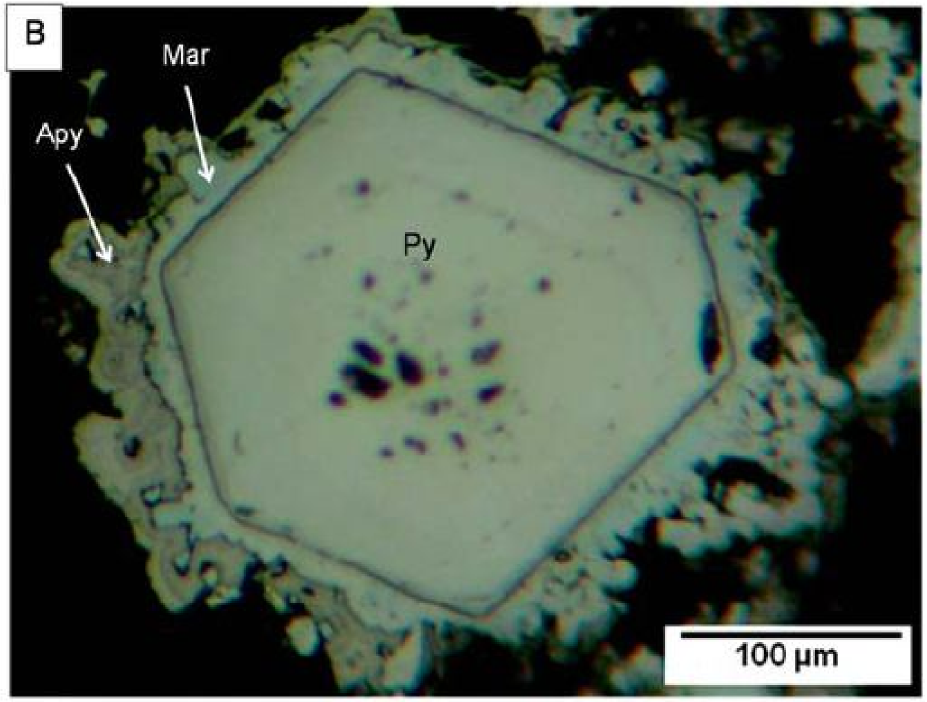

Euhedral pyrite surrounded by marcasite and arsenian pyrite showing zoning pattern.

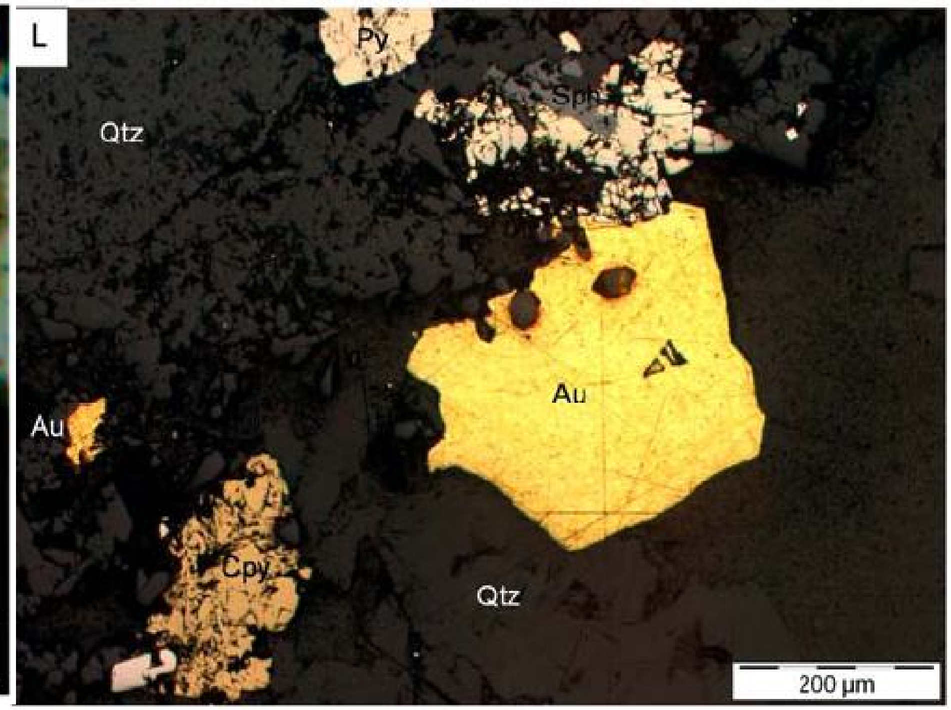

Native gold associated with pyrite and quartz.

Genetic Model

- The Chah Zard gold–silver deposit is a good example of a breccia-hosted **low- to intermediate-sulfidation** epithermal deposit (e.g. Hedenquist et al. 1996; Sillitoe 1999; Einaudi et al. 2003; Sillitoe and Hedenquist 2003).
- This deposit formed in a transtensional environment related to the evolution of the Dehshir-Baft strike-slip fault system.
- The age of Au–Ag mineralization at Chah Zard is younger than those of the large porphyry Cu–Mo deposits (e.g., Sar Cheshmeh, Meiduk, and Sungun) and other epithermal gold deposits (e.g., Sari Gunay) so far discovered in UDMA and may represent a previously unrecognized pulse of mineralization in UDMA.

Geological setting, alteration, and fluid inclusion characteristics of Zaglic and Safikhanloo epithermal gold prospects, NW Iran

SUSAN EBRAHIMI

SAEED ALIREZAEI

YUANMING PAN3

From: Sial, A. N., Bettencourt, J. S., De Campos, C. P. & Ferreira, V. P. (2011) Granite-Related Ore Deposits.Geological Society, London, Special Publications, 350, 133–147.

- The Zaglic and Safikhanloo epithermal gold prospects are located in the **Arasbaran zone,** to the west of the Cenozoic Alborz-Azarbaijan magmatic belt in NW Iran.
- Mineralization is mainly restricted to **quartz and quartz - carbonate veins and veinlets.**
- Gold occurs as **microscopic and submicroscopic grains in quartz and pyrite.**

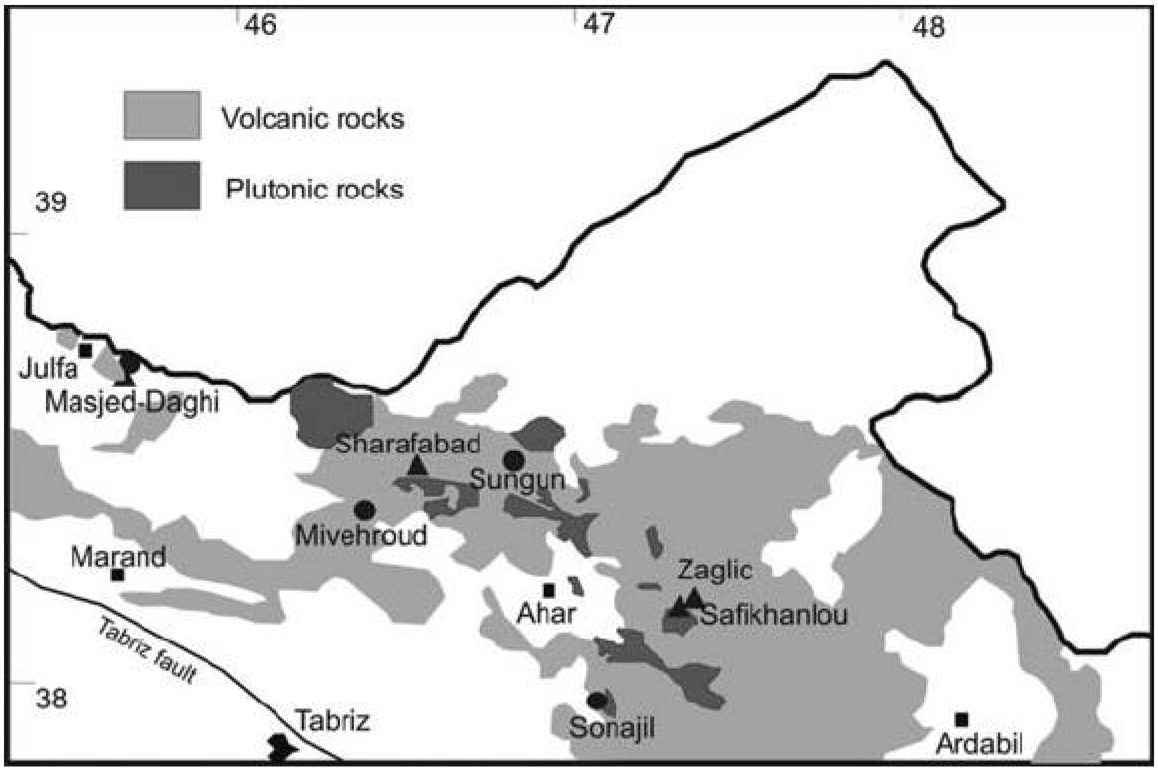

Fig. 2. Simplified map of NW Iran showing the distribution of Cenozoic magmatic rocks. Filled triangles: epithermal deposits; filled circles: porphyry deposits.

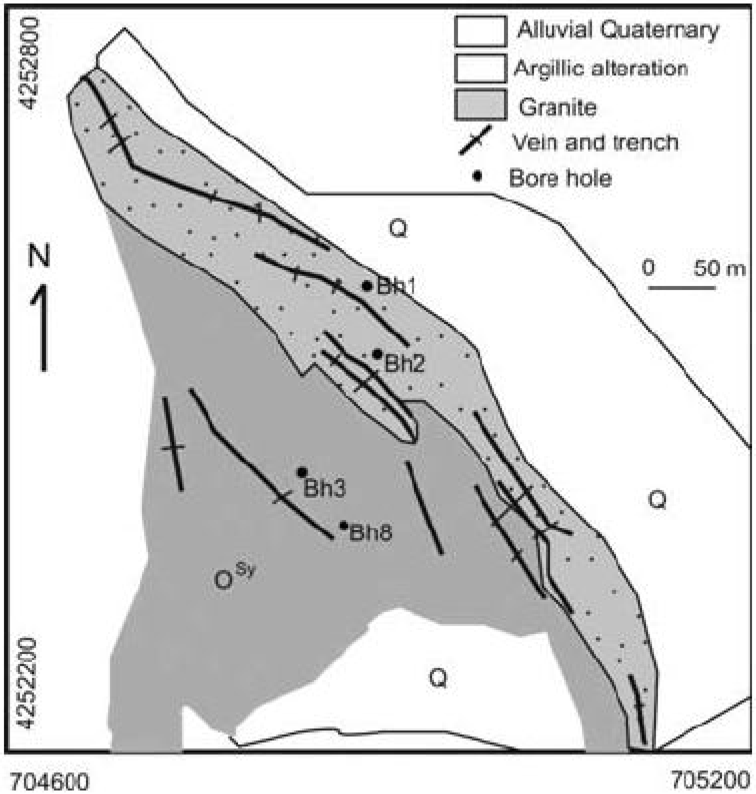

Fig. 3. Geological map of the Safikhanloo prospect, simplified after Mohamadi (2006).

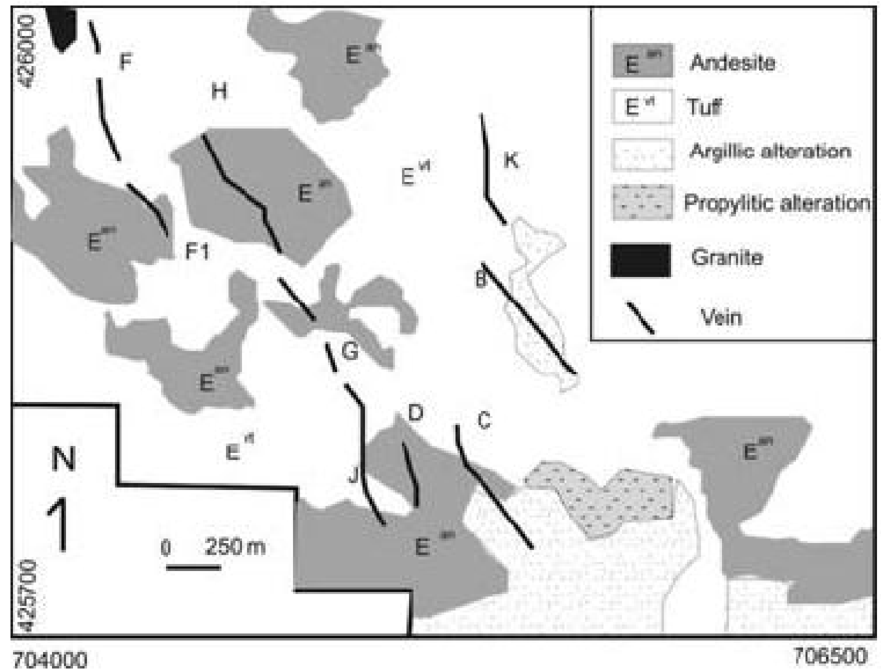

Fig. 4. Geological map of the Zaglic prospect, simplified after Heydarzadeh (2005).

• The least altered country rocks display a trend from calc-alkaline to alkaline, and feature more typical of continental arc/rift magmas.

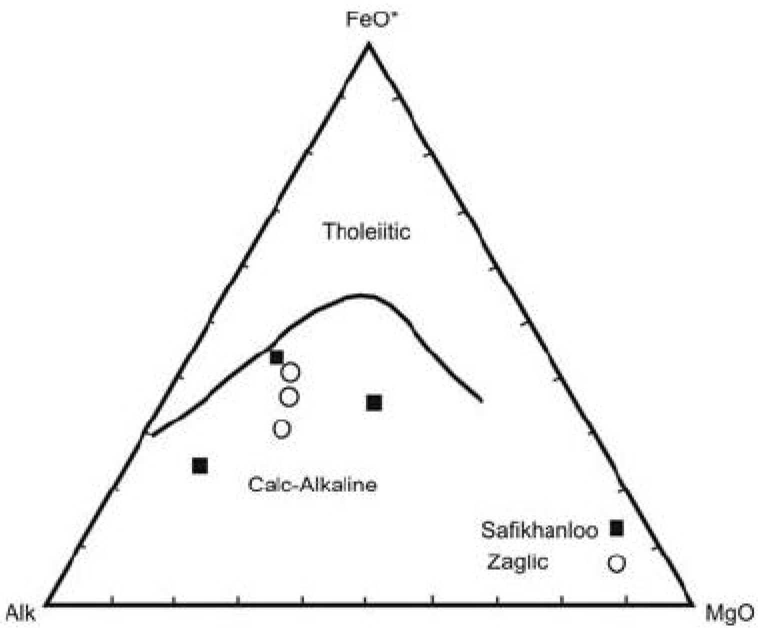

Fig. 6. Plots of samples on the calc-alkaline–tholeiitic discrimination diagram (Irvine & Baragar 1971) showing a calc-alkaline affinity for the country rocks.

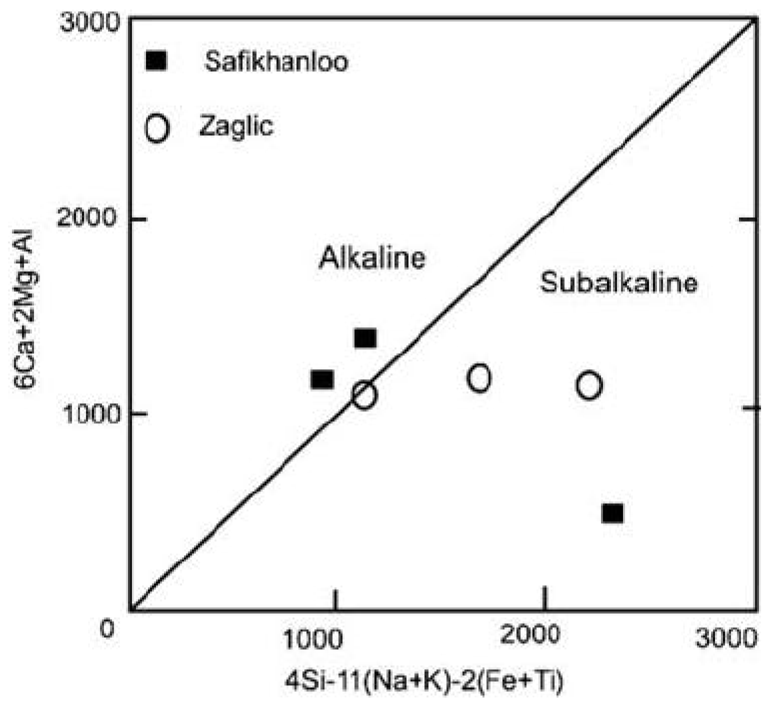

Fig. 7. Plots of samples on the R1–R2 alkaline–subalkaline discrimination diagram of De La Roche *et al.* (1980).

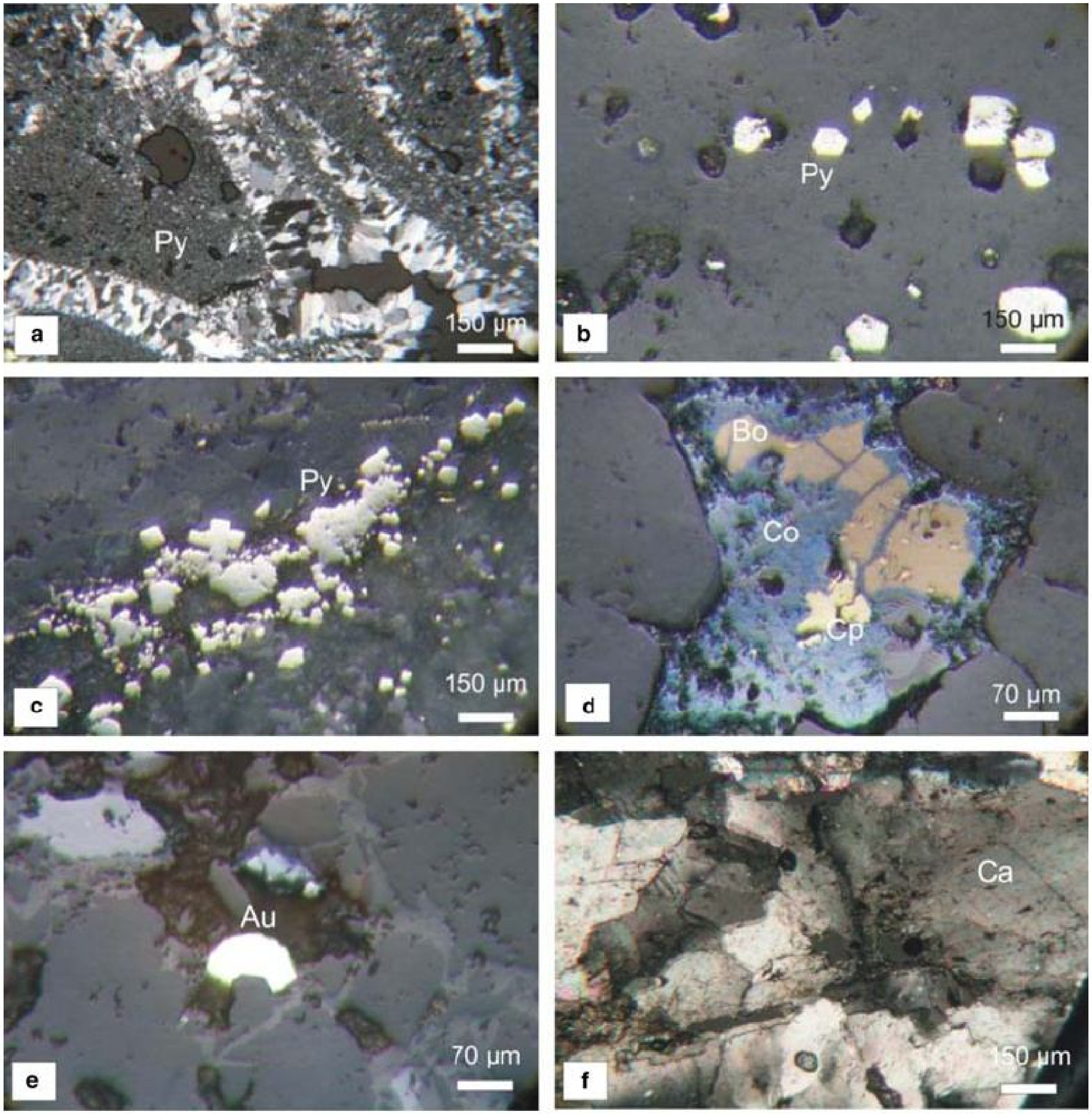

(a) Lenticular dark gray quartz, rich in microscopic pyrite (black spots). **(b and c).** Pyrite from the main stage of mineralization occurring as disseminations (b) and veinlets (c) in silica. **(d)** Bornite (Bo) and chalcopyrite (Cp) replaced by covellite during supergene processes. **(e)** microscopic gold grain (Au) in quartz. **(f)** Coarse-grained (bladed) calcite (Ca) from the main stage of mineralization.

Fluid Inclusion

- For Safikhanloo, homogenization temperatures (Th) vary between 170–230 8C.
- For Zaglic, Th values vary between 190–331C.
- The relatively wide variations in the salinity values (0.17–6.7 and 1.4 to 9.5 wt% NaCl equiv. for Zaglic and Safikhanloo, respectively) could be explained by extensive boiling and vaporization of a low salinity fluid

Genetic Model

- With regards to the dominant intermediate argillic alteration, low contents of base-metal sulphides, homogenization temperatures, and the overall low salinities of the fluids, the Safikhanloo and Zaglic prospects formed in a low-sulphidation epithermalenvironment.